Thermal Storage Solution for the Organic Rankine Cycle

Deliverable:

Final Report

Submission:

April 10th, 2015

Team: # 17

Authors:

Belal Nabulsi

Bruce Orozco

Cory Nelson

Jhamal Holliday

Sponsor:

Verdicorp

Advisor:

Dr. Juan Ordonez

Submitted to:

Dr. Nikhil Gupta

Dr. Chiang Shih

Contents

Table of Figures

Table of Tables

Abstract

As a customer, Verdicorp, a company that produces and sells Organic Rankine Cycle power systems, has asked us to build a thermal storage unit to extend the running time of their ORC system. It was requested that our design specifically take into account the location of the end user with regards to raw material procurement. This led us to pursue a sensible thermal storage method that could be tailored to the location by changing material mediums. Later in the project, our customer acquired a new patent on phase change material encapsulation and decided to refocus our efforts on a latent heat storage device that was previously considered in earlier reports. We have been tasked with developing an efficient way to take advantage of the geometry and thermal properties of the phase change material properties. In response our team chosen a new storage medium called Dynalene MS-1 and heat transfer fluid Duratherm HF. We've also chosen to use existing Shell-and-Tube heat exchanger technology to store and transfer energy by applying several variations.

Introduction

Presented In this report is our current understanding of the Thermal Storage Solution project. The goal of this project is to produce a functional scaled down version of a thermal storage device. Objectives for the final model include that the device display the potential to power Organic Rankine Cycle for up to four hours, ability to respond to energy needs as they're demanded of it, and produces costs at or below the target of 23 cents per kilowatt hour.

The need for thermal storage solutions is currently within a time of growth. As the use of intermittent sources such as solar increases so does this need. When these sources are no longer available power companies need thermal storage devices to continue producing energy. Verdicorp's ORC is in need of such a device to continue providing the heat needed to produce electricity.

Need Statement

A thermal energy storage solution is needed to increase the operation time, efficiency, and overall feasibility of Verdicorp's Organic Rankine Cycle power generator. Using waste or excess heat, the ORC is able to take advantage of a greater portion of the heat produced from intermittent sources to continually generate power. This process will reduce the required fuel needed for the same amount of energy production; after an input source has been depleted or turned off. This produces savings for the customer in fuel and energy costs, as well as reducing the production of any potentially environmentally harmful emissions from the system. The main storage component of the device will be provided by Verdicorp. This component is a patented encapsulated PCM storage cell. The optimal configuration using these cells must be designed to maximize the functionality of the overall system.

Goal Statement

Our aim is to produce a commercially viable thermal energy storage solution for Verdicorp's Organic Rankine Cycle using their patented PCM, environmentally friendly materials, and cost effective manufacturing.

Objectives

- To design and construct a functioning thermal energy storage unit prototype by April 2015, under the present day constraints specified below.
- Insure that said prototype is easily serviceable
- Produce power at 23cent per kilowatt hour
- Applicable in developing markets such as China
- Ability to supply extra power during times of peak operation
- Optimize the heat transfer and energy storage using the latent heat method provided

Project Challenges

While our overall goal remains the same, our project has undergone several changes since it began in August of 2014. The first of which was a change in location from Brazil to the Australian Outback. At the time our team was pursuing a sensible heat storage concept based on materials locally available at the location of the end user. This change to Queensland, AU forced us to reevaluate the materials that would be used in our design. While studying the mineral resources of the Outback we found an ore called bauxite that was commonly available throughout the region and possessed desirable thermal properties like such as high thermal conductivity compared to similarly priced options like concrete and granite. In our sensible storage concept, Bauxite would be used as our storage medium. Then in early December the project was subject yet another change. After acquiring a patent in phase change encapsulation Verdicorp directed the team to refocus on developing a latent heat storage concept. To address this change the team once again reevaluated the available storage materials. Our research led us to Dynalene MS-1 a molten salt that exhibited low corrosion on stainless steels unlike other options and a redesign of our storage device to take advantage geometry of the phase change capsules. The team has chosen to accomplish this by creating a variation of Shell-and-Tube Heat Exchanger, a pre-existing design. However, the tubes would contain the Dynalene MS-1 salt and would not flow through the tank as in a traditional shell-and-tube heat exchanger. Rather, the salt would be vacuumed sealed in the tube and stagnant. This has not been done before as the patent was recently released so we do expect to have highly significant results

While facing the challenges that come regularly in a dynamic industrial environment, the team has refined its process to pool our individual resources to gather and learn new research material. The team has also improved its design process by communicating design issues and discussing solutions as a group, while leaving individuals to specialize in specific areas of the design.

Constraints

A key to the success of the project will be the management of the various constraints that are inherent in the design, or that may arise during the design process. In order to optimize the productivity of the team these constraints must be constantly analyzed and reevaluated. The present constraints of the project are categorized by full and prototype scale

For Thermal Storage Unit (Full Scale):

- Stores Heat for a minimum of 14 hours after heat input.
- Robust system-Corrosive resistant
- Resistant to high thermal cycle fatigue
- Serviceable and cost-effective maintenance
- Design must generate power at or below 23 cents per hour of power.

For Thermal Storage Unit (prototype):

- Maximum operating pressure: 50 psi
- Construction material: 80-20 alloy
- Must be mobile
- Design must be marketable
- Maximum budget for parts and materials: $2000

Performance specifications

- Must not heat the working fluid, R245, of the ORC to temperatures in excess of 170^{o}C
- Ability to deliver energy as demand dictates
- Extends the ORC's operation time by 14 hours when primary fuel source is no longer available (assuming the device is fully charged)

Prototype Design specifications

The energy storage material is a key component to the design, and after careful consideration and talks with our sponsor, it has been decided to implement phase change material as our storage medium. This material must be contained in an insulated environment and be capable of transferring energy with minimal losses and maximum heat transfer. The heat exchanger configuration and piping must be designed to optimize the energy control to and from the system. An example of a possible design is presented in Figure 1. The type of material and heat transfer configuration selected will determine the amount of heat that can be stored and the duration. The device must be capable of storing the thermal energy for at least 14 hours and consistently deliver the heat needed to generate power in the ORC system.

Prototype Sensors and Control

In order to determine if our system is working, temperature sensors will be placed before and after the thermal storage tank. Based on the outcome temperatures, modifications to the pump can be made to pull the oil through the tank slower or faster. Changing the flow of the oil will change the amount of time it is exposed or in contact with the PCM capsules. A flow meter will be used directly after the thermal storage tank and will be used with the temperature sensors to find the appropriate speed to successful transfer the correct amount of heat from the oil to the PCM and vice versa. All of these components must have a max temperature range of at least 200 0C. The typical flow in the system will be between 0.01 and 1.0 gallons per minute (gpm) and therefore a flow meter with these characteristics will be used. Finding controls and sensors that can operate at such high temperatures has been a challenge with the remaining budget.

Background

General Investigation

With the human population growing at an exponential rate, energy demands will soon follow. As resources become scarcer it becomes apparent that energy demands cannot rely on fossil fuels. The world needs to simultaneously find ways to efficiently use the remaining fossil fuel deposits and develop renewable resources for future generations to rely on. Strides have been made to relieve ourselves from the grips of fossil fuels by building solar power plants, wind farms, using natural gas, bio mass, and even marketing electric cars. However, these sources are often intermittent in nature. For example solar plants are unable to produce energy at night. This implies a need for some type of energy storage so that plants can maintain consistent operation. Thermal storage stores excess energy while the renewable source is available and provides energy when the conventional energy source is no longer available.

The idea of thermal energy storage is simple and has been around for some time. No matter the method of thermal storage, the cycle is the same. The system is charged with thermal energy, the energy is stored for some time, and finally the energy is released. The earliest units may be dated to the 1890s when people used compressed air, flashing high temperature water into steam, and implementing water or steam storage tanks [1]. The problem with water is that it cannot retain the heat for very long, even in an insulated tank. Also, there is only so much heat the water can absorb. Therefore, if more heat needs to be stored more water is needed which means more space is needed. So by using water as a thermal medium the storage device is constrained in almost every way including space, amount of heat absorbed, and duration.

Phase change materials (PCM), is another common thermal storage medium. As heat is added the material approaches its melting temperature. As the material begins to change phase it is able to store more heat without increasing the temperature, given that the pressure doesn't go up in the enclosure due to the volume change. Additional heat also increases the amount of energy stored even after the melting process is complete [2]. What makes the process so unique is the fact that lots of heat may be stored in a material without much change in the material's temperature. This has benefits in areas where temperature control is critical. Many classes of phase change materials exist including inorganic, organic, and bio-based. The organic class stems from petroleum bi-products which are manufactured by major petrochemical companies [2]. For that reason, their availability could be limited and prices could vary. While these materials may be toxic, flammable and expensive they have a potentially infinite number of life cycles.

The bio-based class contains organic materials that are naturally existing fatty acids such as vegetable oil. These products are non-toxic, non-corrosive and have infinite life cycles. However, they may be expensive and the risk for flammability increases with high temperature [2]. The inorganic class includes salts which are an engineered hydrated salt solution and deemed to be non-toxic, non-flammable and economical [2].

Recently, molten salts have become quite popular amongst the solar industry for its ability to be pumped as a liquid when hot enough and retaining heat for extended periods of time. Some estimate that solar thermal plants can keep running for six hours after the sun goes down [3]. The process is simple as stated before. The salts are melted or charged, stored in an insulated container

and when energy is needed again, pumped through a heat exchanger to warm the working fluid.4 These salts must be heated by an incredible amount before they turn to gas so the potential to store heat dwarfs that of water and also surpasses many oils. However, it still faces some of its own challenges, at least in the solar industry. The main challenge is optimization in this technology.

The problem with using molten salts as of now lies in the process for heating and storing the salts. Halotechnics is currently working on developing salts to store energy from any source of electricity [4]. Rather than building long expensive troughs as the only way to heat the salts, electricity may be used as a supplement which cut capital cost down. Terrafore Technologies is also trying to cut the price on molten salts by redefining how the heat is stored and dissipated all together. They plan on combining multiple materials together, all with different melting temperatures to cut the number of tanks needed, essentially leaving one tank for heat storage and one for the cold salts.3 This would cut the initial capital cost of building a ecofriendly plant such as a solar one, which is always more appealing to investors.

Detailed Investigation

The Figure below compares two types of heat storage sensible and latent. The heat stored in a sensible heat storage method is like its name suggests sensible. Increased energy stored in the medium can be sensed by the increase in that mediums temperature. Eqn.1, energy stored is equal to the mass times the specific heat and the change in temperature, suggests this linear relationship and in the Figure the heat stored has a linear relationship with temperature for the sensible method. However the latent heat storage method uses a medium that undergoes a phase change in the applicable temperature range. Pure substances change phase at a constant temperature in the Figure the distinction can be made by the point where two diverge. Latent heat storage allows for a significant portion of energy to be stored without and change in temperature. This relationship is defined in Eqn.2, where the length of the portion of energy stored without temperature change is proportional to the heat of fusion.

Eqn1. $E_{thermal\,storage} = mc_p\Delta T$

Eqn2. $E_{thermal\,storage} = m \times [c_p\Delta T + h_{heat\,of\,fusion}]$

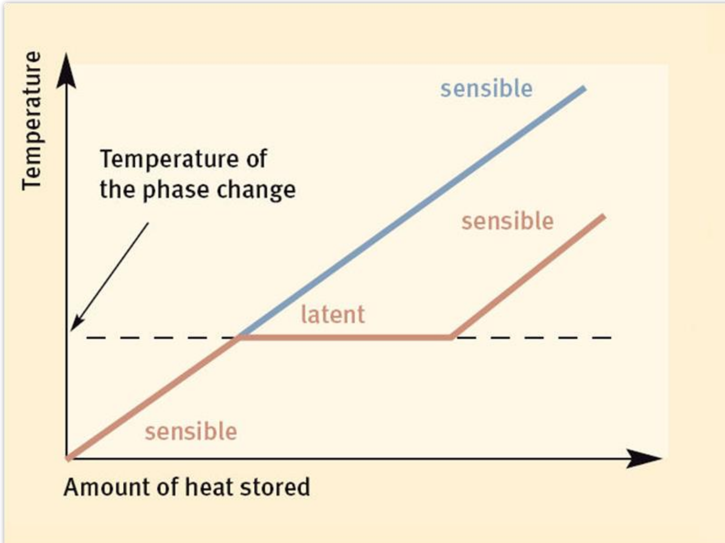

Figure 1 Latent and Sensible Heat Storage

Concept Generation

As mentioned before, the project was flipped on its head after the conclusion of the fall semester. In the fall our design concepts revolved around sensible heat storage while in the spring they focused more heavily on latent. Here is the breakdown of that evolution beginning in the fall.

Fall Semester

1.) Latent Heat Storage Device

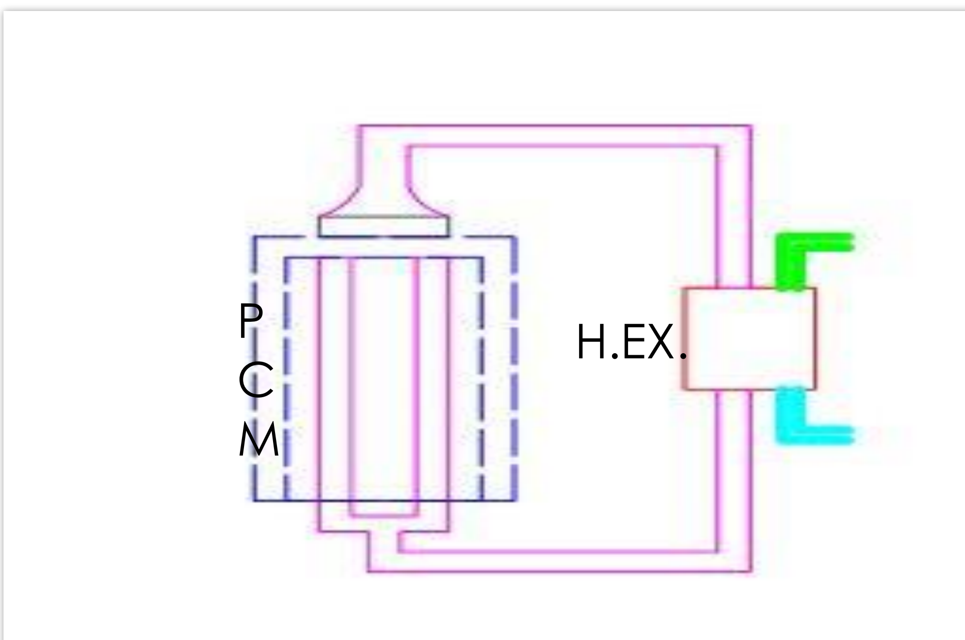

Figure 2 Latent Storage Using built in heat exchanger between air and PCM

The latent heat storage design concept takes excess heat from the heat source in green at the heat exchanger (HEX) using a gaseous working fluid such as air. The air is pushed through the system using a fan. As the air passes through the pipes that run vertically through the phase change material (PCM) the excess heat is stored within the PCM for later use. When the heat source is no longer able to supply the energy needed for operation the air collects the stored heat and delivers it to the ORC. A positive of this design is the decreased need of insulation. For any given amount of energy stored the appropriate PCM will not reach the temperatures that a sensible storage material might. Smaller temperature differentials across the insulation is directly proportional to the heat lost from the storage device. Another positive is the use of a gas as a working fluid, this allows for the implementation of a fan that generally requires less energy to pump through the system thus allowing the customer to increase profit.

<u>Pros</u>:

- Predictable discharge rates
- Higher energy density (J/unit mass)
- Requires less insulation

Negatives of this latent heat design include cost of the phase change material and complexity of the design. Manufacturing & servicing the storage tank alone are prohibitive. To ensure that the heat exchange process between the air and the PCM since. Many PCM's can be highly reactive and potentially corrosive to common metals so careful consideration must be taken for choosing the materials of the piping system. One must also consider the availability of such materials in rural areas. Replacements could not only be costly but time demanding. This design primarily considers A-144 family of organic PCMs that are commercially available. A price comparison of this material to its sensible counterparts is presented later in Table 1 following the description of the sensible heat concept.

<u>Cons</u>:

- Expensive
- Limited temperature range
- PCM reactivity may lead to undesirable maintenance

2.) First Sensible Heat Storage Method

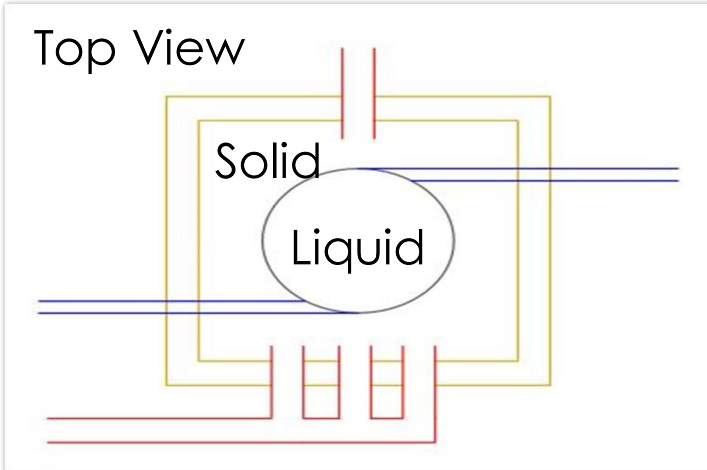

Figure 3 Sensible heat storage schematic using a combination of liquid/solid materials

Our main concern is the storage tank. What is collecting the heat and the ORC cycle itself is not of our concern. Figure 2 provides a simple block diagram for how our tank should work. Heat is gathered from the source and is supplied to the tank at a high temperature. The hot liquid from the source and the liquid from the tank will exchange heat through a heat exchanger. The circulation of the liquid in the tank will enhance convective properties of the liquid which will enhance heat transfer to the pipes within the tank. The liquid in the pipes needs to be heated to either 200oC or 400oC depending on our sponsor's preference, so the more we can enhance heat transfer to the pipes the less piping and tank volume we would need which would mean less money. The heated liquid in the pipes within the tank will then exit the tank and transfer that heat to the ORC's R245a working fluid which will then power the turbine generating 75kWe. After heating the refrigerant in the ORC to about 150oC, the liquid responsible for heating the R245a is recirculated through the tank to begin the process all over again.

Heat transfer to the ORC's R245a does not require a storage tank to lie in-between it and the source. The heat from the source could simply go straight to the ORC heat exchanger, but by doing so poses the risk of shutting down operation as soon as the source heat is cut off. The tank acts as a buffer to maintain a constant temperature output and provide heat even after the source is shutoff. To retain heat for longer periods of time, materials with high heat capacity is needed. The higher the heat capacity, the more energy is required to heat a unit mass of the material by 1 K. On the other side it would take the same amount of energy to lower the temperature of the same unit mass by 1 K which would mean we could have the heat for a longer period of time. A material with a low heat capacity would take less energy to heat it. The faster we can heat up the materials in the tank, the quicker we may reach our goal of 200oC or 400oC. On the other hand, this would mean we would lose heat quickly which would diminish the time we could use it. This gave birth to two of our concepts illustrated in Figure-2 and Figure-3.

The sensible heat storage device displayed in Figure 3 acts as a buffer between the heat source and the ORC. The storage device takes all takes all available heat from the source (red) and delivers a constant output to the ORC (blue) and stores all excess energy for later use. The idea was first conceived with the assumption of the source being an incinerator. The idea was that the hot air waste coming from the incinerator will piped to the tank and that hot gas will conduct heat to the solid material and liquid before it is allowed to exit. The problem with this idea is that gas is a poor conductor, and gas expands so pressure in the tank would need to be regulated and monitored which only adds to the complexity of the system. This led to our second sensible concept illustrated in Figure 4.

3.) Second Sensible Heat Storage Method

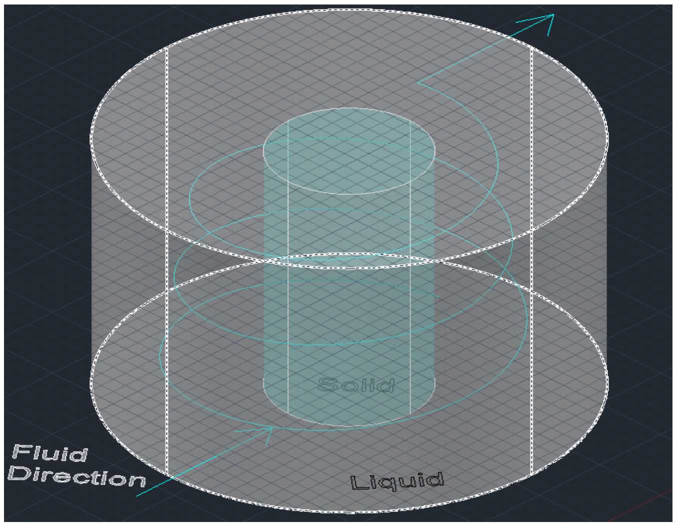

Figure 4 Sensible heat storage concept using a combination of liquid/solid materials

Much like the concept in Figure 2, the concept in Figure 3 also combines solid materials with high heat capacity, with liquids such as mineral oil or molten salt that have a lower heat capacity to get the best of both worlds. The liquid heats quickly first and by conduction transfers part of that heat to the solids in the tank. The liquid is constantly heated by the source until the source energy is depleted or shutoff. Once the source is shutoff, the solids will continue to provide heat to the liquid by conduction for an extended period of time. The cylindrical tower in which the solids lay was by design to create even heat transfer in all directions. The fluid was also made by design to come in from the bottom and leave at the top of the tank because as we all know, heat tends to rise due to buoyancy forces. The max temperature in the tank is therefore most likely to be at the top. By having the fluid travel up the tank, it will continually rise in temperature in a healthy manner rather than being shocked upon entry. Heat will continue to rise until it reaches a max by the time it exists. The hotter the fluid coming out at the exit the better because there will be some heat loss on the way to the ORC's heat exchanger and the closer the fluid is to the heat exchanger the less heat loss we will have. The heat in the tank and the pipes needs to last as long as possible to provide the best performance and therefore proper insulation of this tank is crucial to minimizing any possible kind of heat loss. Some possible materials for insulation are compared in Table-1.

Positives of this design include the relatively low cost of the actual storage materials being considered. Relatively little concern for the thermal expansion of materials since no phase changes take place during operation.

Pros:

- Affordable highly abundant materials
- Wide range of applicable temperatures

Cons:

- Drastically increased weight and space requirements
- Reaches higher temperature therefore requiring more insulation
- May exhibit variations in thermal energy output requiring tighter engineering controls

Thermal Storage Method Selection

Table 1. Concept Decision Matrix

Design	Safety	Cost	Performance		Local Feasibility	Reliability	Environmental Impact	Total Score
			Capacity	Efficiency				
Latent	4	1	5	5	2	2	4	178
Sensible	2	4	3	3	5	4	4	200
Weight	5	10	9	9	8	7	7	

The presented concepts were evaluated in Table 2 using six different points of criterion. Although there are but six, these major metrics encompass several hidden values. The following is a simple definition of the major six metrics. The safety metric was based on any potential danger faced by the operator during regular operation. The cost metric takes into account the price of raw materials and ease in which the particular concept could be manufactured. The performance metric was broken down into the storage material's ability to store the necessary energy capacity, the application versatility of the material, and the ability of the material to deliver energy to the ORC.

The reliability metric is based not only on the probability of mechanical failure of the device but also on the customer's ability to service the device in the event of failure. Unlike other metrics, Local Feasibility and environmental impacts are more straightforward. Local feasibility was based on the ability of customers to obtain replacement materials for the storage device and Environmental impact is indirectly proportional to any damage assumed by environment's exposure to materials present with the storage device.

Material Available Near Birdsville, Australia

Table 2. Materials

Minerals	**Thermal conductivity (W/m*K)**	**Specific Heat (kJ/kg*K)**	**Melting Point (°C)**	**Density (kg/m^3)**	**Extraction/Collection Process**
Sand	0.15-0.20	0.8	1,600	1922	Collected(68,147 miles^2)
Granite	1.7-4.0	0.79	1215	1650	Excavated and crushed
Clay	0.6-2.5	0.92	800	1602	Collected(68,147 miles^2)
Limestone	1.26-1.33	0.908	825	2371	Collected(68,147 miles^2)
Silica (gibber rock)	1.5	0.73	1414	2050	Excavated and crushed
Iron Ore	80.4	0.45	1538	2500	Mined
Nickel	90.9	0.44	1455	8908	Mined
Bauxite	30	2	1650	1281	Mined
Sensible Liquids	**Thermal conductivity (W/m*K)**	**Specific Heat (kJ/kg*K)**	**Temperature Range (°C)**	**Density (kg/m^3)**	**Cost per kg (US$/kWh)**
Mineral oil	0.12	2.6	200-300	770	0.3
Synthetic oil	0.11	2.3	250-350	900	3
Silicone oil	0.1	2.1	300-400	900	5
Nitrate salts	0.57	1.5	250-450	1825	1
Carbonate salts	2	1.8	450-850	2100	2.4
Liquid Sodium	71	1.3	270-530	850	2
Insulators	**Thermal conductivity (W/m*K)**	**Specific Heat (kJ/kg*K)**	**Melting Point (°C)**	**Density (kg/m^3)**	**Cost per ft^2 (US $)**
Glass Cloth	0.126	N/A	450	80	$0.50 (At 4 in thick)[8]
Plain Blanket	0.126	N/A	500	80	$1.16 (At 2 in thick)[9]
Mineral Wool Slab	0.087	N/A	649	64	N/A
Mineral Wool Blanket	0.079	N/A	649	112	$0.62 (At 4 in thick)[8]
Sectional Pipe Insulation (SPI)	0.095	N/A	649	120	N/A
Wire Mesh	0.087	N/A	649	64	N/A
FI 48 Hi-Temp	0.032	N/A	480	48	N/A

Minerals abundantly found in the Outback include granite, sand, limestone, clay, gibber rock or silica, iron ore, nickel, and bauxite. These minerals could all contribute to the heat conduction and insulation needed in successfully storing heat. Not only will they be able to extract the heat from the incoming heat source but they will also be able to store that heat long after the heat source is depleted. Sand, clay, limestone, gibber rock, and granite are all found either on or within a few feet of the earth's surface all over the outback. Birdsville lies in the middle of the Simpson Dessert where these minerals are all extremely abundant. The other minerals are popularly mined in Australia and are readily available for distribution from numerous companies. Insulators will also play an important factor in maintaining a minimal reduction in heat due to losses. The insulators in table 1 were chosen due to their different applicability and they are all candidates for our final design due to their high melting points. The sensible liquids shown in Table 1 are the candidates to be used as the transport medium for the heat within the thermal storage unit, as well as to create a desired temperature gradient within the storage. The liquids of interest come in two types either oils or molten salts; the oils offer a higher heat capacity than the molten salts, but the molten salts offer a higher heat conduction than the oils. Molten salts are used in today's solar power generation systems because they provide efficient, moderate-cost thermal energy storage that is compatible with the high temperatures and pressures of modern steam turbines.

Final Fall Semester Concept

Previously, sensible storage was chosen to be the most applicable form of storage for this particular application. Below in Figure 1 is a schematic of the updated sensible concept. Although sensible storage will reach higher temperatures for the same amount of energy stored thus requiring more insulation, sensible storage was selected over latent storage because of its monetary savings in initial cost but also in consideration of future maintenance costs caused by the corrosive properties of the phase change materials that are used in latent storage. The availability of sensible storage materials also played a large role in this decision. Verdicorp's targeted markets for this device often include isolated areas such Birdsville Australia, located in the Australian outback, so it was a priority that replacement parts & materials should be easily portable or locally available. It was also determined that this was infeasible with phase change materials since no local sources were available in the surrounding area of Queensland Australia.

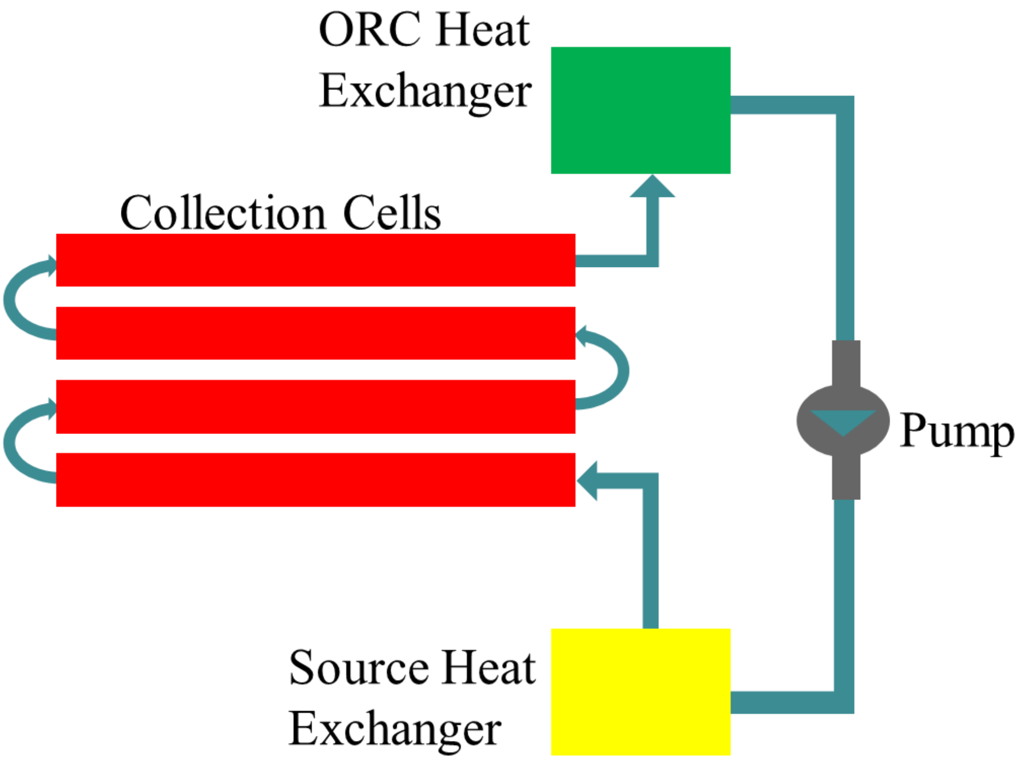

Figure 5. Sensible Heat Storage System Concept

The selected concept in Figure 1 was inspired by a solar parabolic trough heat addition system, the heat transfer fluid passes through blue pipe in Figure 1 gaining waste heat from the heat source in yellow box representing the sources heat exchanger. The heat transfer fluid leaves the source at after reaching a max temperature of 275°C. The fluid then enters a system of collection cells shown in red. There the fluid sheds its excess heat into the four well insulated 25m long cells and drops the temperature of the fluid to an acceptable 200°C before entering the Organic Rankine Cycle heat exchanger. The excess heat is stored in the cells for later use. Flow through the system is controlled by the pump on the right. The flow of heat during the charging cycle is represented by the block diagram in Figure 2.

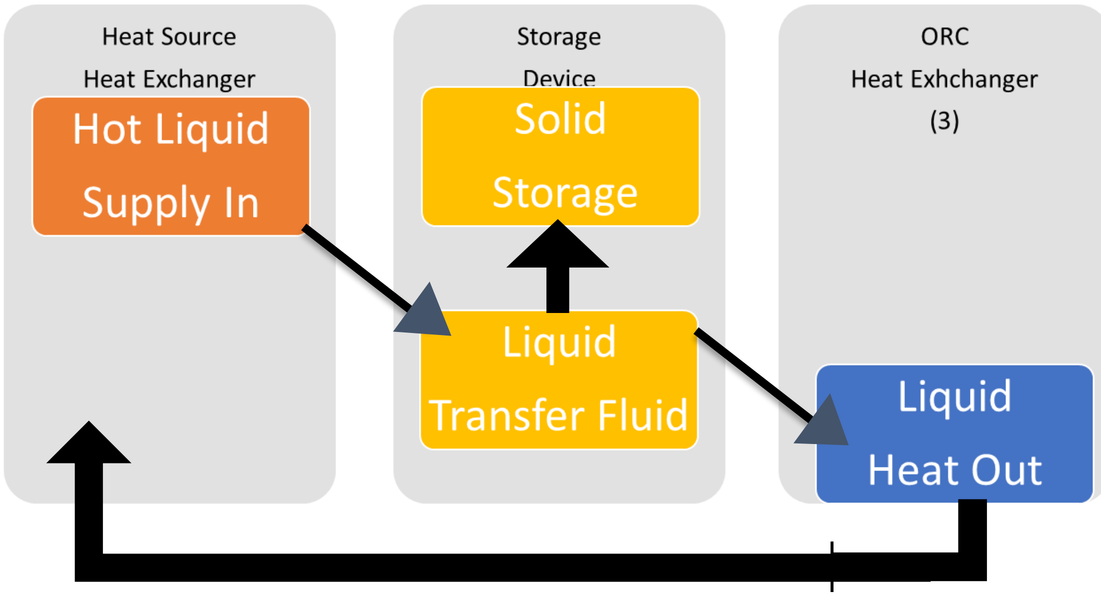

Figure 6 Heat Flow Block Diagram

When the heat source is exhausted, the pump continues to circulate the fluid. The cold fluid enters the cells and gains heat from the excess heat stored earlier that day until reaching 200°C. After choosing the form of storage and concept, the team moved on to solid storage material selection i.e. the materials used in the collection cells. Table 1 below shows the decision matrix used to select the appropriate heat transfer fluid and input output selection.

Temperature Range Selection

Selected temperature output: 200°C

The selected temperature input to the Organic Rankine Cycle (ORC) was chosen to be 200°C. This temperature was chosen because the higher proposed temperatures may have caused part degradation within the ORC. The working fluid of the ORC was designed to vaporize at 150°C so parts were not designed to withstand temperatures in considerable excess to this temperature. Higher operation temperatures also put limitations on liquid storage materials that could be implemented in the thermal storage unit and led us to specifying the maximum inlet temperature of our storage device.

Selected temperature input: 275°C

Increasing the upper limit of the temperature input to the storage unit has significant benefits such as decreasing the amount of material needed for storage, but the drawbacks to increasing this temperature cannot be ignored. Like the output temperature selection the input selection plays a large part in determining the liquids that can be implemented within the storage device. As the temperature is increased the options for heat transfer fluid becomes limited to expensive and often corrosive heat transfer fluids such as liquid sodium. Ultimately, the output temperature was based on the liquid heat transfer fluid medium, Mineral Oil. By setting the upper inlet temperature to 275°C, a temperature well within the operational temperature of the Mineral oil, we were able to safely use the most cost effective liquid available among our list of considered choices. After choosing the liquid we moved on to selection of the solid storage mediums.

Material Selection

Table 3. Liquid Storage materials

Liquids	Cost	Corrosivness	Temperature Range	Thermal Conductivity	Specific Heat	Total
Mineral Oil	5	5	1	1	5	**157**
Synthetic Oil	2	5	2	1	5	**136**
Silicone Oil	1	3	4	1	5	**124**
Nitrate Salts	4	2	2	2	3	**118**
Carbonate Salts	2	1	5	3	3	**123**
Liquid Salts	2	1	3	5	3	**121**
Weight	**10**	**10**	**9**	**8**	**8**	

The heat transfer fluid at least twice the cost of the solid storage materials that will be discussed later. They are also the limiting factor on the range in operation temperatures since they are easily susceptible to degradation from high temperatures. Table 1 shows the basis by which Mineral Oil was chosen. Despite having higher temperature application ranges the salts corrosive abilities under minded the reliability of the system. The salts also came with higher costs. What set Mineral Oil apart from the other oils was its relatively inexpensive it was. Cost analysis placed Mineral Oil at $0.30 per kg while its closest competitor was over three times the price at $1.00 per kg. Having chosen the heat transfer fluid the temperature range during system operation could be determined.

Table 4. Solid Storage Materials

Sensible Minerals	Cost	Thermal Cycling	Thermal Conductivity	Specific Heat	Environmental Friendliness	Volume	Total
Granite	4	2	2	3	4	2	**124**
Clay	1	1	1	4	4	2	**87**
Limestone	5	2	1	4	4	3	**137**
Iron Ore	3	3	5	2	2	3	**128**
Nickel	1	5	5	2	3	5	**134**
Bauxite	4	5	4	5	4	1	**174**
concrete	5	3	1	4	4	3	**144**
Weight	**10**	**7**	**8**	**8**	**6**	**3**	

Table 2 is comparison of several solids that were found to be readily available in Birdsville. This means that all of these solids are either excavated in the Queensland area or easily transportable to the area. Based on our criteria presented in Table 2 above, we have selected bauxite and concrete. Certain secondary costs will be considered in later evaluation but the material abundance of bauxite and its desirable thermal characteristics have placed this material as the front runner, while the low cost of concrete and its ability to be easily formed into complex geometries makes it a close second. To avoid the incursion of secondary costs in producing complex shapes with the raw bauxite it was decided that the two materials would be used in conjunction with one another. The two solid materials are shown side by side in Figure 3. In the Brick Design section of this report, the specifics of how the solids will be combined will be presented.

Figure 7 Raw Bauxite & Concrete Structure

Brick Design

As shown in the material selection section of the report, it was decided that bauxite and concrete will be used in conjunction with one another to avoid the extra cost of creating complex shapes of bauxite alone. Compared to other mined minerals found deep in the Earth's crust like diamond, bauxite ores are usually found a little under Earth's surface as solid rocks and are sold in the form of pellets with a diameter close to an inch. Concrete should serve as the matrix to hold bauxite pellets together since it is easily formed. Many questions now remain as to how the two will be combined.

Although concrete is easily formed it is also very brittle. Cracks tend to occur frequently under the right conditions. Because the working fluid will be under some amount of pressure and high temperature, the fear is that cracks will form and repairs will become frequent. The overall collection cells will be approximately 25m in length and so having one solid piece of concrete wouldn't make any sense from a maintenance standpoint. In an effort to reduce maintenance costs and downtime, it was decided to design bricks of concrete that would connect together along the length of the cell as well as around the circumference of the cell. Therefore, in the event of a crack somewhere along the pipe, rather than replacing the entire collection cell only a few bricks would be replaced saving time and money.

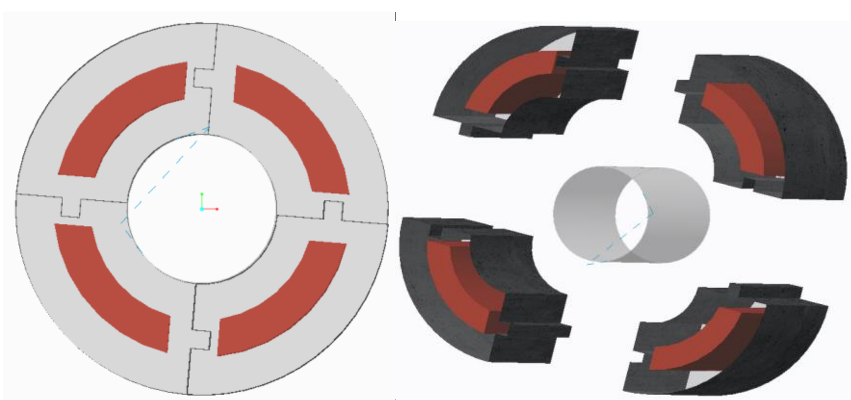

Figure 8 Solid Material Storage Bricks composed of Bauxite & Concrete

Figure 4 depicts a proposed brick design. The red shown in the figure symbolizes bauxite while the surrounding gray symbolizes concrete. The inner circle where the working fluid is projected to flow is designed to be 8 inches in diameter while the outer circle is approximately 2 meters in diameter. Bauxite has great conductivity and specific heat compared to other solids so the idea of concentrating that heat is quite appealing. However, this design has its flaws. Because the bauxite is in the form of pellets it needs to be contained. Having the bauxite sandwiched between two layers of concrete poses the threat of impeding heat transfer to the bauxite since concrete has relatively low conductivity. The charging time would take much longer compared to the bauxite coming into direct contact with the working fluid which may cause problems on days where charging time is limited. However, for those days where there is a long period of heat supply, it would be better to have this resistance layer to slow the heat transfer process because if the rate was too high and there wasn't proper temperature and valve control, the rocks could get dangerously hot, changing the properties of the material or worse, causing rapid degradation of the working fluid. Perhaps an alternative to having the bauxite concentrated in the middle of the concrete brick would be to disperse it throughout the entire brick. In the process of mixing the cement, the bauxite pellets could be used as an aggregate to the cement solution which would ultimately lead to a brick with the conductivity between that of concrete and bauxite. This is something that has not been done before to anyone's knowledge and so the properties and benefits of such concrete cannot be theorized and would need physical experimentation. It could, however, be the answer to a more thermally conductive concrete that the world is looking for.

The right of Figure 4 exploits the bricks geometry and how they would all come together. The idea came from Lego blocks where one shape can make a museum of designs. By having one shape be the basis of the entire pipe, manufacturability and assembly of the system becomes much faster. The faster it goes up, the faster it can make money. One mold would be all that's needed and because its only cement, no real technical knowledge is needed to complete the mold. Remember this type of system would be implemented in rural third world areas. The ability to hire locals to create these molds is a major commercial selling point for many reasons. For one, the area is more welcoming of your product because it aids in creating jobs which is beneficial to the immediate economy of that area and the overall well-being of the locals. For two, Verdicorp wins because they won't have to pay these workers as much allowing them to hire more to get the job done faster. So you see there is a win-win for both parties. One flaw in this design is that the bricks would need to be connected in the axial direction which poses a maintenance problem after completion. Say for example a crack was found in a brick which happens to lie in the middle of the collector cell. There would need to be a more complex process for replacing that brick rather than simply plugging a new brick in that spot and moving on. There would need to be enough clearance space to allow room for a new brick to slide into the empty slot. The bricks themselves would also need to be light enough for removal by hand using one to two workers.

Overall, the materials make sense to choose for testing. The question is how will they perform together as a unit? To better the chances of success it was decided to test the two different configurations previously discussed. One as shown in Figure 4 where the bauxite is concentrated in the middle of the brick and the other with the bauxite dispersed throughout the entire brick. The results will be compared with the conclusion of testing.

Analysis

Energy Requirements

A Major requirement of any energy storage device is that it be capable of storing the energy required of it. Taking the sum of energy added to storage from Table 4 in the Appendix provided by Verdicorp and multiplying it by the duration of time by which this rate of energy was added It was found that this device should be capable of storing up to 860GJ of energy. To evaluate whether or not our design was capable of storing this energy without reaching temperatures in excess of 200^{o}C Eqn.3 was used. Where the excess energy stored was equal to difference between the amount stored and the amount required for storage.

Eqn. 3 $E_{excess} = E_{Stored} - E_{Required}$

Eqn. 4 $E_{Stroed} = m_{Bauxite} C_{pB} \Delta T + m_{concrete} C_{pC} \Delta T$

Eqn. 4 was defined as the amount stored energy stored in the Concrete and Bauxite combination. Energy stored is a solid sensible material is defined as the mass of that material times the specific heat of that material multiplied by its change in temperature. The change in temperature was from 23^{o}C to 200^{o}C. The upper temperature was set to 200^{o}C to prevent the fluid from reaching temperatures in excess of 200^{o}C when the charging cycle ended. Analysis found that our design yielded 200MJ in excess energy that could be lost to the environment.

Major Dimensions

The dimensions of solid portions of the collection cells were found based on the need to have enough mass to hold the required energy and have a thermal resistance low enough to dissipate the heat even when the heat added to the storage is at its highest rate to insure that the heat transfer fluid does not reach the Organic Rankine Cycle above the correct temperature. The inner pipe was set to be 0.2 meters in diameter and the subsequent layers of concrete, bauxite and concrete to be 0.3m, 1.6m, and 0.1m thick respectively. The overall resistance was modeled as the equivalent resistance of convection and conduction and assumed perfect contact. Sample Calculations can be found in the appendix. To reduce requirements on the thermal resistance, the heat transfer process was complimented by the systems pump system which is capable of controlling the exposure time between the heat transfer fluid and solid storage materials.

Cost Analysis

The cost of the raw storage materials including the heat transfer fluid were calculated and presented in Table 3. These calculations were based on bauxite costing $016/kg, Concrete $0.18/kg, and Mineral Oil for $0.3/kg. Further optimization is expected to lower the initial cost and thus allow to surpass our goal of $0.23/kWh. The energy used to calculate these values was taken as the energy stored per cycle time the number of cycles.

Table 5. Raw Material Cost Estimation

Storage Mediums	Initial Cost	Cost per Cycle	9yr Life Cycle Cost
Cost	$830,000	$0.29/kWh	$1e^{-4}/kWh

Scaled Prototype

The scaled prototype will be 1/25 the scale of the full scale solution. This means that each of the four collection cells will be 1 meter in length and of thickness 16cm. the pump will also be sized accordingly. All other flow parameters such as non-dimensional Reynolds and Nusselt numbers will be maintained as close as possible to validate our concept. The heat source will be modeled by an electric resistance heater and the success will be measured by the ability of the prototype to produce a consistent outlet temperature. This will be gauged by placing a thermocouple at a point where the flow leaves the collection cells. Another thermocouple will be placed at the inlet to the cells and flow of the heat transfer fluid will be changed accordingly by adjusting the pump.

Spring Semester

As mentioned previously, at the end of the fall semester our sponsor urged us to explore latent heat storage and select a system, including materials that would best work with the patented PCM capsules he wanted to use. These capsules would be approximately 2 inches in diameter and would contain salt of our choice to act as a heat storage medium through phase change. The greatest advantage of these capsules is that they are vacuumed sealed, meaning no pressure buildup during phase change while still offering sufficient surface area for heat transfer to take place. Knowing that these tubes would need to fit into a larger tank, our research led to shell and tube heat exchangers. These heat exchangers are incredibly common in industry as they are a highly effective method to transfer heat. There are many different designs to a shell and tube heat exchanger but they all behave the same way. One fluid flows through tubes while the other flows around the tubes. The fluid flowing around the tubes is dictated by baffles, which also help support the smaller tubes and damp vibration of those tubes. We explored a number of these baffle designs but focused on namely two, as seen below.

1.)

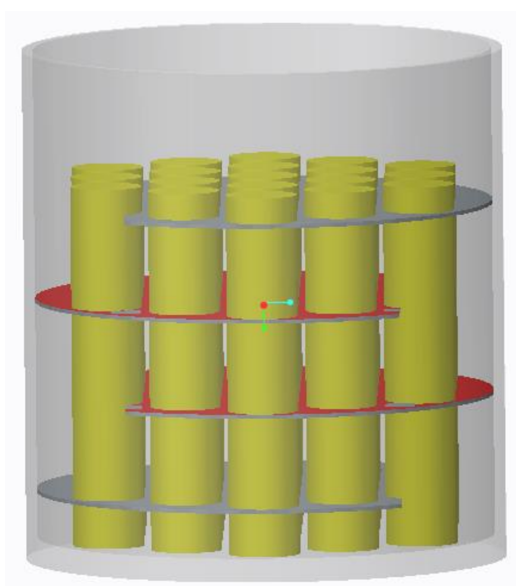

Figure 9 Single Segmental Baffle Concept

In this baffle configuration the fluid would flow in from one side of the tank and would zig-zag either up or down to the other side depending on where the inlet is placed. This concept limits fluids flow in the longitudinal direction and focuses the fluid flow in the lateral direction. This forces the outside (or shell side) fluid to pass each tube in a more erratic manner which increases the turbulence of the fluid and therefore increase the heat transfer. Baffles are identical and are merely rotated 180o from baffle to baffle. The fact that they are identical means simpler manufacturing because they robot would be programmed to cut the same shape multiple times. However, with increased heat transfer comes the price of pressure drop. The pressure drop could be battled by reconfiguring the tube layout to a square patter rather than a triangular patter (explained later) but this would hurt heat transfer.

2.)

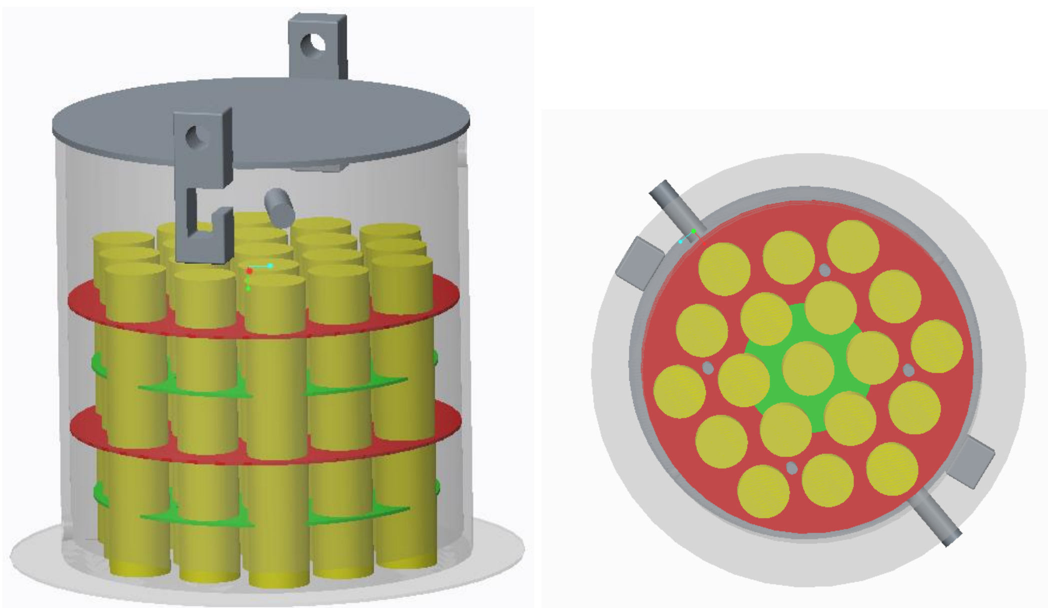

Figure 10 Disc and Doughnut Concept

In this concept the shell side fluid would enter the tank from the bottom and be forced to alternate between the tank wall and tank center. The circular pattern here ensures a more symmetrical fluid flow which can be a major advantage. In the heat transfer realm, it is imperative that the tank be uniform in temperature otherwise unwanted temperature gradients would be introduced leading to unpredictable, or undesirable results. This concept also carries the advantage of lower pressure drop which would lower overall pump requirements and ultimately cost. However, again with lower pressure drop leads to lower heat transfer. The fluid in this case travels more parallel with the length of the tubes which creates a more laminar type of flow meaning less effective heat transfer.

Concept Decision Matrix

Single Segmental Configuration		**Disk and Doughnut Configuration**	
Pros	**Cons**	**Pros**	**Cons**
Easy to manufacture	Higher pressure drop	Lower pressure drop	Harder to assemble
Proven and used extensively	Not ideal in high vibration situations	Better symmetrical flow	Heat transfer suffers due to less cross flow
Great heat transfer	Likely to produce dead zones if not careful resulting in increased fouling	Great for high vibration	Fouling is a greater concern for this type

Material Selection

	Product	Melting Temp.	Volume Expansion	Longevity	Corrosiveness	Cost	Total
Salts	Dynalene MS-1	4	5	5	5	3	**200**
	Dynalene MS-2	5	4	5	4	2	**182**
	50%NaOH-50%KOH	2	4	1	3	5	**141**
	Product	**Max Temp.**	**Volume Expansion**	**Longevity**	**Corrosiveness**	**Cost**	**Total**
Heat Transfer Oils	Duratherm HF	5	3	5	5	5	**212**
	ExxonMobil Synthetic	4	2	3	3	5	**159**
	Paratherm	5	3	4	4	2	**165**
Weight		**10**	**9**	**8**	**9**	**10**	

Final Design

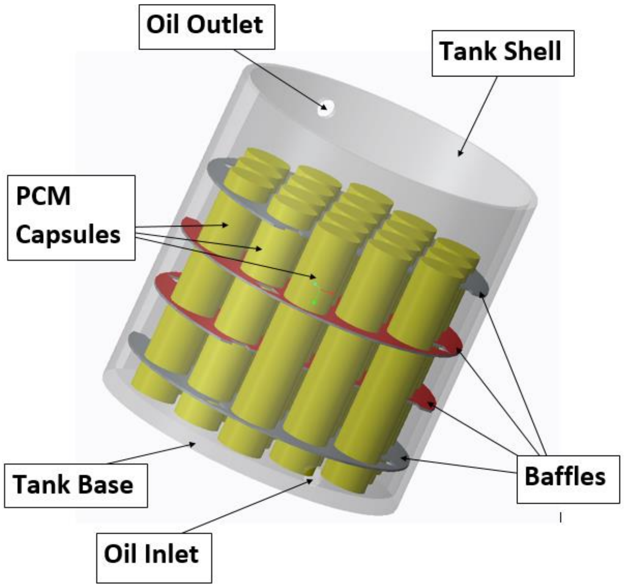

Figure 11 Final Chosen Design CAD

The PCM material will be contained in approximately 2" ID (inner diameter) & a 2.375" OD (outer diameter) cylindrical tubes about 1ft tall placed throughout the tank with baffles incorporated to allow the tank to act as a shell and tube heat exchanger. Shell and tube heat exchangers are often employed in industry in part for their serviceability but also because they maximize surface area while minimizing floor space which ultimately saves money. The idea is simple, one fluid flows through the tubes while another flows around the tubes in a direction dictated by baffles. Heat transfers from one fluid to the other by modes of conduction and convection. However, when it comes to actually designing the system it becomes quite complex as there are many variables to consider, each of which directly impacts strength of heat transfer, serviceability, and pump requirements. Examples of these variables include tube configuration, baffle cuts, and baffle spacing.

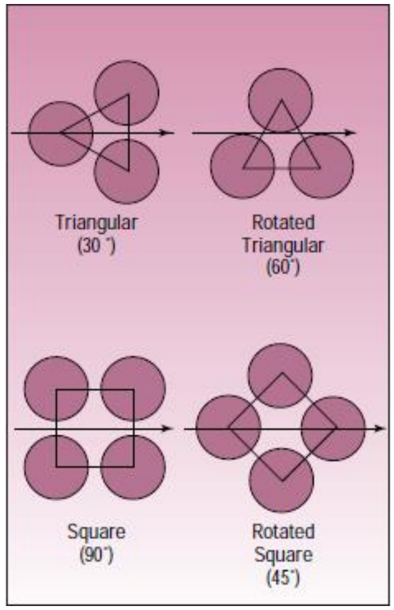

Figure 12: Pipe Configuration

Tube configuration is the most important when it comes to strength of heat transfer and serviceability. There are generally four types of configurations as seen in Figure 2. Keep in mind the space between each tube is dictated by the tube pitch. The tube pitch for triangular geometry is 1.25 times the OD of the tube while for square geometry it is 1.25 times the OD or the OD plus 6 mm, whichever is closer [5].

It should be noted that in Figure 2, the black arrow depicts fluid flow. According to this fluid flow, the triangular pattern offers the highest amount of turbulence and therefore the highest heat transfer coefficient. Not only that, but it also accommodates the greatest amount of tubes within a given space compared to the square pattern due to its geometry, which reduces space required which reduces capital cost. However, the downfall with the triangular geometry is that it is not easily serviceable due to the reduction of space between each tube. Square configurations are necessary when cleaning and serviceability is a major concern. The rotated square layout is used when Re<2000 to help increase turbulence and therefore heat transfer [5] Because of limited serviceability, triangular pattern is limited to applications where there is expected to be clean shell side operation or an operation that can employ chemicals to do the cleaning. As for the rotated triangular configuration, it does not offer as high a heat transfer coefficient as normal triangular and still possess the same problem when it comes to serviceability so therefore rarely employed.

For our application in particular, the shell side fluid will be the Duratherm HF heat transfer oil. The main concern when using oil as far as serviceability is the buildup of sludge. However, oil sludge can be treated with a variety of chemicals without the need of manual labor the same way it is treated in an automobile engine. After consideration of the pros and cons of each configuration and the materials of our design, it was decided that the triangular configuration would suit our needs best. It offers the best heat transfer coefficient, the smallest footprint, and manageable serviceability considering oil sludge can be treated with chemicals. For the sake of comparison, we will also test the rotated square configuration and compare charging/discharging times, space required, and exit temperatures. The expectation is that the exit temperature for the triangular configuration will be higher than that of the square layout because the triangular layout offers a higher heat transfer coefficient. Now with a deeper understanding of how the fluid will interact with the tubes, it is now necessary to develop how the oil will flow through the entire tank. Fluid direction is dictated by the use of baffles, how they are cut, and how they are spaced. Baffles are vital in shell and tube design because the allow fluid to flow across tubes rather than parallel which increased heat transfer coefficient and cuts the length of the system down which reduces costs. Baffles are also important for supporting tubes so they don't sag and also to minimize vibrations induced on the tubes which become increasingly important as fluid velocity is increased. Figure 3 showcases examples of baffle cuts and spacing to demonstrate what works and what doesn't work.

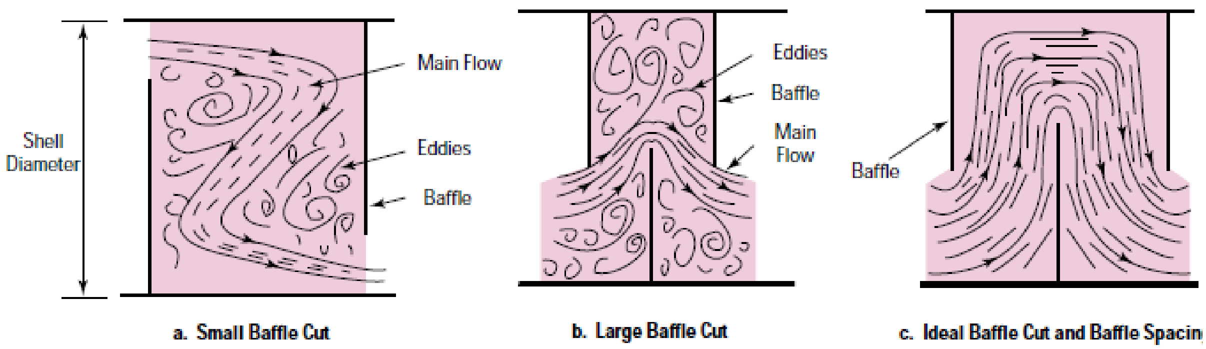

Figure 13: Examples of projected fluid flow for various baffle cuts and spacing.

As seen in Figure 3, pushing for small baffle cuts may increase heat transfer coefficient but will result in poor fluid distribution. The same may be said for having baffle cuts too big in an attempt to decrease pressure drop. The objective is seen in Figure 3(c). The more fluid moves, the better the overall heat transfer. The formation of eddies will lead to a less than satisfactory system with a lower efficiency than expected. Also having a disproportionate cut will lead to repeated acceleration and deceleration of fluid flow which is not as effective as constant motion in terms of pressure drop to heat transfer. It is recommended the baffle cuts are between 20% and 35% of the shell inside diameter [5]. We will employ a 30% to push for a balance of pressure reduction without sacrificing much heat transfer loss.

As far as baffle spacing, the Tubular Exchanger Manufacture's Association (TEMA) sets the minimum spacing to be a fifth of the shell inside diameter or 2 in, whichever is bigger [5]. Setting the spacing too small leads to more difficult cleaning and poor fluid distribution while spacing too large will lead to primarily parallel fluid flow which is less effective at transferring heat than cross flow. It is shown in a study that as baffle spacing is reduced, the pressure drop increases more rapidly than does the heat transfer coefficient. The optimum spacing is 30% to 60% of the shell inside diameter. We will employ a 40% spacing to balance pressure drop and heat transfer. In summary, our prototype will stand vertically with cylindrical PCM capsules oriented in a triangular patter for one test and a square pattern for a separate test with baffles cut to 30% of the shell inside diameter.

Flow Properties

An analysis of the flow and heat transfer properties of the two chosen design concepts was conducted in order to further understand the impact of baffle geometry on fluid behavior and select the optimal design for prototyping. In order to properly analyze and differentiate between the two designs the major differences in geometry must be accounted for, but there are some parameters that are similar to both designs. Eqn.5-12 are geometric quantities that are due to the triangular arrangement of the capsules or tubes and are equivalent for both configurations. The equations are for tube pitch, clearance between tubes, distance between the tube and the storage tank wall, uniaxial area between tubes, tube hydraulic diameter, tube surface area, cross flow area between tubes, and the free flow area outside the tubes, respectively. These equations are all functions of the tube diameter which remains constant for both designs and take into account factors such as baffle spacing, number of tubes at each section, and the shell inner diameter. By implementing these geometric equations the vertical and horizontal fluid profiles that are apparent in both configurations can be properly accounted for.

Eqn.5 $$tube_P = 1.25 * tube_D$$

Eqn.6 $$tube_C = tube_P - tube_D$$

Eqn.7 $$tube_W = \frac{shell_{ID} - 4 * tube_P + tube_D}{2}$$

Eqn.8 $$tube_{UA} = \sqrt{3} * \frac{{tube_P}^2}{4} - \frac{\pi}{8} * {tube_D}^2$$

Eqn.9 $$tube_{DH} = 4 * \frac{tube_{UA}}{\pi * {tube_D}^2}$$

Eqn.10 $$tube_{SA} = \pi * tube_D * baffle_H * N_{tubes}$$

Eqn.11 $$area_{CF} = (tube_C * (N_{tubes} - 1) + 2 * tube_W) * baffle_H$$

Eqn.12 $$area_{FF} = (tube_P * (N_{tubes} - 1) + 2 * tube_W + tube_D) * baffle_H$$

For configuration 1, the segmented baffle design, the flow properties were calculated at 12 sections across each of the 5 levels of the storage tank for a total of 60 points of interest. The inlet pipe was assumed to be perpendicular with the side of the tank, and the fluid direction to be parallel to the tank floor. In this design the majority of the fluid direction is assumed to be flowing horizontally and acting normal to the surface of the PCM capsules. The fluid direction changes at the baffle cut area where all of the flow is assumed to be flowing vertically along the capsules. Eqn.13 and Eqn.14 account for this vertical flow behavior at the baffle cut, which are the baffle entry area and baffle hydraulic diameter, respectively.

Eqn.13 $$baffle_{EA} = 0.2 * shell_{ID} * (2 * (tube_P + tube_W) + tube_D)$$

Eqn.14 $$baffle_{DH} = \frac{2 * baffle_{EA}}{0.2 * shell_{ID} + (2 * (tube_P + tube_W) + tube_D)}$$

For configuration 2, the disc and donut baffle design, the computations were done in a similar manner as configuration 1, with 12 sections per level of the storage tank where the fluid parameters are computed. The difference is the inlet flow is assumed to be entering through the center of the tank from the bottom, and the majority of the fluid direction is assumed to be flowing vertically along the capsule's length for all sections and across each level. In the disc and donut design, the annular area between the tubes and tank wall of the disc baffle is where the fluid flows vertically is also the same area as the center of the donut where the fluid also flows vertically. The diameter of the circular flow duct in the donut is 0.1524m and the flow area is computed with the use of Eqn.15. Although the flow area is the same for the disc and the donut baffles the characteristic length and/or hydraulic diameter of the baffles are different. The hydraulic diameter used for the disc is derived from the general relation of multiplying 4 times the flow area divided by the flow perimeter this is seen in Eqn.16, while the hydraulic diameter for the donut is the hydraulic diameter of the tubes previously seen in Eqn.9.

Eqn.15 $$baffle_{DD} = \pi * \frac{(0.1524)^2}{4} - 4 * \pi * \frac{tube_D{}^2}{4}$$

Eqn.16 $$baffle_{HD} = 4 * \frac{baffle_{DD}}{\pi * 0.3429}$$

The process for computing the flow properties at each section for both configurations involved first to find the inlet conditions of the storage tank. The heat input was assumed to be 4500W and at a temperature difference of 217°C from ambient. The mass flow rate, fluid velocity, Reynold's number, and Prandlt number was calculated using these assumptions and with the use of Eqn.17-20.

Eqn.17 $$\dot{m} = \frac{Q_{in}}{C_P * \Delta T}$$

Eqn.18 $$V = \frac{\dot{m}}{\rho * Area}$$

Eqn.19 $$Re = \frac{\rho * V * D}{\mu}$$

Eqn.20 $$Pr = \frac{\mu * C_P}{K}$$

Depending if the inlet flow was laminar or turbulent, according to the Reynold's number, the friction factor of the inlet pipe was found using Eqn.21-22 for laminar and turbulent flow, respectively, as well as the Nusselt's number, which is constant at 4.36 for laminar flow or found using Eqn.23 for a smooth pipe with turbulent flow.

Eqn.21 $$Fr_L = \frac{64}{Re}$$

Eqn.22 $$Fr_T = (0.79 * \ln Re - 1.64)^{-2}$$

Eqn.23 $$Nu_{T,SP} = 0.125 * Fr_T * Re * Pr^{\frac{1}{3}}$$

Once the inlet fluid properties were computed these were used as the initial conditions entering the tank and the same analysis process was used at each of the 12 sections at every level of the storage tank. The inlet mass flow rate was assumed to remain constant through-out all 60 sections of the tank, but the remaining parameters do change across each level. The Nusselt's number at each section would change due to geometry, Eqn.23 is a relation for square ducts as well as generic circular pipes and was used to compute the parameter for free flow outside the tubes and Eqn. 24 is the relation for flow over a cylinder and was used for the cross flow in between tubes.

Eqn.24 $$Nu_{T,RD} = 0.023 * Re^{0.8} * Pr^{0.3}$$

Eqn.25 $$Nu_{CYL} = 0.3 + \frac{0.62 * Re^{\frac{1}{2}} * Pr^{\frac{1}{3}}}{[1 + (\frac{0.4}{Pr})^{\frac{2}{3}}]^{\frac{1}{4}}} [1 + (\frac{Re}{282{,}000})^{\frac{5}{8}}]^{\frac{4}{5}}$$

After the velocity, Reynold's number, and Nusselt's number was calculated at each point of interest across the entire storage tank, the heat transfer coefficient is also computed at each section using these obtained values. Eqn.25 is the equation used to compute the heat transfer coefficient and involves the thermal conductivity, Nusselt's number and characteristic diameter or length. The length used for configuration 1 was the hydraulic diameter due to the free flow area around the tubes and assumed to be a rectangular duct, this diameter changes at each section due to geometry. In configuration 2, the hydraulic diameter had more variation, but was the same for the cross flow sections under the baffles, away from the baffle cut areas or vertical flow areas. The diameter used for the disc was the actual diameter of the disc which was found to be 0.3429m, the diameter for the donut flow area was assumed to be the tube hydraulic diameter which was previously stated.

Eqn.26 $$H = \frac{Nu*K}{D}$$

The computations of the Reynold's number for configuration 1 and 2 are depicted in Fig.14 and Fig.15, respectively. The resulting computations show that although the Reynold's number for each configuration are within the same range, configuration 1 has a higher frequency of turbulent flow across each level of the storage tank, while at the baffle cuts the Reynold's number drops significantly. This drop in value would suggest a laminar flow through the baffle cut area and less likely to cause vibrations in the baffle frame while the flow transitions from level to level.

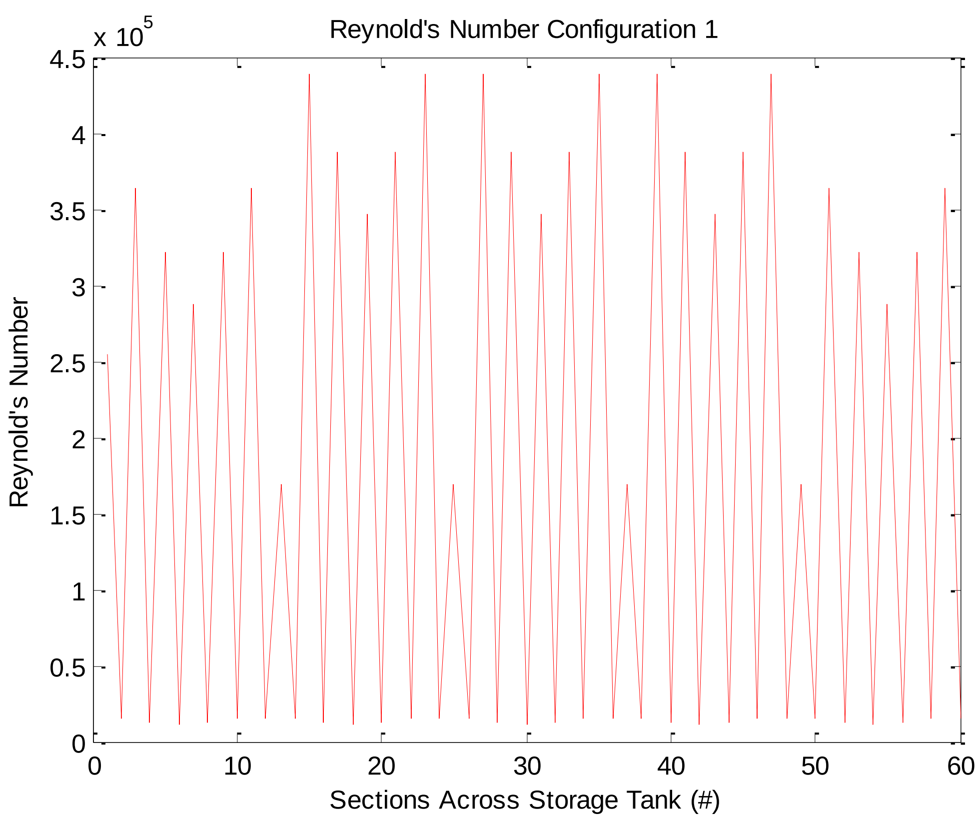

Figure 14 Variation of Reynold's number for Configuration 1

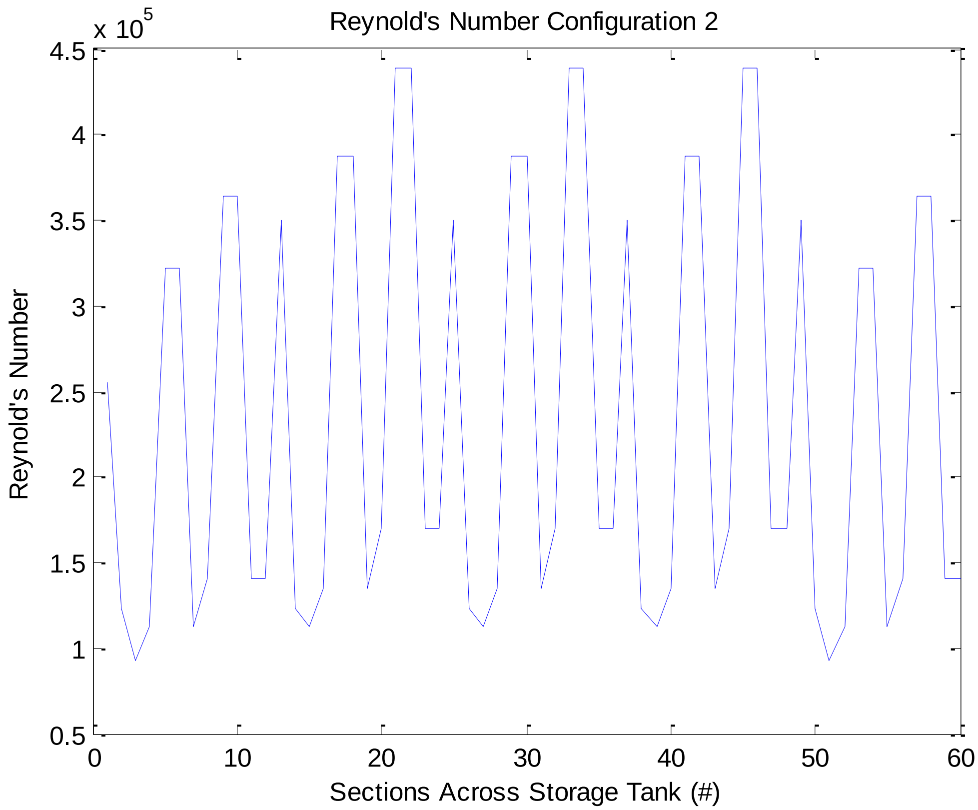

Figure 15 Variation of Reynold's number for Configuration 2

With these values of Reynold's number the Nusselt's number is also expected to have a similar trend with each configuration as well. Fig.16 and Fig.17 depict the Nusselt's number computations across the entire storage tank for configuration 1 and 2, respectively. As expected, configuration 1 has a larger range of values, but has a higher frequency of variation per level than configuration 2. It can be assumed that overall configuration 2 would have a higher heat transfer rate due to the findings of the Nusselt's number, but the configuration must be suitable for both charging and discharging of the storage tank. According to the findings it seems that configuration 1 has a more balanced baffle configuration for both charging and discharging. The MATLAB code used to develop this analysis can be found in the Appendix.

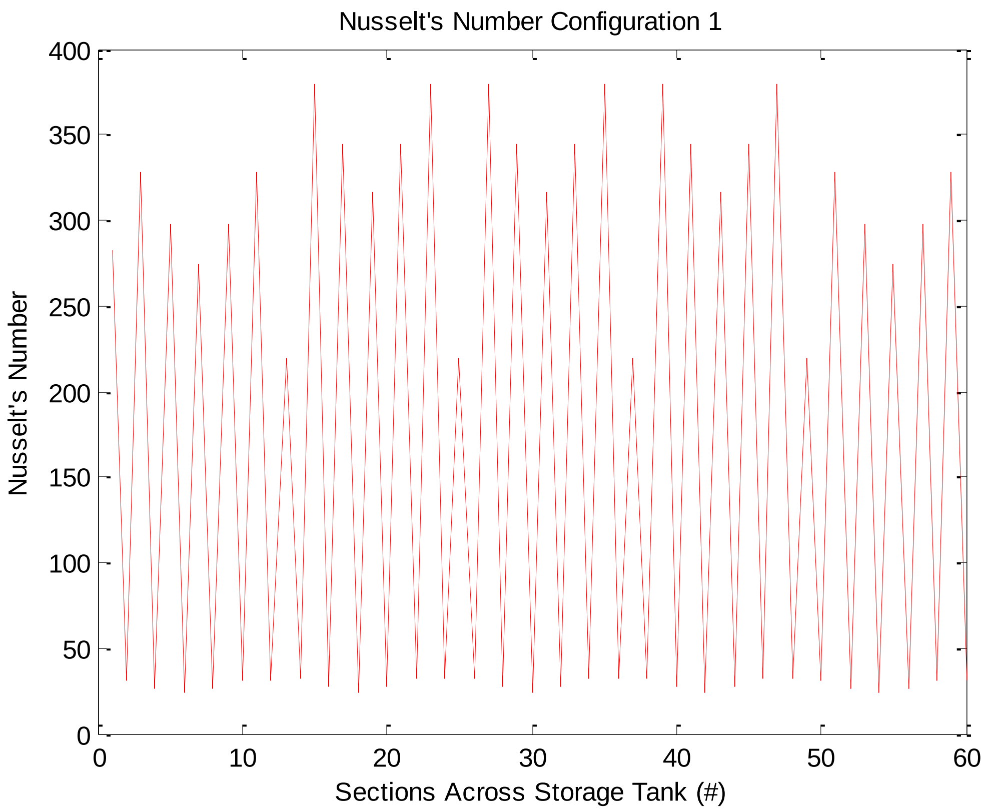

Figure 16 Variation of Nusselt's number for Configuration 1

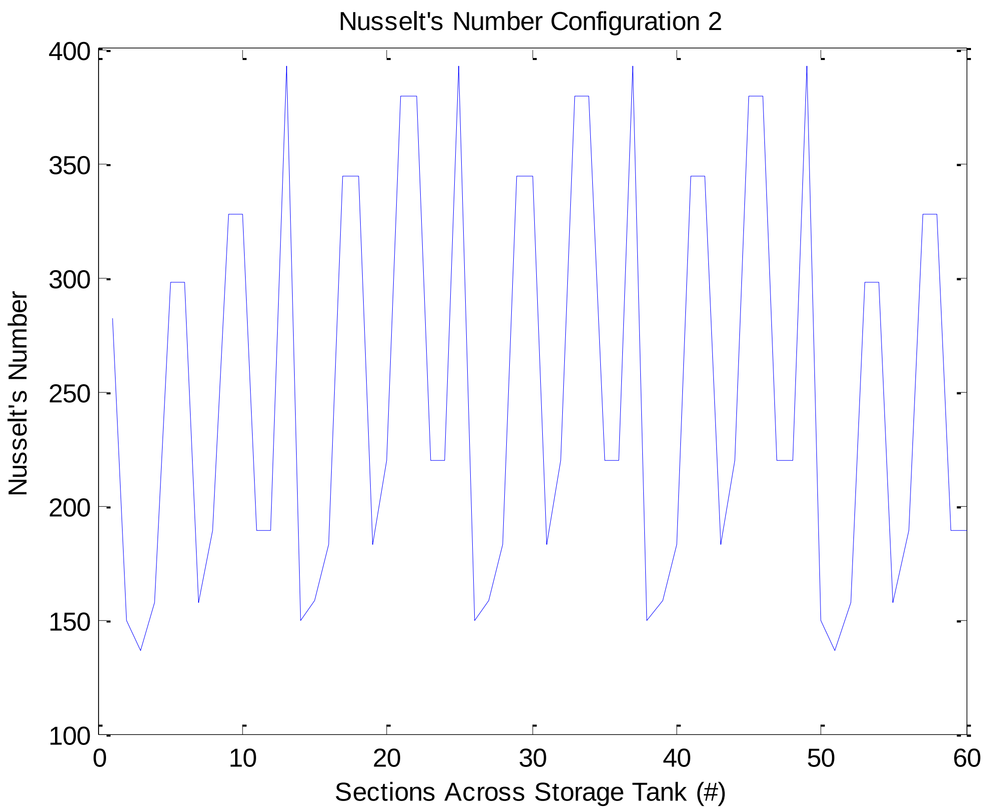

Figure 17 Variation of Nusselt's number for Configuration 2

Thermal Simulation

A simulation of the final design was used to predict the behavior of the system. This simulation was broken down into two parts a charging cycle and a discharging cycle. The following are the assumptions made and their major results with respect to both parts:

Charging Assumptions

- Input Duratherm HF Temperature of 240^{o}C
- Dynalene MS-1 PCM Thermal Resistance modeled as conduction through liquid phase
- Dynalene MS-1 melting Temperature of 225^{o}C
- Efficiency Taken as the amount of energy added to storage over the energy available for storage (which is the energy dissipated from Duratherm HF after a temp drop from 240^{o}C-170^{o}C
- Losses were estimated to be 205W based on tank being held at a temp of 240^{o}C in ambient room temperature conditions
- Flow rate: 0.27GPM
- All capsule area in between baffles were exposed to the same surrounding temperature

Charging Results

- Fully charged in 2 hours and 15mins
- Outlet temperature of the thermal storage approaches melting temperature of Dynalene MS-1 225^{o}C
- Average efficiency of 70 % based on the amount of energy stored to the amount of excess energy available for storage
-

Discharge Assumptions

- Flow rate or less: 0.27GPM
- Full Energy Stored: 9600 kJ
- Useful Energy Stored or energy above 170^{o}C: 4953.89 kJ
- Full Load of 2274W (70^{o}C drop)

Discharge Results

- Ratio of useful to Full: 0.58
- Operation Time on Full Load of 2274W (70^{o}C drop): 34 minutes
- Pressure drop (testing system): 7Pa

Simulation Methods

The method used to determine these results took into account the transient nature of this project complex heat transfer. A major factor in the complexity of analyzing the concept design stemmed from it transient attributes with regards to heat transfer. The first step in our analysis was to determine the major components of heat transfer resistance. Identifying these components would allow us to determine where the design could be optimized. Equations 1-3 were used to compute the resistances of the convection from Duratherm HF to the capsule wall, the conduction through the 304 Steel wall, and the conduction through the Dynalene MS-1 PCM material. The thermal circuit formed can be found in Figure. The results of this analysis were plotted in Figure, which clearly shows that the largest resistance is found in convective portion of the resistance. One of design goals was now to minimize these effects.

In order to narrow down the actual operation point in terms of flow rate another calculation was run to find the necessary flow rate to achieve the desired temperature drop across the PCM storage tank.

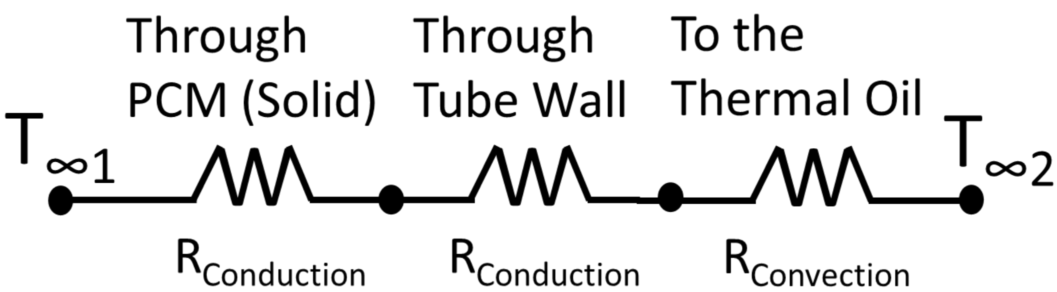

Figure 18 Thermal Resistance Network from Capsule origin (left) to surrounding fluid(right)

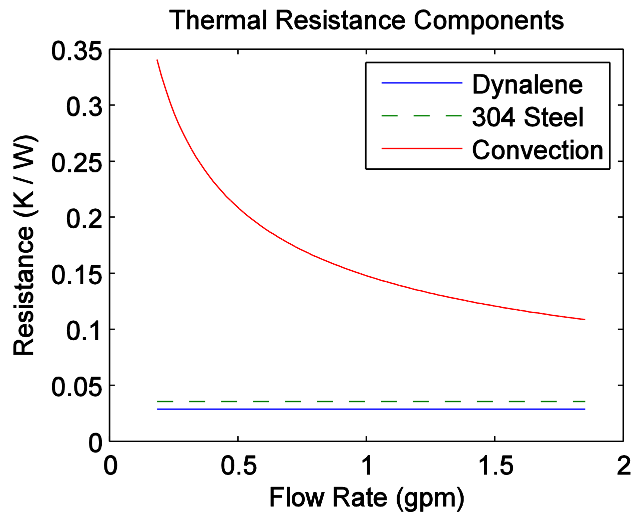

Figure 19 Breakdown of system Capsule Resistance

Unlike conventional shell and tube heat exchangers the fluid moving through the shell side of the exchanger was not exchanging heat with a fluid at some constant inlet condition temperature. Instead the tube side, which in this case is the PCM material was stationary within the tube and therefore the temperature difference from the shell side from to the tube would change with time and at an infinite amount of time the temperature difference would approach zero. To find an applicable range of flow rates the temperature drop across as a function of the capsule's internal temperature was graphed against the flow rate in Figure. It was found that the flow rate should be maintained at or below 0.27gpm to achieve any significant temperature drop. After determining a flow rate a full simulation could now be run.

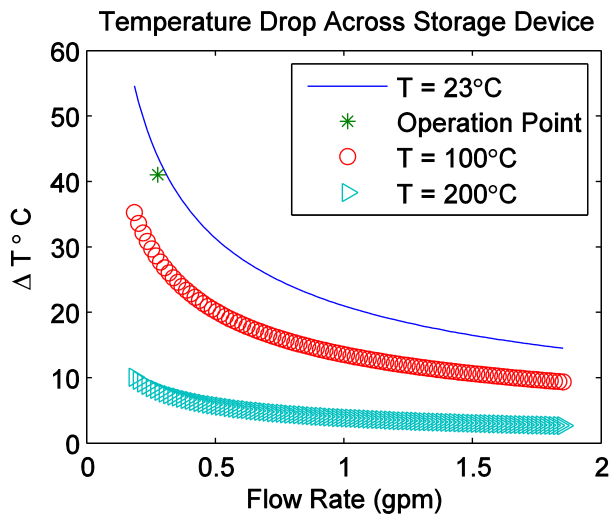

Figure 20Temperature Drop across Storage Tank

The full simulation broke down the tank into four discrete levels that were divided by the baffles. Each level was 3.05 inches in height and spanned the diameter of the tank, 15.75 inches. The transfer fluid flowing through each level was assumed to have the same bulk temperatures. Meaning that every capsule on that level was assumed to be exposed to the same surrounding temperature and said to melt at the same time. The amount of heat transfer from Duratherm to the Dynalene storage medium was found using Equation. This equation was a slight modification of the general heat transfer equation to include transient considerations for the capsule's temperature. Temperature at the origin of the capsules were found using Equation from Cengal, that solves the two dimensional heat transfer equation for short cylinders, Equation. Solving this equation for the temperature at the origin, and all other spatial coordinates, of the capsule allowed us to calculated the amount of heat transfer and determine the heat transferred and as a result the bulk temperature of the Duratherm leaving one level and entering another. Then the process was repeated for every level until reaching the output temperature of the tank. Finally the total amount of energy stored was added to the sum of energy stored. Data from the simulation was recorded at 15 minute intervals.

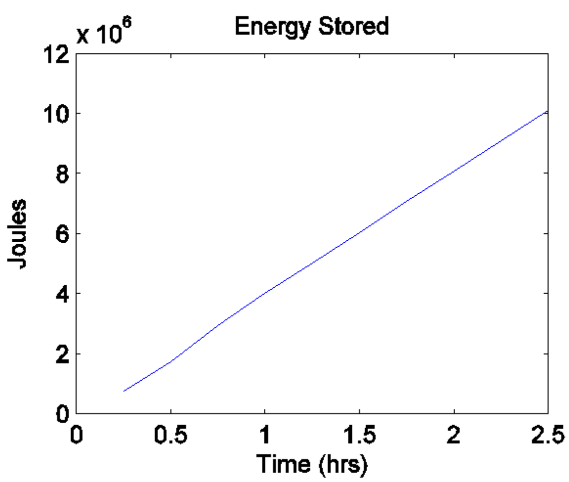

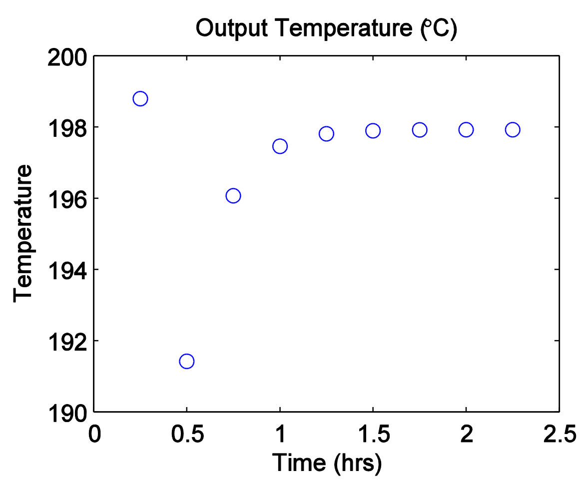

The results of this simulation showed that the thermal storage tank was fully charged in 2 hours and 15 minutes assuming that the inlet temperature of the tank was maintained at 240 degrees Celsius. The output temperature settled around 200 degrees Celsius . The efficiency was also calculated using the ratio of heat added to storage versus the heat available for storage, or the energy required to cool the Duratherm temperature from 240 degrees Celsius to 170 degrees Celsius.

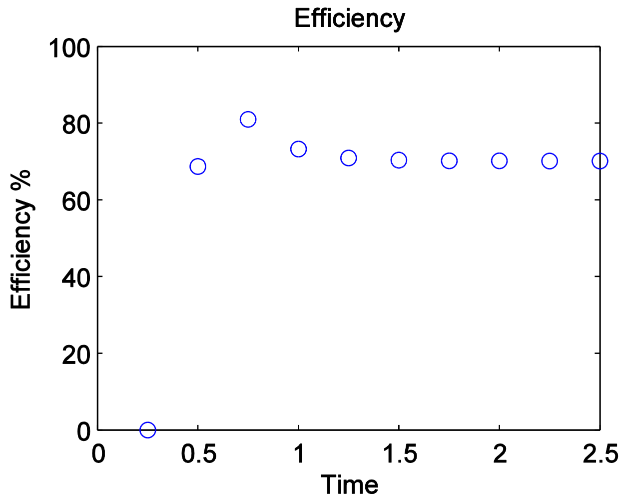

The amount of time that it takes for the storage tank to fully discharge its useful thermal energy was found by using Equation. The full load was taken to be 2274W and the useful energy stored, or the heat energy that is above 170 degrees Celsius to be 54313 KJ of energy. The losses from the system were taken to be 205W to the environment. It was found that the tank would be fully expended of useful energy in 34mins. This means that over 58% energy stored could actually be used to power the load and that this energy could only be used for a fraction of the time that it took to store that energy.

Eqn.27 $$t = useful\ energy/(Losses + Load)$$

Design for Manufacturing

Once all of the parts were sourced and ordered we were able to begin manufacturing the baffles. Using the water jet machine provided by the College of Engineering, we cut 19 holes in an aluminum sheet and then cut out the outer diameter of the circle. The baffle cut was then made making the baffles a semi-circle which will allow for the desired flow of the oil. When the salt arrived, Verdicorp began creating the phase change material (PCM) capsules. This process is patented and little details were given but, in summary the salt was poured into a steel cylindrical pipe, heated to an extremely high temperature, cooled, and solidified. This process was repeated multiple times for each PCM capsule. The baffle frame was created using four threaded rods and were spaced 3.05” apart. The tank was then constructed by welding the base to the bottom of the large cylindrical pipe shown in Figure – 1. It was then water tested to ensure no oil will leak out during the testing and operation processes. Inlet and outlet holes were drilled and threadolets were welded to the outside of those holes. Plugs were inserted into the threadolets to protect the holes from any damage until the system was ready for complete assembly. A top was manufactured by welding an aluminum ring, with a diameter slightly smaller than the inner diameter of the tank, to the base of a circular plate. A scrap piece of smooth metal was shaped into a half of a square and then welded to the top, opposite the side of the aluminum ring, as a handle. The next two components of the project were manufactured simultaneously. The heat source was constructed by using a 6” diameter circular pipe with a cap welded on one side. The inlet and outlet holes were drilled in the same manner as the tank and the threadolets were welded to both of the holes. The top cap was created by cutting 4 holes in it equally spaced apart one for the thermocouple and three for the heat cartridges to be

Figure 21Tank with baffles frame installed inserted into. Since the heat cartridges need to be protected from the oil a thin metal alloy tube was inserted into the holes and welded to the cap within the heat source. The wires for all four components inserted into the heater cap will all stick out for easy wire connection and assembly. Two brackets were welded to the side of the heat source for easy mounting to the 80/20 frame shown in Figure – 2.

At the same time the load that represents the ORC was being constructed using a car heat exchanger and two small fans. The housing was constructed using a wall track material donated by Lowes. The piping and fin car heat exchanger was inserted into the housing and secured. An aluminum sheet was used to mount the fans onto the housing. Two holes the size of the fan were cut out of that aluminum sheet in order to

Figure 22 Heat Source

allow air flow over the fin and piping heat exchanger. Figure – 3 shows an aluminum sheet with the fans attached being secured to the heat exchanger housing.

Figure 24 Heat Load Representing ORC

The pump was assembled and mounted to a thick sheet of metal for stability and easy mounting shown in the right side of Figure – 1. Once all of the components were assembled individually they were all mounted on a vertical frame of 80/20 material on wheels. The heat exchanger load was mounted to the top of the frame to avoid blowing hot air directly at whoever is testing the system. A base sheet of aluminum was mounted to the frame to provide a surface for the pump and tank to be attached to. The heat source was mounted vertically in the center of the 80/20 frame and piping was used to connect all of the components. Insulation was added to the tank, heat source, and piping to prevent unnecessary heat loss in the system.

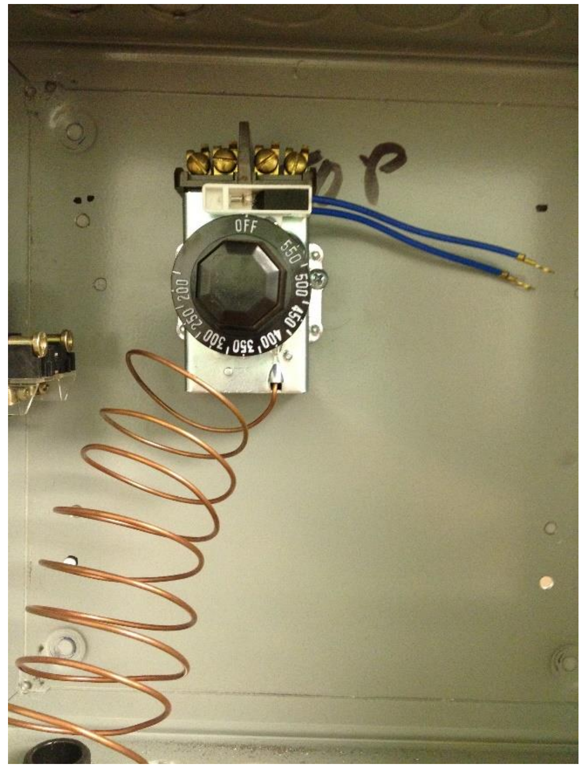

Figure 25. Switch within control box

A switch, shown in Figure – 4, was connected in series with the heat cartridges to provide a way to prevent overheating. This switch was mounted in a control box to protect it from the heat provided to the rest of the system. The flowmeter was placed right after the pump before the heat source. Thermocouples were used to display the temperatures directly before and after the thermal storage tank. These temperature displays will show if the system is successfully storing the heat within the PCM capsules and if that heat is being transferred sufficiently.

The overall assembly went quite smoothly and ended up taking less time than expected. We set aside two weeks for construction and it took just over a week to complete. The most difficult part of the assembly was being able to visualize where all the components would fit on the 80/20 frame and how the piping would be oriented.

When considering the overall setup of the system and the project scope we were able to eliminate any extra components during the design phase. The incorporation of a reheat system and a cold storage tank in to our hot storage tank would make our simple system much more advanced and a better demonstration of Verdicorp's project goals.

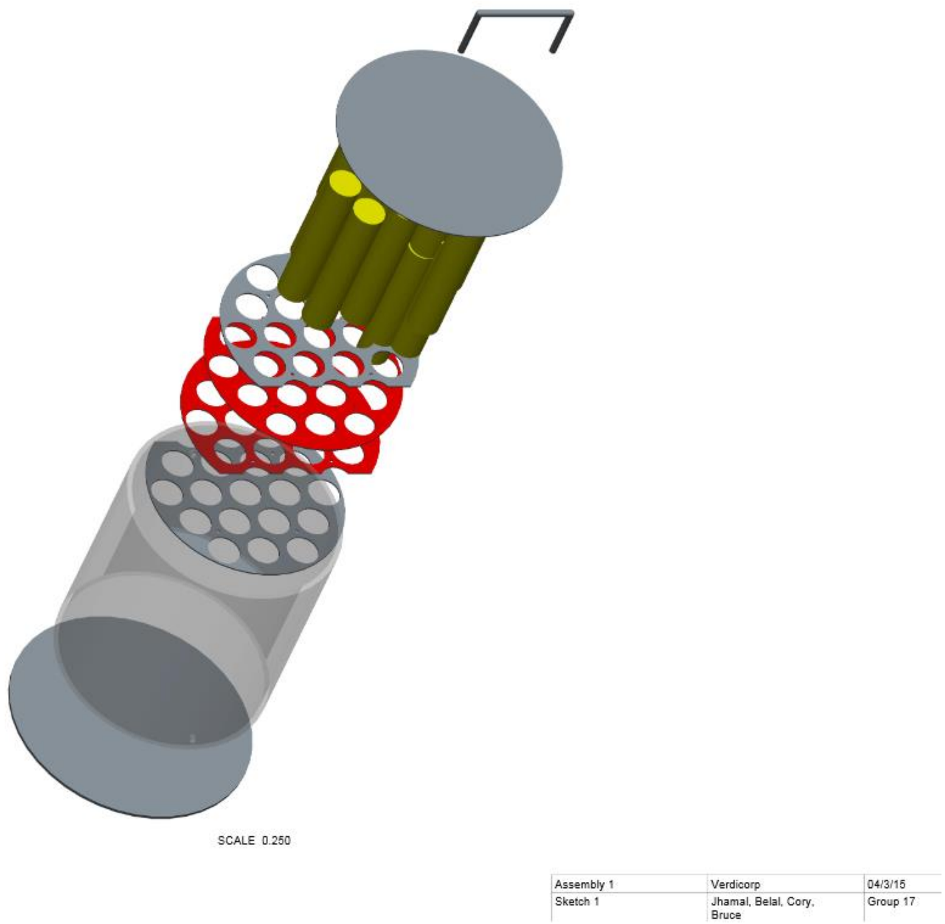

Figure 26. Exploded View of thermal storage tank

Electrical Wiring

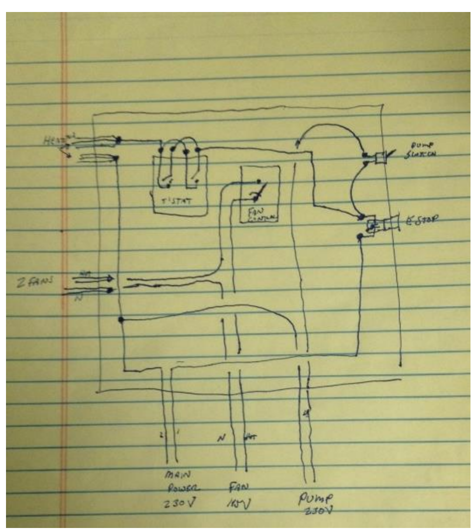

Figure 27 Electrical Wiring Schematic

Design for Reliability

The main use of the prototype is to be used as a test rig for Verdicorp to experiment with different PCM salts as well as different capsule/baffle configurations on a small scale. The prototype will also be used as a portable model to demonstrate the PCM capsule technology to possible future customers.

With this in mind, the prototype is not meant to be an actual small scale operating thermal storage system, it is meant more to collect data under monitored use, and not to be left unattended as the large scale version would operate. The controls on the prototype are completely analog and must be monitored during use to prevent over-heating of the heat cartridges and possibly burning the working fluid. The mass flow rate must be regulated manually over the operating cycle of the prototype to simulate the controls of the full-scale device. Apart from these concerns with the controls, the prototype is designed very robust for its application.

The prototype is expected to run for multiple data gathering cycles before a maintenance must be conducted. The baffles and capsules will have to be cleaned due to fouling of the working fluid, depositing residue onto any component that is in contact with the oil. The copper piping system will also have to be flushed and possibly brushed for the same reasons. After each operating cycle it is recommended to check the interior of the tank for any anomalies, such as misalignment of the baffle frame and ruptures in the PCM capsules. The fittings and valves should be tightened after every ten cycles of operation, as well as the bolts holding down the pump and tank due to high vibration loading onto the frame. An FMEA table is depicted in Figure-7 which illustrates all major possible modes of failure.

In order to increase the reliability of the prototype a mechatronic system should be implemented with the use of the thermal sensors to control the mass flow rate, pressure, and heat input into the system. These controls would make the system safer and make data collection easier for the operating technician.

FMEA (FAILURE MODE AND EFFECTS ANALYSIS)

Failure Modes Effects Analysis

Team #:	17
Project Title	Verdicorp's Thermal Storage Solution for Continuous ORC

Key Process Step or Input	Potential Failure Mode	Potential Failure Effects	SEV	Potential Causes	OCC	Current Controls	DET	RPN	Actions Recommended	Resp.	Actions Taken	SEV	OCC	DET	RPN
What is the Process Step or Input?	In what ways can the Process Step or Input fail?	What is the impact on the Key Output Variables once it fails (customer or internal requirements)?	How **Severe** is the effect to the customer?	What causes the Key Input to go wrong?	How **often** does cause or FM **occur**?	What are the existing **controls** and procedures that prevent either the Cause or the Failure Mode?	How well can you **detect** the Cause or the Failure Mode?		What are the actions for reducing the occurrence of the cause, or improving detection?	Who is Responsible for the recommended action?	Note the actions taken. Include dates of completion.				
Pump	Rust, metallic flakes, and/or debris entering pump.	Pump malfunction will lead to a loss of pressure through the system.	8	Lack of proper grinding/cleaning of tank and piping components.	2	All components in contact with flow must be cleaned of debris.	5	80	Flush system with distilled water or motor oil without pump.	Assembly Technician.	Grinding of rust/debris, throughly vaccumed.	8	2	5	80
Heat Source	Heat cartridges over-heating and failing.	No heat input into working fluid.	8	Improper use of controls and/or lack of monitoring of system.	6	Temperature dial and thermal sensors.	4	192	Monitoring system thermocouples and thermometers.	Operation Technician.	Limit electrical input into heat cartridges through thermostat.	8	6	4	192
Thermal Storage Tank	Working fluid leaking from top and through welds.	Irregular flow, loss of pressure, loss of working fluid.	6	Improper attachment and securement of tank lid, incomplete	3	Lid secures under it's own weight.	3	54	Leak test storage tank, force close storage tank lid to top.	Assembly Technician.	Place locking mechanism onto lid.	6	3	3	54
Baffles	Misalignment and/or movement of baffle assembly.	Unstable flow in tank, improper heat transfer to PCM capsules.	5	Improper securement of baffle assembly, opration pressures higher than recommended.	4	Baffle assembly secured under its own weight and weight of PCM capsules.	7	140	Force close baffle frame between top and bottom of tank.	Assembly Technician.	Elongate baffle assembly links to lock it into place.	5	4	7	140
PCM Capsules	Rupture of capsules due to thermal expansion.	Contamination of PCM salt, corrosion of all components in contact with working fluid.	10	Improper securement of caps onto capsules, overfilling capsules with salts.	3	Testing individual capsules in convection oven before put into assembly.	8	240	Conduct multiple thermal loading tests on individual capsules before assembly and testing.	Operation Technician.	Reduce amount of salt in capsules if necessary.	10	3	8	240
Load	Melting of electrical wiring and/or major components of fans.	Power and control loss of load fans.	6	Mounting low heat resistance components near high temperature components.	3	Thermocouple monitoring.	5	90	Zip-tie wiring and/or relocate low temperature resistant components away from heat sources.	Assembly Technician.	Relocate delicate components away from heat sources.	6	3	5	90
Piping	Leaks and/or ruptures.	Loss of working fluid, melting of wiring and other components, safety hazard.	8	Improperly tightened valves and fittings, higher pressures in system than recommended.	3	Teflon tape applied to all valves and fittings.	3	72	Test piping pressures without heat inputs.	Assembly Technician.	Test piping with water at high pressures at ambient temperatures	8	3	3	72
Assembly Frame	Disassembly of major components.	Pipe ruptures/leaks, disconnection of wiring, loss of materials.	9	Vibration loading, loose bolts and hardware, improper weight distribution on frame.	5	Check tigthening on all bolts, balance weight loads on frame.	3	135	Placement of damping materials under pump and storage tank.	Assembly Technician.	Test pump at high pressures using water and without piping and wiring assembled.	9	5	3	135

Figure 28 Failure Analysis Chart

Design for Economics

Our project revolves around creating a commercially viable thermal energy system for Verdicorp. The system would be placed in Birdsville, Australia to provide extended power to about 300 people. The scale of the project therefore is massive. After relentless research on the subject of thermal energy storage using phase change material, we have determined that 6,121 PCM capsules will be needed for the full scale model. These capsules would fit in a cylindrical aluminum tank 18ft in diameter, 22ft tall, and 1 inch thick. The materials alone to fill the tank with PCM salt and heat transfer oil would cost an upwards of $3.7 million, including the empty tank and capsules themselves. However that doesn't include cost of pump, flowmeter, piping, fittings, and everything else involved with the system. Let's not forget the cost of physically constructing the system. As one can infer, the bill for this project increases rapidly very early on.

The prototype on the other hand was relatively inexpensive and gives a great approximation for what to expect on the full model. To this point, the group has spent $1,442.41 of the $2,000 budget as seen in Figure-9. This includes all simulation, planning, purchasing, and physically building the system. Keep in mind Verdicorp creates Organic Rankine Cycle systems in their warehouse so they have an array of scrap metal and parts we were able to implement into our model, saving the team quite a bit of money. Sheet metal for the baffles, the pump, and heat source are all examples of things we were able to salvage out of there junk pile. They also have many thermocouples throughout the building and were able to use those in our system as well. The heat load was purchased by Verdicorp under a separate account and was therefore not included in the team's budget. Individual components and their cost may be seen in Figure-8.

After researching and discussing this project with advisors and sponsors, the team is not aware of anyone implementing a system such as this. There are systems that use PCM capsules, but they are contained in small spheres rather than large cylinders. Cost estimates for those kind of systems are incredibly hard to find. The best comparison the team could make is to compare the cost of our prototype and services to one of a professional consulting company. Ultimately what we provided to Verdicorp is a simulation of what to expect with the constraints given and building a physical system to prove those theories. We did all that for less than $1,500. Verdicorp could have went with PCM Thermal Solutions, a consulting company based out of the Chicago area, to provide them with advice and direction on their project, but it would have cost them $3,000. This only includes a simulation and advice for future work. The $3,000 figure does not include a physical system to back up their theories. Figure-xxx brilliantly compares the group's bill to that of PCM Thermal Solutions. The team essentially saved Verdicorp $1,500 providing the same services and also building the physical model on top of that.

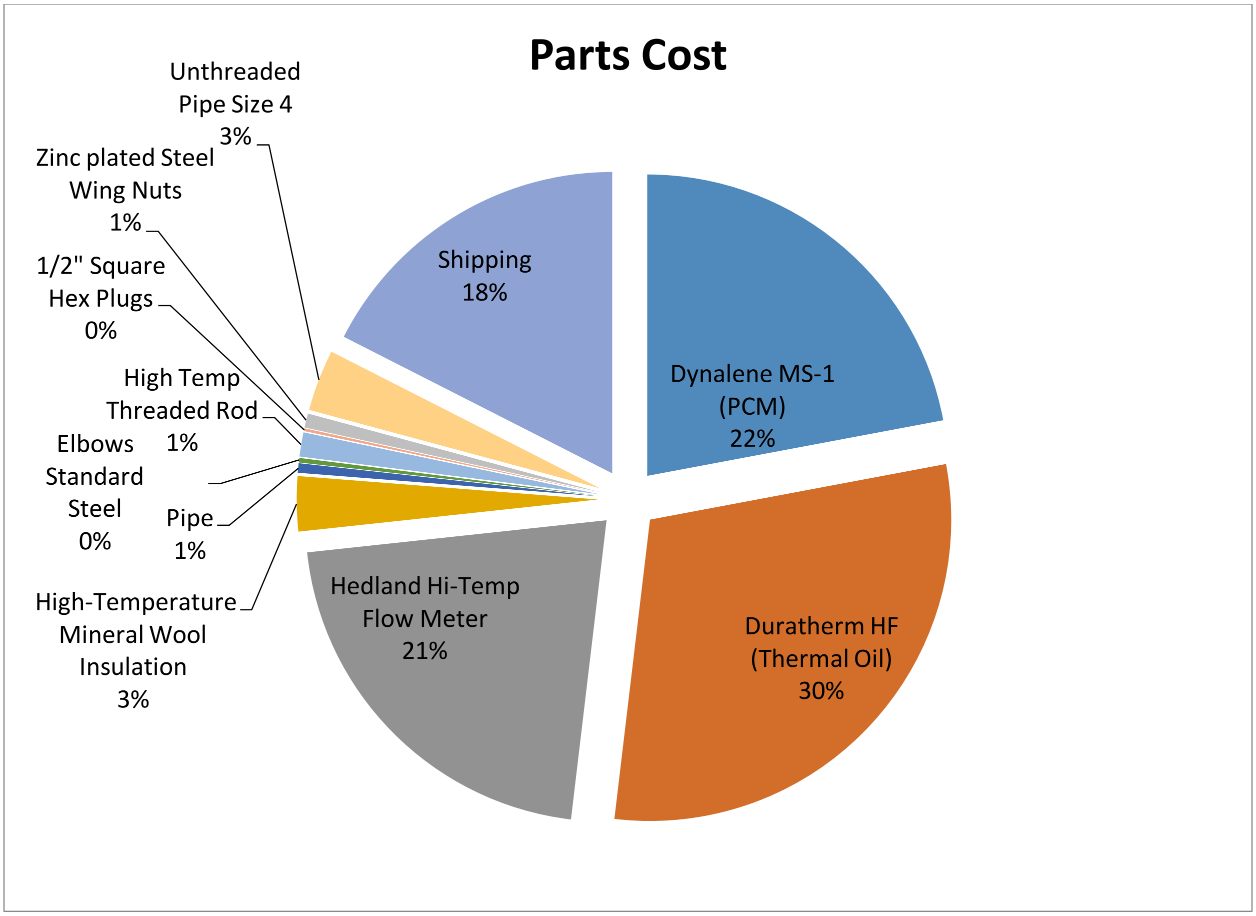

Figure 29 Budget Breakdown

BUDGET GRAPH AND STATEMENT

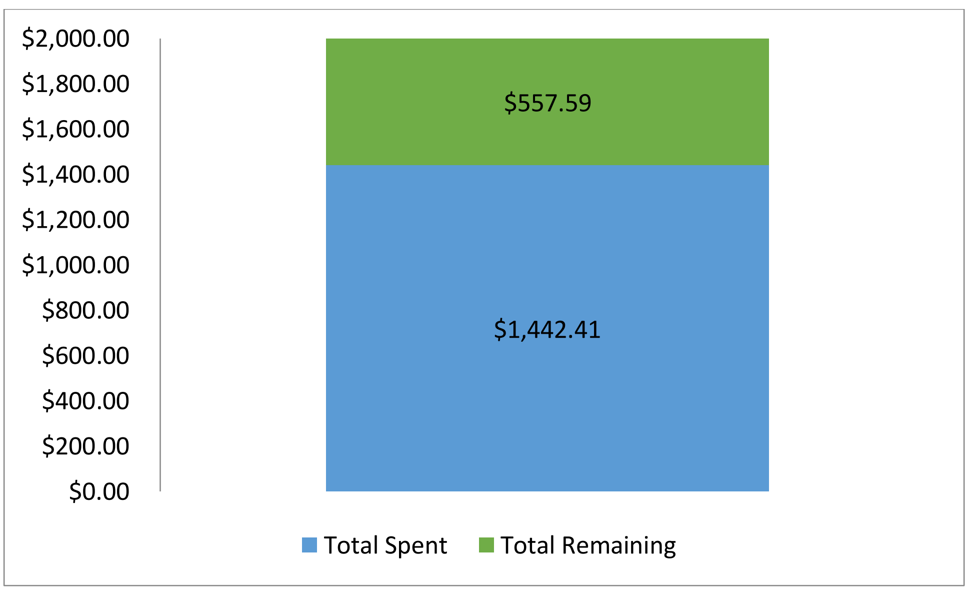

Figure 30. Overall Budget

A BAR GRAPH COMPARING OUR PRODUCT TO OTER COMMERICAL PRODUCTS LIKE OURS

http://www.pcm-solutions.com/thermalstorage.html

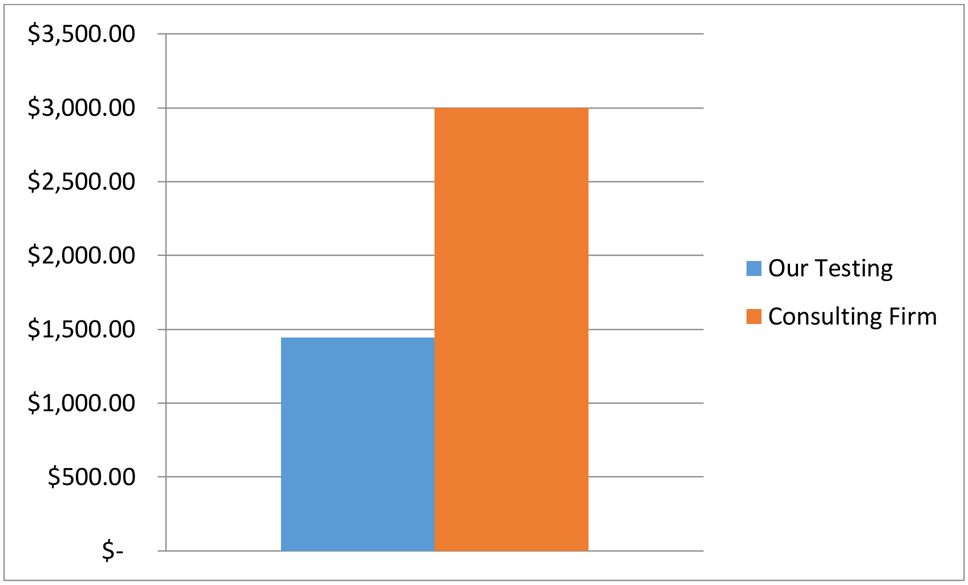

Figure 31. Our Analysis vs. a Competitor

Our project requires many components to perform well but the most important comes from the materials that we use to transfer and store the energy. After all, that's what our project revolves around. After tirelessly researching and communicating with our sponsors we came to the conclusion of using Dynalyne MS-1 as our PCM material and Duratherm HF as our heat transfer fluid. Many advantages led us to this decision. Many PCM materials were available for us to choose from but it was important to our sponsor that the freezing point be as high and as safe as possible for us to test. That number was decided by our sponsors as around 200°C. Dynalene was the easiest to have shipped since they were in the US and offered extensive data that other companies did not provide. Duratherm HF was another easy choice for our sponsors since they already had an account with the Duratherm Company and were satisfied with their products. Technical data for both are listed in Table 1 below.

Table 6. Material Properties Phase Change Material and Heat Transfer Fluid

Dynalyne MS-1 Properties	**Values**	**Duratherm HF Properties**	**Values**
Freezing Point	225°C	Flash Point	276°C
Max Operating Temp	565°C	Max Bulk Temp	338°C
Latent Heat	117 J/g	Auto ignition	393°C
Thermal Conductivity	0.50 W/mK	Viscosity	5.63 cSt (@208°C)
Specific Heat	1.40 J/gK	Density	44.1 lb/ft^3 (@260°C)
Density	1.9 g/cm^3	Thermal Expansion Coeff	0.1101 %/°C
Viscosity	4.0 cP	Thermal Conductivity	0.075 BTU/hr F ft (@260°C)
Freezing Contraction	3%	Heat Capacity	2.587 kJ/kg K (@260°C)

Other important equipment include the pump, heat load, heat source, temperature sensors, valve and flowmeter whose important properties are listed below in Table 2. The pump is a refurbished one that Verdicorp worked on themselves offering 3/4 hp which would be able to handle the flow rate we expect for our system which is about 0.25 gpm. Tank has been leak tested to ensure nothing will leak during operation.

Table 7. Major Component Dimensions and Data

Hayden liquid to air heat exchanger (heat Load)	**Values**
Dimensions	24in x 12in x 1.5 in
Fan (Mechatronics: Model UF25GCA12)	
Dimensions	10in Diameter 5in width
Electrical Input Load	60/75 W
Input Voltage	115V
Flowmeter (Headland H601-001 HT) NPTF	
Flow range	0.1-1gpm
Max temp	260°C
Dimensions	6.6in x 2.01in
Valve (B&G Circuit Setter)	
Max Temp	121°C
Dimensions	3/8 in inlet and outlet diameters
Thermocouples	
Type	K
Max Temp	1250°C
Tank	
Dimensions	17in x 16 in OD (15.25 in ID)
Material	A-36 low grade Hot rolled steel
PCM Capsules	
Dimensions	12 in x 2.375 in OD (2in ID) Schedule 10
Pipe Material	304 Stainless steel
Piping	
Dimensions	1/2in ID
Material	Standard low grade steel
Pump	
Mechanical Power	3/4 hp
Electric Input	230V
Heat Cartridge	
Power Output	1500W
Maximum Temperature	550 degrees Fahrenheit
Dimensions	10in x 3/8in Diameter

Design of Experiment

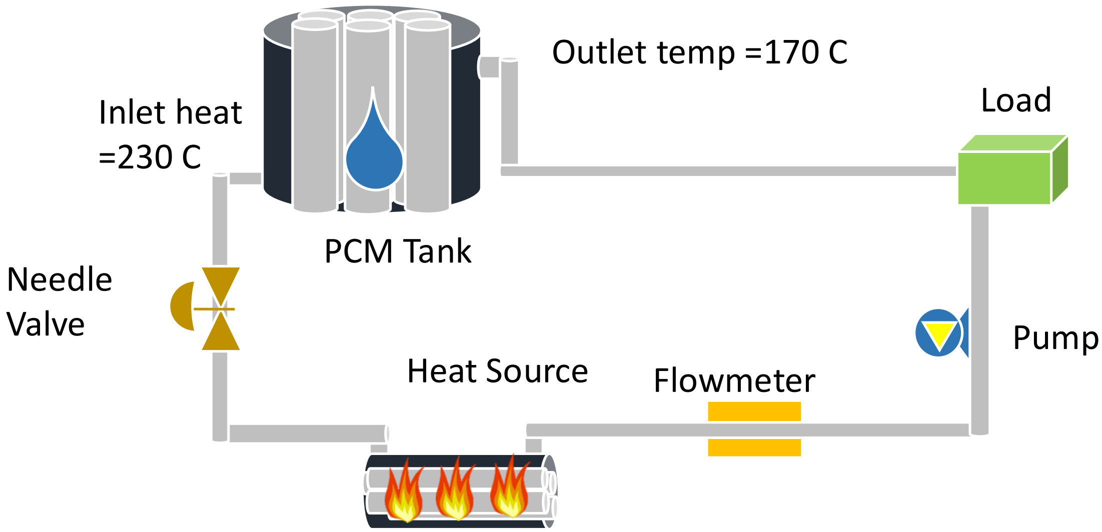

Figure 32 Final System Diagram

Project Assembly

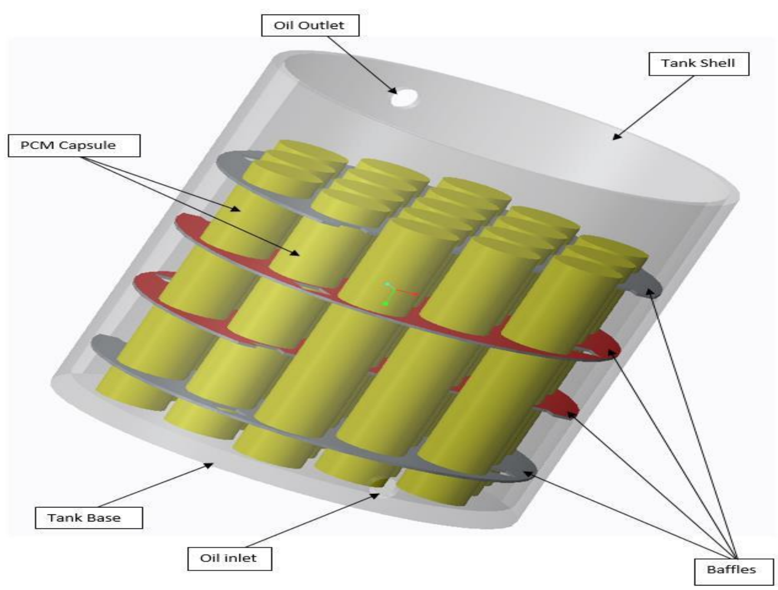

Figure 33 Final Chosen Design

Inlet and outlet diameters for the pump is 3/8 in which is slightly smaller than the piping diameter of 0.25 in we need to achieve our flow rate. 1/2 to 3/8in couplings will be needed for that portion of the system. Same thing goes for our heat exchanger which is provided by Verdicorp as well. It has inlet and outlet diameters of 3/4 in so we will 3/4 to 1/2in reducers for that portion of the assembly. The heat load will simulate the ORC in its consumption of the heat. It resembles a radiator on a smaller scale and will have two fans blowing atmospheric air onto it fins and pipes to improve the cooling effect. To ensure that all the air powered by the fans reach the pipes and fins, a thin metal box will enclose the device and two holes will be cut out for the top for the fans to be mounted on. The other side of the device will be free to the atmosphere. The flowmeter and valve will be placed after the heat load to ensure that the equipment will stay within its operating temperature. The oil will be heated by resistance cartridges that will be placed in a wider pipe that will link in series with the rest of our system. As the oil flows through it, it will get heated to the desired temperature before entering the tank. These cartridges are rated at 1000 W and will be provided by Verdicorp. The cartridges are controlled via applied voltage and the amount of watts applied may be varied via controller. It is imperative that when the cartridges are on they have a constant flow over them or else they will burn up internally and become useless. An overall system can be found in the Appendix Figure 2.

Operation Instruction

Before beginning the operation, one must insure that all components are tightly connected to ensure no leaks during operation. After ensuring that components are tight sealed the power should be turned on. Since it is crucial to determine that the pump, heat cartridges, and heat load are all receiving power the operator must witness the illumination of the light indicators that signal the power delivery. One light will indicate the heat source cartridges being turned on. At this point the pump will begin to push Duratherm through the piping system. The operator must inspect the flow on the flowmeter and adjust the flow of the system using the circuit setter. The flow should be adjusted to a maximum of 0.27gpm. Before the charging cycle can begins the bulk transfer fluid must be heated to 230 ^{o}C. This operation takes up to 1 hour. During the start of any charging cycle the heat load should be adjusted so that no temperature leaving the load exceeds 200^{o}C. The operator must continually monitor the three thermocouples over 15 minute intervals to ensure this. After 2.5 hours the system will be fully charged and the testing can begin. Next the heat source is turned off. Then the circuit setter will once again be used to adjust the flow rate until the thermocouple directly after the tank maintains a steady temperature output of 170 ^{o}C. Once the flow rate is set the temperature reading across all thermocouples will be recorded at a maximum of 5 minute intervals for the following 40 minutes.

Troubleshooting

The heat cartridges need a steady flow to dissipate heat or else they will burn up internally rendering them useless. We will have inlet and outlet temperature sensors before and after the heat source that monitor the temperature of these components. If the output temperature exceeds the 230 ^{o}C power to the system should be cut and allowed to cool. Once cooled to room temperature the cartridges should be inspected for damage. If the cartridges are undamaged, the pump only should be turned on and the operator should monitor the flowmeter and ensure that it reads the expected value. If the flow is not as expected there may be some impedance in the piping network that must be cleared before operation can resume. Another problem we may encounter is having the temperature coming out too hot from the load. The circuit setter Verdicorp has chosen has a relatively lower operating temp so if allowed to exit at too high a temp it may ruin the circuit setter. To avoid we will turn down the heat source or add a regular house fan to blow air on the device to further convective heat transfer. We may encounter the problem of not vacuum sealing the PCM capsules due to lack of knowledge and time on Verdicorp's part since they are the ones manufacturing it. If that is the case we will drill holes into the caps of the capsules and lead copper pipe from the top of the capsule to the top of the tank to act as a vent so that we do not see pressure build up within the capsules.

Regular Maintenance

To prevent sludge from building up in the tank, the Duratherm transfer fluid should be removed from drained from the system at least once a month and the tank should be cleaned of any built up debris. This will insure that an impeded flow will be maintained during operation. The circuit setter should be replaced every 6 months as well since it will likely be running near max temperature for almost every test at a $50 cost per part to the end user. As mentioned previously, the heat cartridges are prone to burn out. Therefore they should be inspected once a month for full functionality to ensure that the heat transfer fluid achieves the melting temperature of the phase change material in the expected time frame.

Spare Parts

The parts listed below are components ant the recommended quantities of those components that should be kept in stock to ensure reliable operation.

- (1) Heat Cartridge in case of early burn out
- (2) Thermocouples
- (1) ½" NPT B&G Circuit Setter

Environment, Safety, and Ethics

In recent years one of the main project requirements in the industry has been a small environmental footprint. By preventing air pollution, contaminated waters, noise pollution, as well as many other impactful negative contributions to the environment, future generations will reap these benefits in the years to come. Green energy is a source of power created using recycled materials, renewable resources, and leaves little to no environmental impact. Solar and geothermal power plants are an excellent advancement in the green energy industry. By creating a thermal storage solution for these renewable energy power plants we are able to contribute to the green energy sector's progress.

Our particular thermal storage unit prototype has a very little environmental footprint. We chose to use an electric pump to eliminate the use of fossil fuels during testing. In the full scale application this pump will be powered by the system itself and will not need any outside source of electricity eliminating any environmental impact. Furthermore we chose heat transfer materials that had very little impact on the environment if uncontained or spilled.

Although our system reaches extremely high temperatures we decided to not pressurize the entire system to prevent any combustions. An emergency shutoff switch was installed just in case hot oil begins to overflow or leak onto the floor. This emergency shutoff switch will cut all power to the heat cartridges, and the pump which should prevent any extra damage to the system or environment. The "Load" or cooling system was placed strategically at the top of the system so that the hot air will be blown away from and above any observers or testers. Most of the piping as well as the heat source is in the back of the system away from where any operators or observers would stand. A sensor with a temperature switch was installed within the heat source to prevent overheating and extremely high temperatures which could lead to damages to specific components within the system. Insulation was applied to all open piping as well as the thermal storage tank and heat source to prevent accidental contact with an unfamiliar observer.

The integrity of pursing the completion of a project ethically has been lost by some engineers under immense pressure. No shortcuts were taken to advance this project along. The safety of the customer and operator were of the utmost importance throughout the design and assembly process. Factors of safety were incorporated to ensure this was true.

Project Management

- **Schedule**

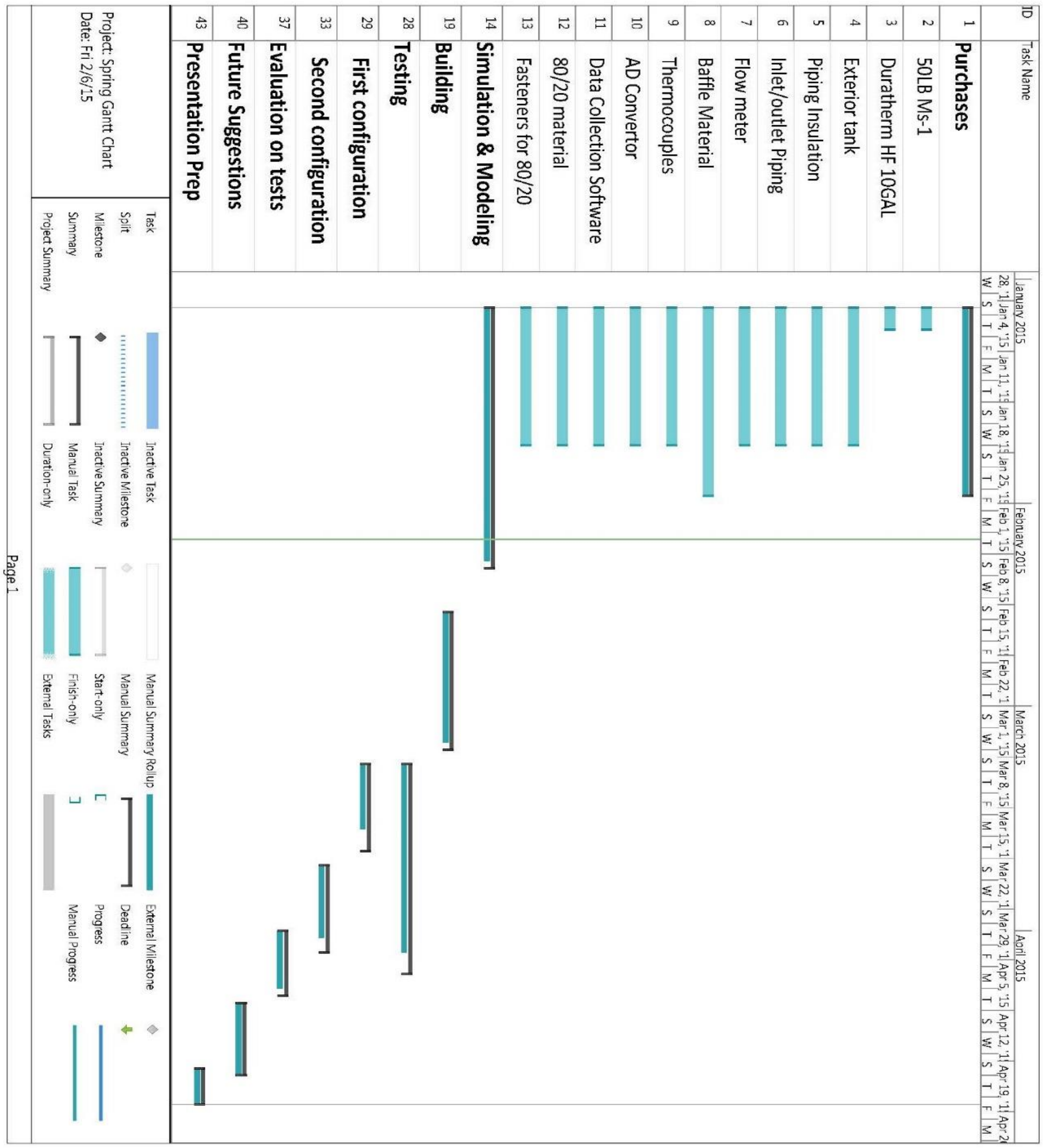

Figure 34: Gantt Chart

By setting short term goals our team will be able to assure our client of a product that meets their needs and is finished by the appropriate deadline. The Gantt chart, Figure 4, will help us complete these short term goals throughout the semester. It will also help us manage unforeseeable obstacles since our overall timeline for the project will be laid out. Any new tasks that need to be added will be done immediately in order to give our team as much time as possible to adjust to the changes. It is critical to the project to manage our time wisely and the Gantt chart will be our guide.

ID	Task Name	Duration	Start	Finish
1	**Purchases**	**20 days**	**Mon 1/5/15**	**Fri 1/30/15**
2	50LB Ms-1	3 days	Mon 1/5/15	Wed 1/7/15
3	Duratherm HF 10GAL	3 days	Mon 1/5/15	Wed 1/7/15
4	Exterior tank	15 days	Mon 1/5/15	Fri 1/23/15
5	Piping Insulation	15 days	Mon 1/5/15	Fri 1/23/15
6	Inlet/outlet Piping	15 days	Mon 1/5/15	Fri 1/23/15
7	Flow meter	15 days	Mon 1/5/15	Fri 1/23/15
8	Baffle Material	20 days	Mon 1/5/15	Fri 1/30/15
9	Thermocouples	15 days	Mon 1/5/15	Fri 1/23/15
10	AD Convertor	15 days	Mon 1/5/15	Fri 1/23/15
11	80/20 material	15 days	Mon 1/5/15	Fri 1/23/15
12	Fasteners for 80/20	15 days	Mon 1/5/15	Fri 1/23/15
13	**Simulation & Modeling**	**26 days**	**Mon 1/5/15**	**Mon 2/9/15**
14	Vertical Configuration	1 day	Sun 2/8/15	Sun 2/8/15
15	Horizontal Configuration	1 day	Sat 2/7/15	Sat 2/7/15
16	CAD Modeling	25 days	Mon 1/5/15	Fri 2/6/15
17	Submit Drawings to Verdicorp to begin cutting	1 day	Fri 2/6/15	Fri 2/6/15
18	**Building**	**14 days**	**Mon 1/19/15**	**Thu 2/5/15**
19	Create Capsules	14 days	Mon 2/16/15	Thu 3/5/15
20	Create Heat Exchanger	14 days	Mon 2/16/15	Thu 3/5/15
21	Weld bottom to tank	1 day	Mon 2/16/15	Mon 2/16/15
22	Cut Baffels	1 day	Mon 2/16/15	Mon 2/16/15
23	Frame for baffels	3 days	Mon 2/16/15	Wed 2/18/15
24	Connect pipes	1 day	Thu 3/5/15	Thu 3/5/15
25	Place capsules/oil in tank	1 day	Thu 3/5/15	Thu 3/5/15
26	Screw top on tank	1 day	Thu 3/5/15	Thu 3/5/15
27	**Testing**	**21 days**	**Mon 3/9/15**	**Mon 4/6/15**
28	**First configuration**	**10 days**	**Mon 3/9/15**	**Fri 3/20/15**
29	Test 1	2 days	Mon 3/9/15	Tue 3/10/15
30	Test 2	2 days	Fri 3/13/15	Mon 3/16/15
31	Test 3	2 days	Mon 3/16/15	Tue 3/17/15
32	**Second configuration**	**10 days**	**Mon 3/23/15**	**Fri 4/3/15**
33	Test 1	2 days	Mon 3/23/15	Tue 3/24/15
34	Test 2	2 days	Thu 3/26/15	Fri 3/27/15
35	Test 3	2 days	Tue 3/31/15	Wed 4/1/15
36	**Evaluation on tests**	**7 days**	**Wed 4/1/15**	**Thu 4/9/15**
37	Performance of first configuration	3 days	Wed 4/1/15	Fri 4/3/15
38	Performance of second configuration	3 days	Mon 4/6/15	Wed 4/8/15
39	**Future Suggestions**	**7 days**	**Sat 4/11/15**	**Mon 4/20/15**
40	Brainstorm how to improve	5 days	Sat 4/11/15	Thu 4/16/15
41	Present suggestions to sponser	1 day	Mon 4/20/15	Mon 4/20/15
42	**Presentation Prep**	**5 days**	**Mon 4/20/15**	**Fri 4/24/15**
43	Prepare board	3 days	Mon 4/20/15	Wed 4/22/15
44	Present	1 day	Fri 4/24/15	Fri 4/24/15

Figure 35. Project Schedule

As seen in Figure 5, our team will wrap up any final purchases by the end of January. We have already ordered the items with the highest lead times including the PCM, the oil, the tank, the thermocouples, and sheet metal for the baffles. We will promptly begin building when the materials come in which is estimated to be the middle of February. We begin testing after construction is complete which is estimated to be toward the beginning of March. While we wait for the material to come in we will evaluate each configuration using CAD and COMSOL to get some approximations of what kind of flow and temperatures we should expect. The schedule in Figure represents projected deadlines and actual undertaking of certain tasks may begin earlier than reported.

Resources

Throughout the manufacturing and assembly process many resources were utilized. Since Verdicorp is a local company, we were able to use their facilities. A conference room with a white board was made available for meetings and brainstorming. Veridcorp's Lab Manager, Mr. Parsons acted as our main contact with the company. When it came to advice on parts, system construction, and power supply, Verdicorp's Project Manager, Lewis Neely contributed greatly to the success of our system. All parts that were ordered, were shipped directly to Verdicorp saving us the huge inconvenience of transporting parts. Verdicorp also allowed us to use their assembly floor to construct and store our thermal storage system. Having access to a complete repertoire of tools, scrap metals, excess insulation and other spare parts made the assembly process run much smoother than originally anticipated. The only downside to using Verdicorp as our work station was the limited hours of operation.

Procurement

Once the constraints and volume parameters were determined, mass and volume calculations were used to find how much salt and oil would be needed. After careful research, specific salts, DynaleneMS-1, and an oil, Duratherm, were found and the suppliers were contacted. Quotes were given for our required amounts of each product and orders were placed shortly after. More research and analysis will be done to determine how much piping and which fixtures we will need to order within the next few weeks. The remaining budget will be a huge factor when determining which suppliers to order from and which sensors will be absolutely necessary. Specialized welding will be form the desired tank shape and to create the PCM capsules. Verdicorp's skilled employees will play a huge role helping us with these processes.

For our thermal storage solution a budget was set at $2,000. From this $480 was used for the Dynalene MS-1 molten salt, and $442.84 was used for the Duratherm thermal oil. That leaves us with $1077.16 to spend on piping, insulation, sensors and controls, and other unforeseen purchases. After having the tank provided for us by Verdicorp, a large chunk of the budget can now be distributed elsewhere, like purchasing metallic plates for baffle material.

Bill of Materials

Part # Part Name

1. Tank
2. Top
3. Handle
4. Base
5. Lock and Lift Pin
6. Baffle
7. Rod
8. Shell
9. Heat Cartridge
10. Heater Cap
11. Heater Cap 2
12. Flow Meter
13. Pump
14. Fan
15. PCM Capsules
16. 80/20 Frame
17. Control Box
18. Heater Switch with Sensor
19. Pump Switch
20. Fan Switch
21. Emergency Stop
22. Condenser Coil with Fins
23. Threadolets
24. Tank Insulation
25. Pipe Insulation
26. Heater Insulation
27. Copper Piping
28. Three Way Valve
29. Circuit Setter
30. Base Plate
31. Wheels
32. Dynalene MS-1 (Salt)
33. Duratherm (Oil)

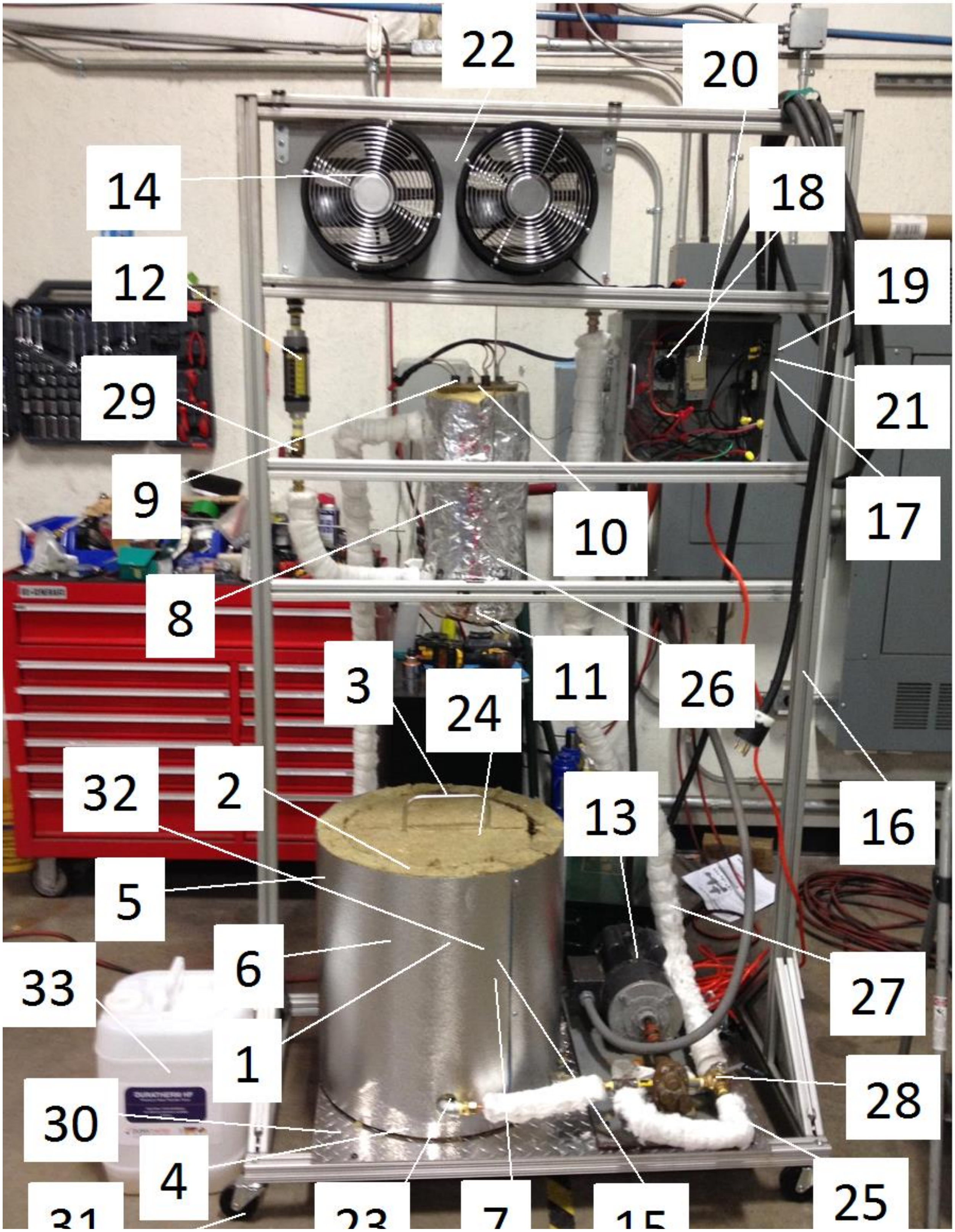

Figure 36 Final Design Part Breakdown

Communications

Communication between the team, faculty, and Verdicorp has been crucial to keeping this project on track for success since this project has been prone to numerous changes throughout its development. From location changes to priority changes that depend on the customer's perceived needs and suggestions pushed by the involved faculty the project has evolved to fit new requirements as they're introduced. To ensure a balance between time spent working and time spent in meetings, Communication with our sponsor has been on has been on a regular bi-weekly basis along with deliverables on our progress during the weeks that we do not meet. Meetings with our faculty advisors has been less formal because of their close proximity and many suggestions have been taken from in-class deliverables and presentations. Good communication between the three parties involved allowed the team to respond to location changes and this process is will be maintained through completion of the thermal storage prototype.

Conclusion

Utilizing all resources available to us, our group will design, create, and present a thermal storage solution to our customer. The materials used in this scaled down model will be chosen with three things in mind, cost, effectiveness, and accessibility. Each group member will be allocated specific tasks and the scheduling of those tasks will be managed using the Gantt chart in Figure 4. In the upcoming weeks materials research will be completed and appropriate materials for the selected thermal storage unit will be chosen. The selection process of materials and parts will depend on the available budget and how well they meet the design requirements. Our design process continues to be the "funnel" methodology. Once drawings are created and materials are ordered the manufacturing process will begin.

References

[1] Google Books. (2014, September 22). *Thermal Energy Storage (1st ed.)* [Online]. http://books.google.com/books?id=EsfcWE5lX40C&pg=PA93&lpg=PA93&dq=methods+of+thermal+energy+storage&source=bl&ots=7XQn2Ozyuw&sig=vw4lHt7F0F3BKmzDdWgtIAq-dcY&hl=en&sa=X&ei=qEwcVKuAL8-YyATlsYHACw&ved=0CE8Q6AEwBDgK#v=onepage&q=methods%20of%20thermal%20energy%20storage&f=false

[2] Heat and Cold Storage with PCM. (2014, September 22). *Reinhart & Gupta Energy Efficiency Systems (1st ed.)* [Online]. Available: http://rgees.com/technology.php

[3] IEEE Spectrum. (2014, September 22). *Terrafore Looks to Cut Molten Salt Energy Storage Costs in Half (1st ed.)* [Online]. Available: http://spectrum.ieee.org/energywise/green-tech/solar/terrafore- looks-to-cut-molten-salt-energy-storage-costs-in-half

[4] MIT Technology Review. (2014, September 22). *Molten Salts May Be An Alternative to Batteries for Electricity Storage | MIT Technology Review (1st ed.)* [Online]. Available: http://www.technologyreview.com/news/525121/molten-salts-might-provide-half-price-grid-energy-storage/

[5] Mukherjee, R , (2014, December 20) *Effectively Design Shell-and-Tube Heat Exchangers*. *(1st ed.)* [Online] Available: http://www.mie.uth.gr/ekp_yliko/CEP_Shell_and_Tube_HX.pdf

Appendix

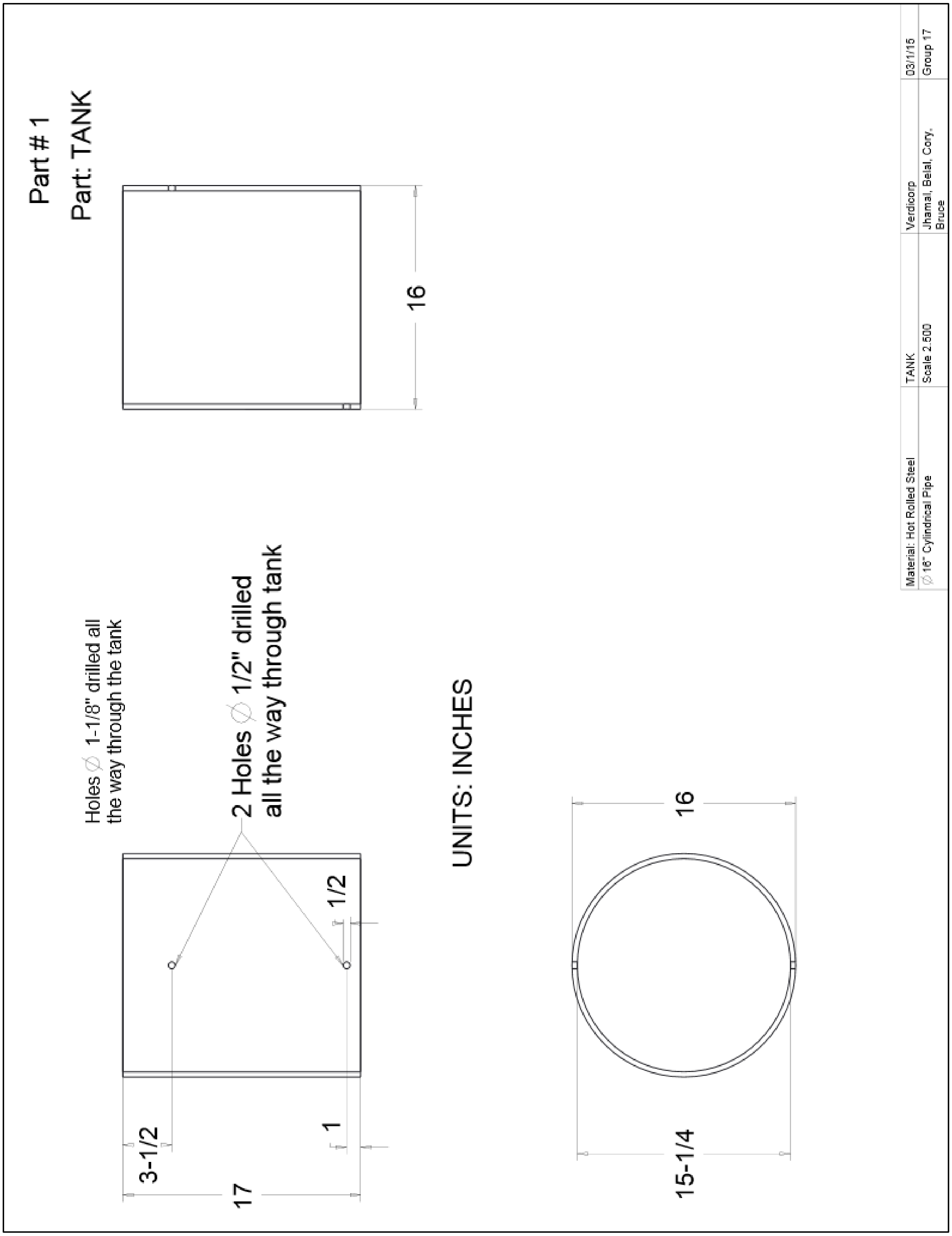
Part # 1
Part: TANK
16
Holes ∅ 1-1/8" drilled all the way through the tank
2 Holes ∅ 1/2" drilled all the way through tank
1/2
UNITS: INCHES
16
3-1/2
1
17
15-1/4
Material: Hot Rolled Steel
∅ 16" Cylindrical Pipe
TANK
Scale 2.500
Verdicorp
Jhamal, Belal, Cory, Bruce
03/1/15
Group 17

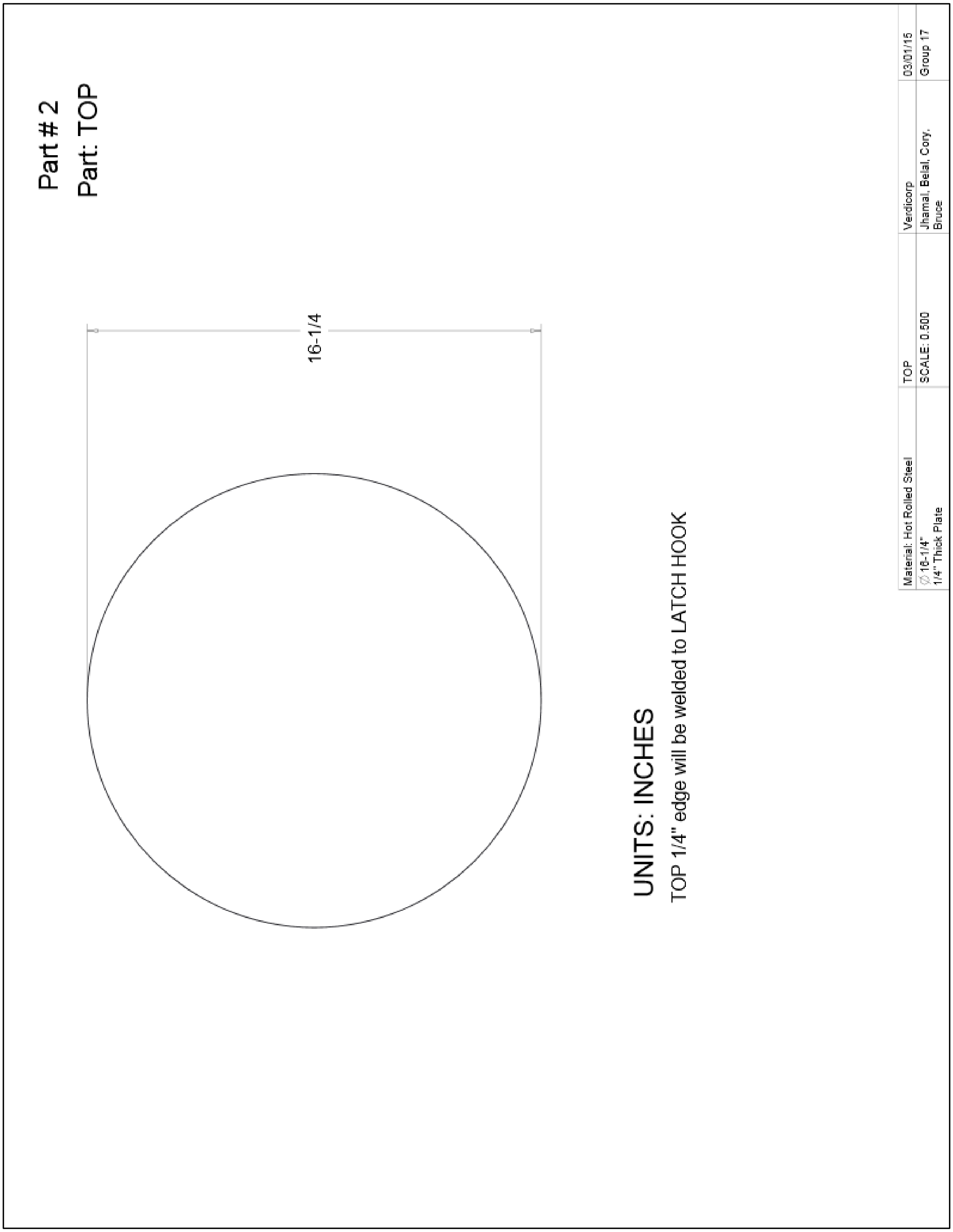
Part # 2
Part: TOP
16-1/4
UNITS: INCHES
TOP 1/4" edge will be welded to LATCH HOOK
Material: Hot Rolled Steel
∅ 16-1/4"
1/4" Thick Plate
TOP
SCALE: 0.500
Verdicorp
Jhamal, Belal, Cory, Bruce
03/01/15
Group 17

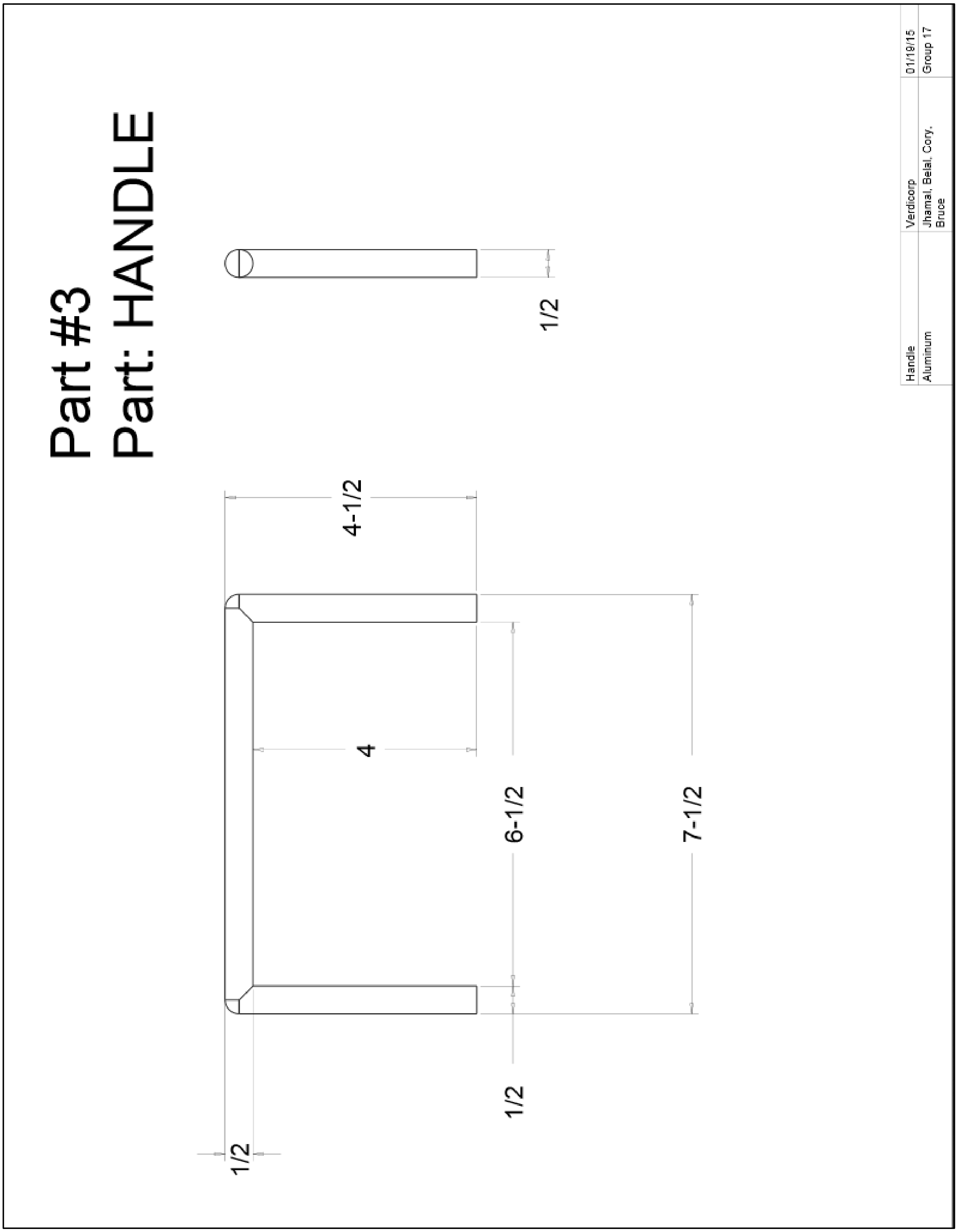
Part #3
Part: HANDLE
1/2
4-1/2
4
6-1/2
7-1/2
1/2
1/2
Handle
Aluminum
Verdicorp
Jhamal, Belal, Cory, Bruce
01/19/15
Group 17

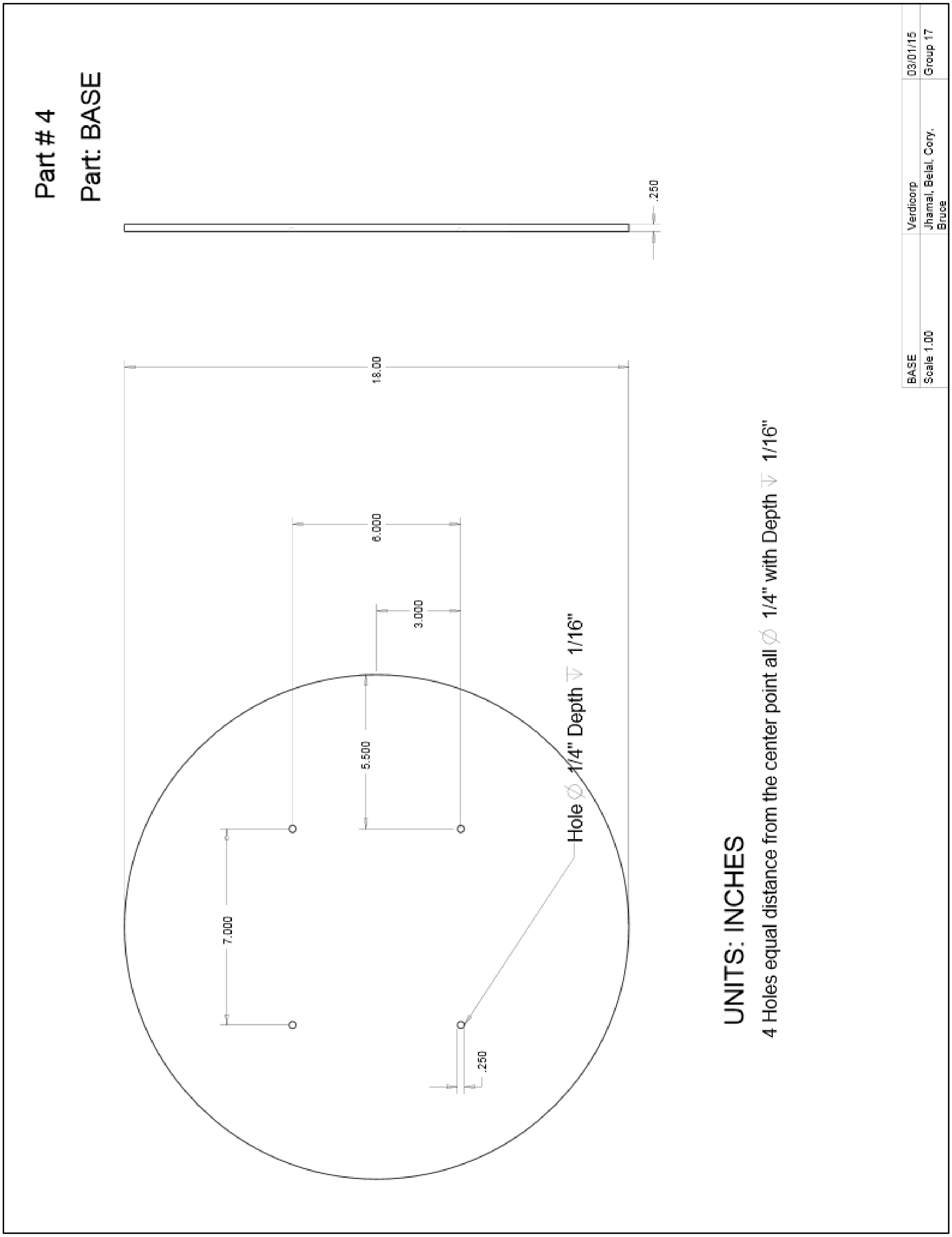

Part # 4
Part: BASE
18.00
8.000
3.000
5.500
7.000
.250
.250
Hole ∅ 1/4" Depth ⊽ 1/16"
UNITS: INCHES
4 Holes equal distance from the center point all ∅ 1/4" with Depth ⊽ 1/16"
BASE
Scale 1.00
Verdicorp
Jhamal, Belal, Cory, Bruce
03/01/15
Group 17

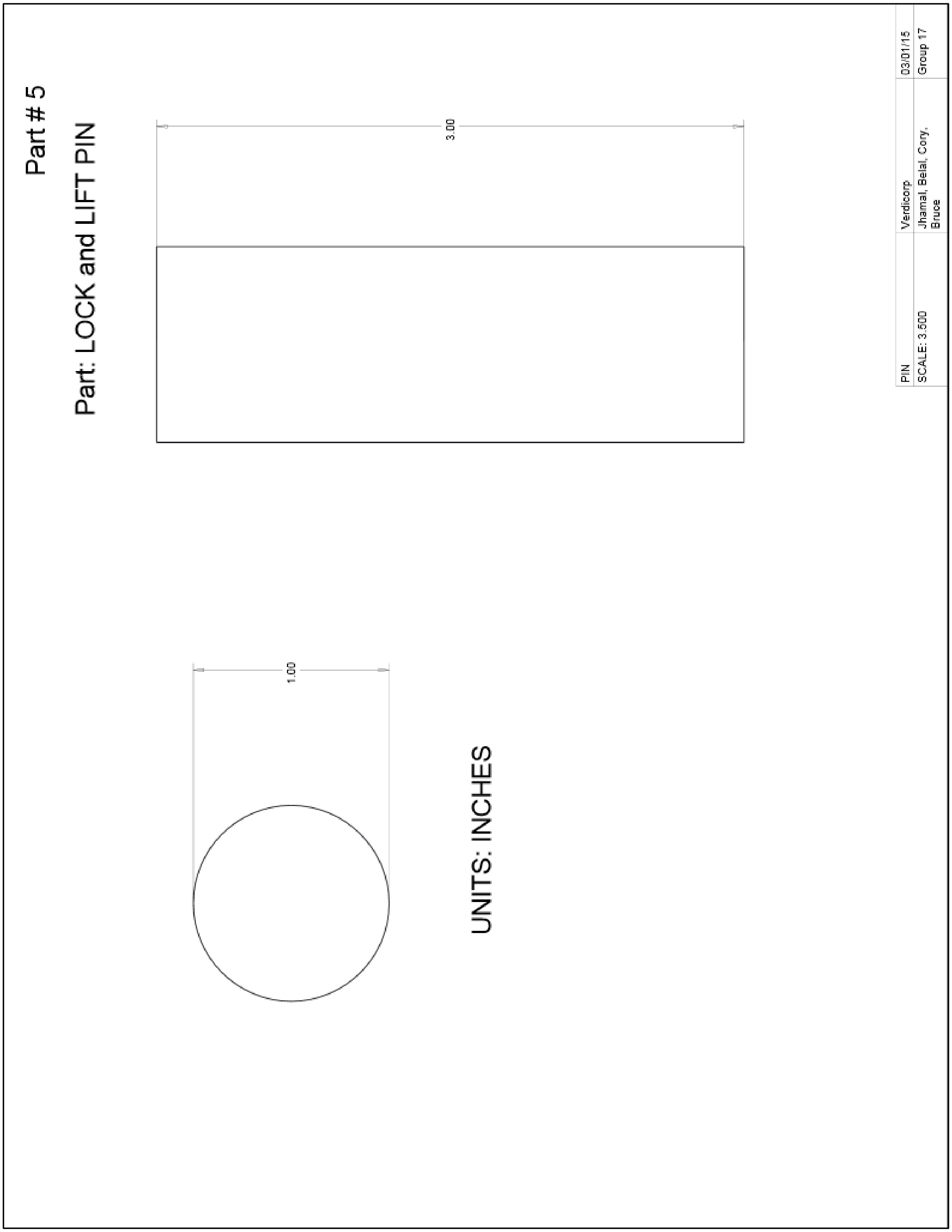
Part # 5
Part: LOCK and LIFT PIN
3.00
1.00
UNITS: INCHES
PIN
SCALE: 3.500
Verdicorp
Jhamal, Belal, Cory, Bruce
03/01/15
Group 17

Part # 6

Part: BAFFLE
DESIGN 1

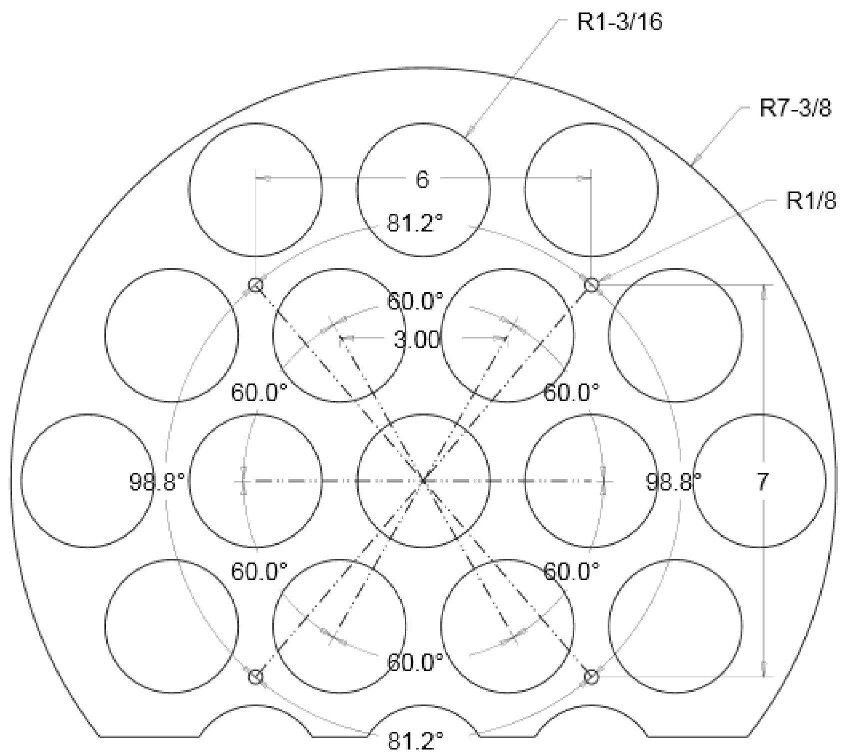

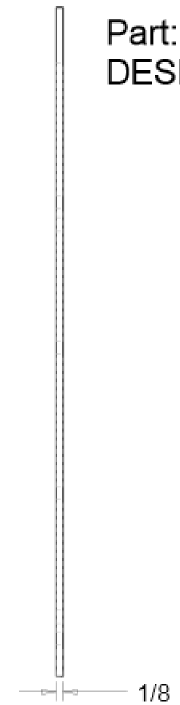

UNITS: INCHES

Distance between centers of all 2-3/8" holes is 3"

BAFFLE DESIGN 1	Verdicorp	2/28/15
UNITS: INCHES	Jhamal, Belal, Cory, Bruce	Group 17

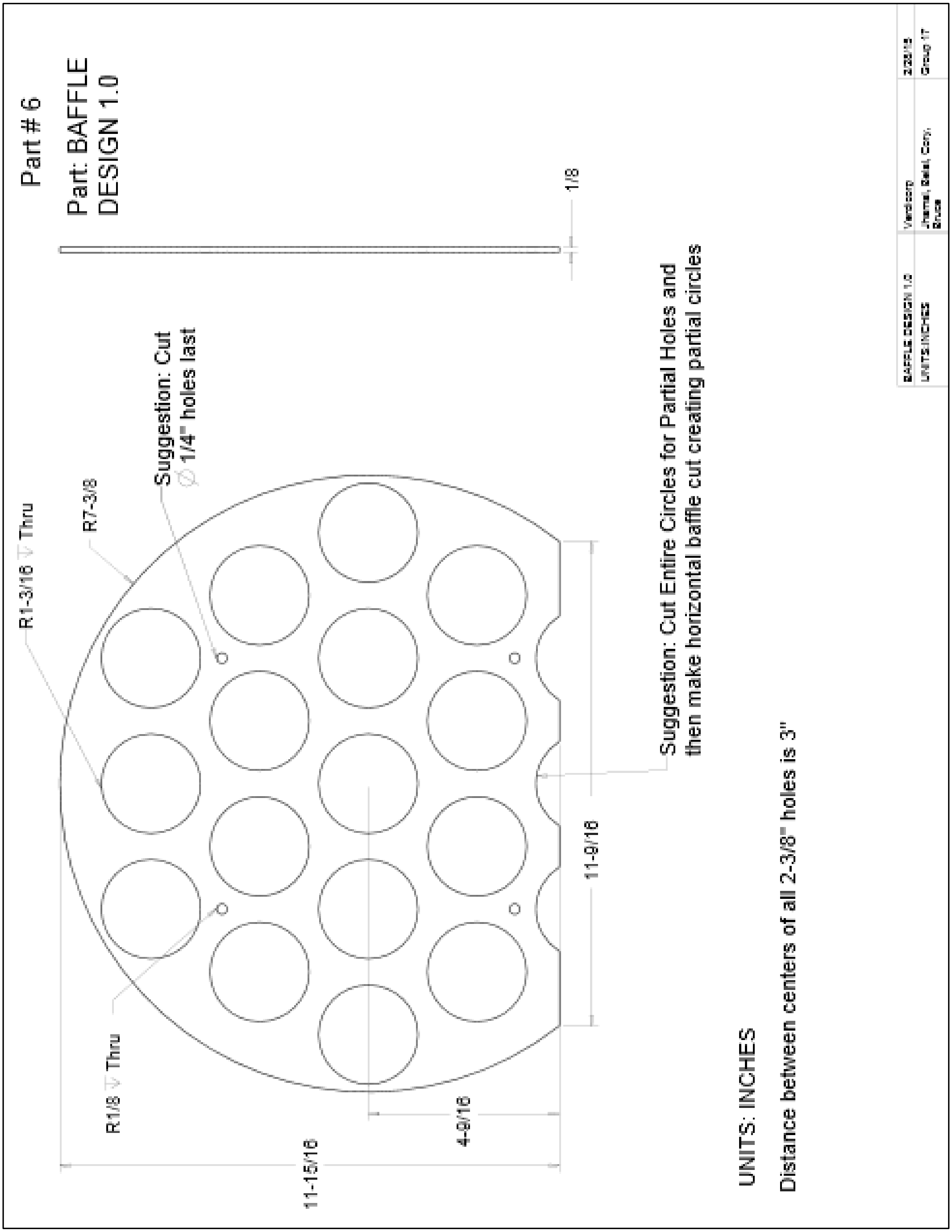
Part # 6
Part: BAFFLE DESIGN 1.0
1/8
R1-3/16 Thru
R7-3/8
Suggestion: Cut ∅ 1/4" holes last
Suggestion: Cut Entire Circles for Partial Holes and then make horizontal baffle cut creating partial circles
11-9/16
R1/8 Thru
4-9/16
11-15/16
UNITS: INCHES
Distance between centers of all 2-3/8" holes is 3"
BAFFLE DESIGN 1.0
UNITS:INCHES
Group 17

Part # 7

Part: ROD

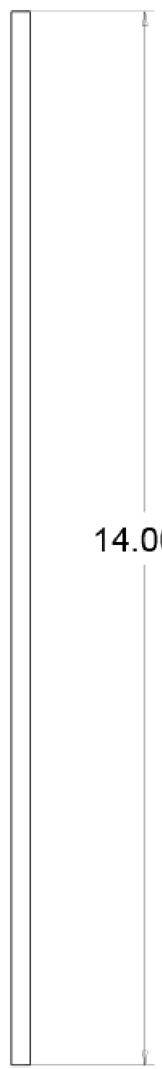

SCALE 1.000

UNITS: INCHES

Threaded rod will be cut into four 14.0" pieces and will be used to frame the baffles

Material: Med. Strength Steel	ROD	Verdicorp	03/01/15
1/4" Threaded Rod	Various Scale	Jhamal, Belal, Cory, Bruce	Group 17

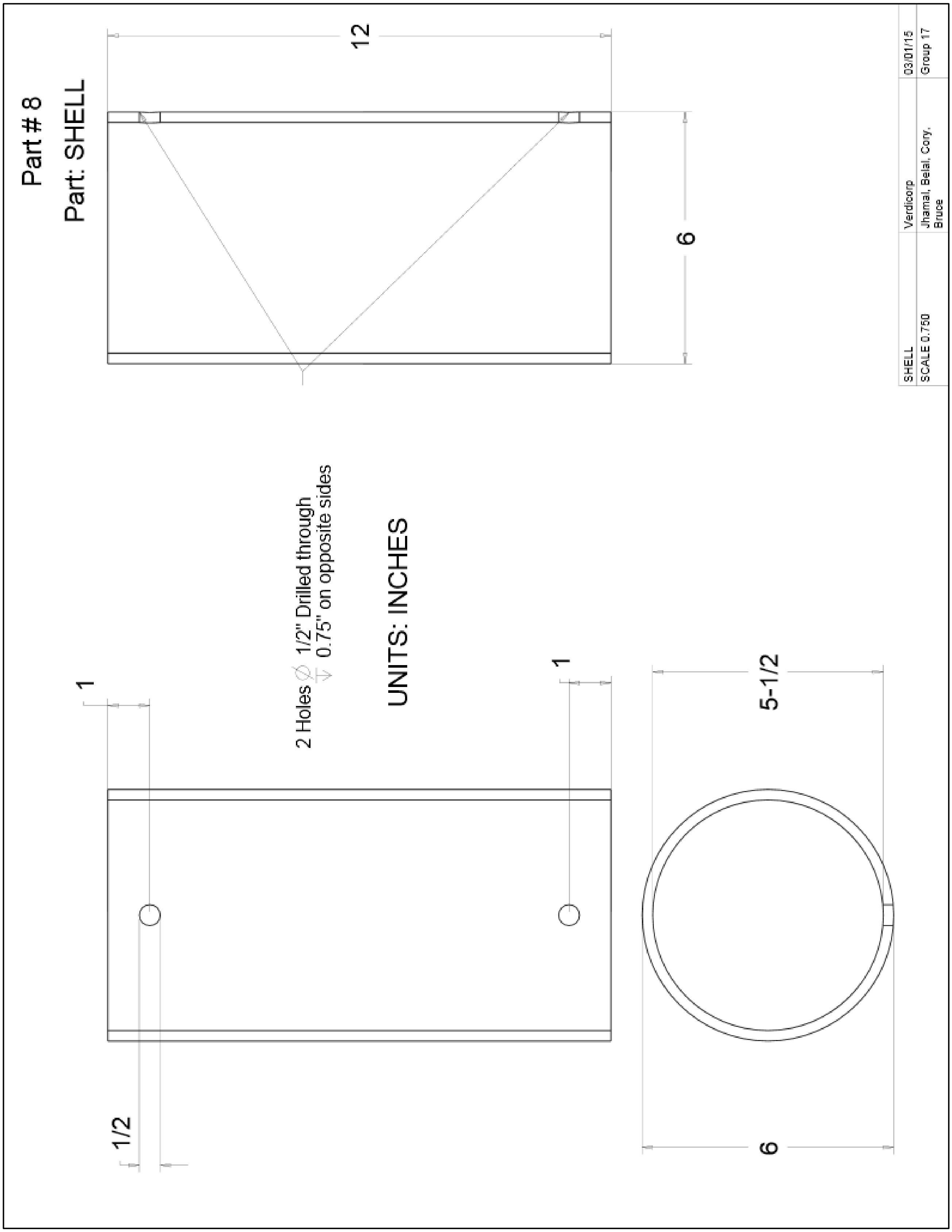
Part # 8
Part: SHELL
12
6
2 Holes ∅ 1/2" Drilled through
0.75" on opposite sides
UNITS: INCHES
1
1
5-1/2
1/2
6
SHELL
SCALE 0.750
Verdicorp
Jhamal, Belal, Cory, Bruce
03/01/15
Group 17

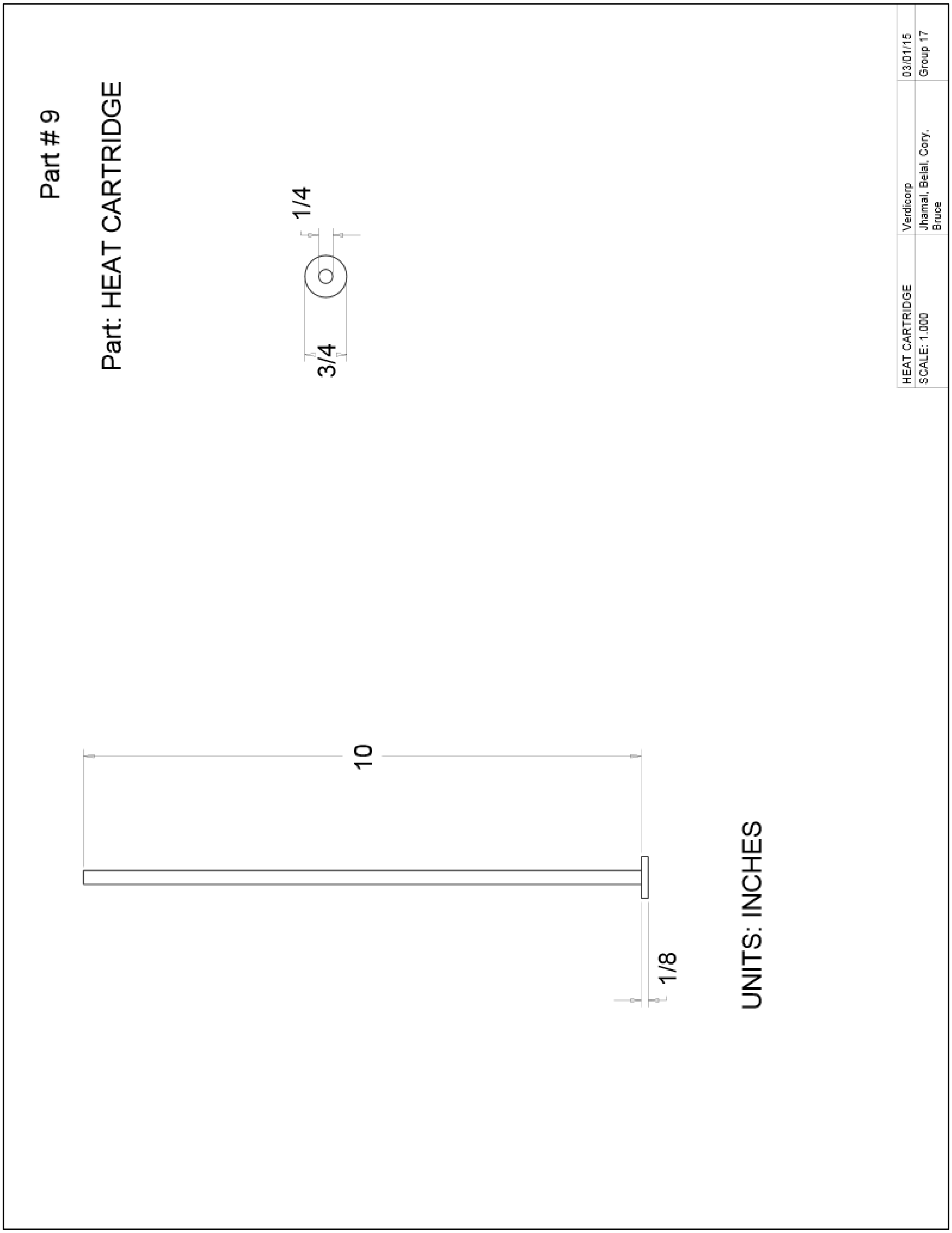
Part # 9
Part: HEAT CARTRIDGE
1/4
3/4
10
1/8
UNITS: INCHES
HEAT CARTRIDGE
SCALE: 1.000
Verdicorp
Jhamal, Belal, Cory, Bruce
03/01/15
Group 17

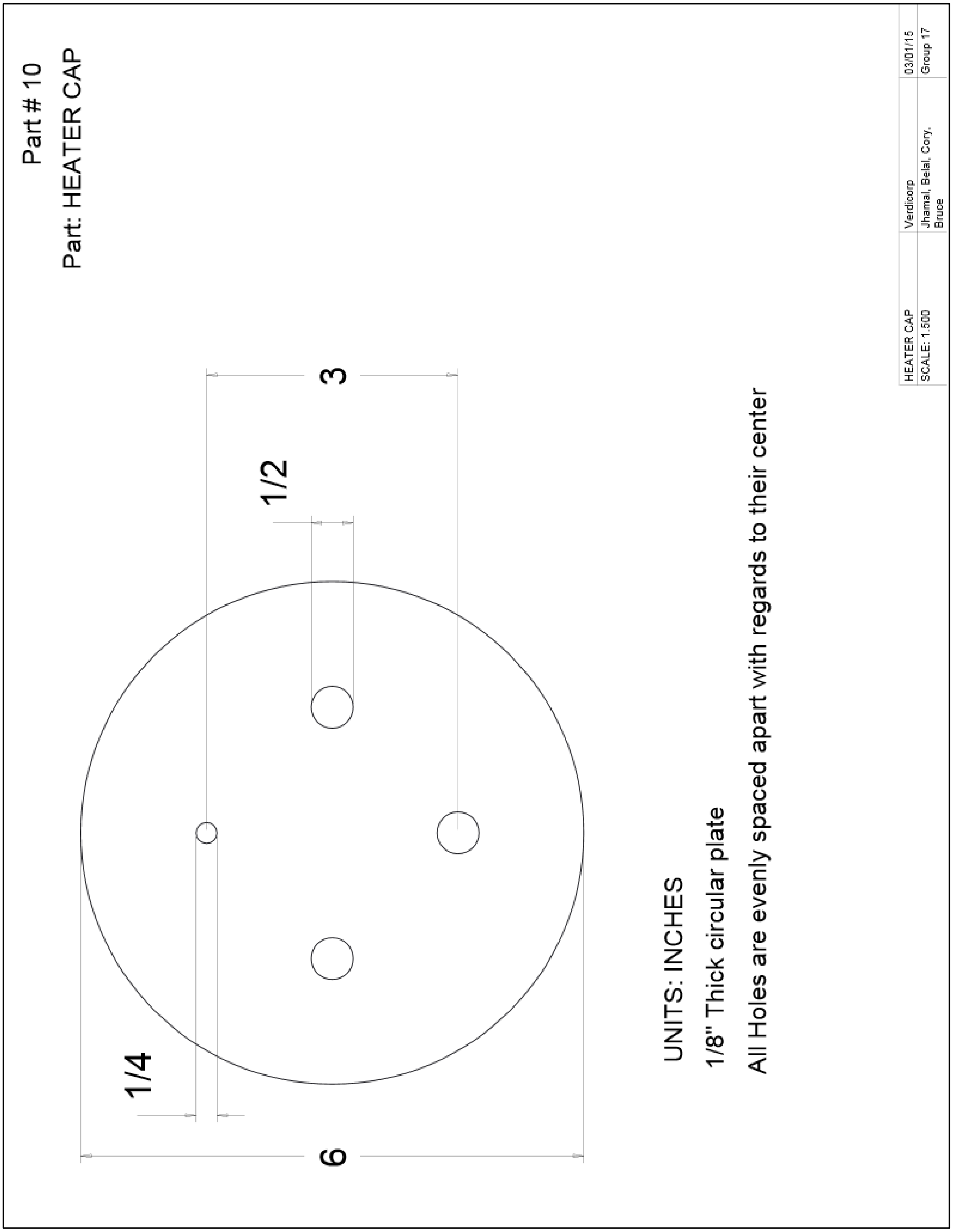
Part # 10
Part: HEATER CAP
3
1/2
1/4
6
UNITS: INCHES
1/8" Thick circular plate
All Holes are evenly spaced apart with regards to their center
HEATER CAP
SCALE: 1.500
Verdicorp
Jhamal, Belal, Cory, Bruce
03/01/15
Group 17

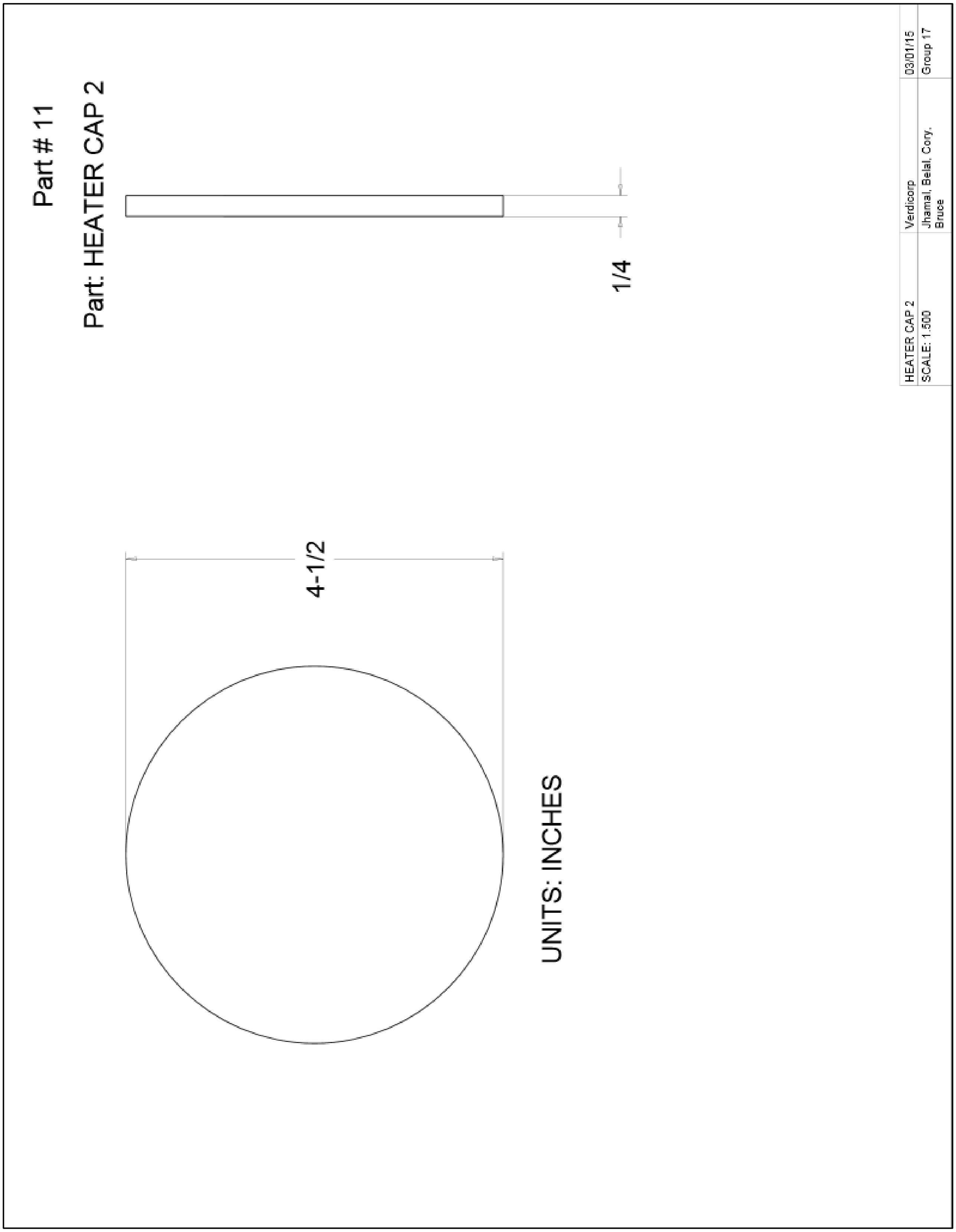
Part # 11
Part: HEATER CAP 2
1/4
4-1/2
UNITS: INCHES
HEATER CAP 2
SCALE: 1.500
Verdicorp
Jhamal, Belal, Cory, Bruce
03/01/15
Group 17

```
clc, clear all, close all
% TES Parameter Study ====================================================
% Storage Unit Geometry/Properties
shell_h = 0.4318;                         % shell height (m)
shell_od = 0.4064;                        % shell outer diameter (m)
shell_id = 0.38735;                       % shell inner diameter (m)
shell_v = pi*((shell_id)^2/4)*shell_h;    % shell volume (m3)
tube_d = 0.0523875;                       % capsule diameter (m)
tube_l = 0.3048;                          % capsule length (m)
tube_v = pi*((tube_d)^2/4)*tube_l;        % capsule volume (m3)
tube_p = 1.25*tube_d;                     % distance capsule to capsule (m)
tube_w = (shell_id-(4*tube_p+tube_d))/2;  % distance capsule to wall (m)
tube_c = tube_p-tube_d;                   % clearance between capsules (m)
tube_n = 19;                              % quantity of capsules
tube_ua = (sqrt(3)*tube_p^1/4)...         % capsule uni-axial area (m2)
    -(pi/8*tube_d^2);
tube_dh = 4*((tube_ua)/(pi*tube_d/2));    % capsule hydraulic diameter (m)
baffles = 4;                              % quantity of baffles (#)
baffle_h = 3.05*0.0254;                   % baffle spacing (m)
baffle_t = 0.125*0.0254;                  % baffle thickness (m)
baffle_entry = 0.2*shell_id...            % baffle entry area (m2)
    *(2*tube_p+tube_d+2*tube_w);
baffle_dh = 2*(baffle_entry)/...          % baffle hydraulic diameter (m)
    (0.2*shell_id+(2*tube_p+tube_d+2*tube_w));
baffle_sa = pi*((shell_id)^2/4)-....      % baffle surface area (m2)
    (tube_n*(pi*(tube_d)^2/4))-baffle_entry;
entry_h = 3.675*0.0254;                    % height of first/last levels (m)
% HTF Duratherm Properties
rhoL = 706.98;                     % density of duratherm at 260C (kg/m3)
CL = 2.609*10^3;                   % heat capacity (J/kg*k)
KL = 0.130;                        % conductivity duratherm at 260C (W/m*K)
visco_l = 10.45*10^-6;             % duratherm viscosity at 100C (m2/s)
minor = 1.1;                       % minor loss 90 deg turn coefficient
% PCM Dynalene MS-1 Properties at 300C
latent = 117*10^3;                 % latent heat (J/kg)
KP = 0.50;                         % conductivity (W/m*K)
CP = 1.40*10^3;                    % heat capacity (J/kg*K)
rho_pcm = 1900;                    % density (kg/m3)
visco_pcm = 0.004;                 % viscosity (Pa*s)
% Thermodynamics =========================================================
Tmin = 150+273;                             % minimum temperature oil K
Tmax = 240+273;                             % maximum temperature oil K
Tm = 225+273;                               % melting point PCM K
Ta = 23+273;                                % ambient temperature K
Temp = linspace(Ta+1,Tmax,50);              % temperature range oil K
delta_t = Tmax-Ta;
mass_oil = rhoL*(shell_v-(tube_n*tube_v));
E_oil = mass_oil*CL*(delta_t);
mass_pcm = rho_pcm*tube_n*tube_v;
E_pcm = mass_pcm*(CP*(delta_t)+latent);
E_total = E_oil+E_pcm;
qmin = E_total/(8*3600);
qmax = E_total/(3600);
qin = linspace(qmin,qmax,50);               % heat addition range J/s
% Flow Properties Study ==================================================
% Inlet Condition Arrays
mass_flow = zeros(length(qin),length(qin)*length(qin));
```

```
Uinf = zeros(length(qin),length(qin)*length(qin));
Re_inf = zeros(length(qin),length(qin)*length(qin));
Nu_inf = zeros(length(qin),length(qin)*length(qin));
fr_inf = zeros(length(qin),length(qin)*length(qin));
H_inf = zeros(length(qin),length(qin)*length(qin));
inlet = linspace(0.5*0.0254,3.75*0.0254,50);   % inlet diameter (m)
Pr = (visco_l*CL)/KL;                           % prandlt duratherm
Ks = 16;                                        % conductivity steel (W/m*K)
% Configuration 1 Arrays
T_s = zeros(60,length(qin)^3);
T = zeros(60,length(qin)^3);
Q = zeros(60,length(qin)^3);
A = zeros(60,length(qin)^3);
V = zeros(60,length(qin)^3);
Re = zeros(60,length(qin)^3);
Nu = zeros(60,length(qin)^3);
H = zeros(60,length(qin)^3);
R = zeros(60,length(qin)^3);
% Configuration 2 Arrays
T_s2 = zeros(60,length(qin)^3);
T2 = zeros(60,length(qin)^3);
Q2 = zeros(60,length(qin)^3);
A2 = zeros(60,length(qin)^3);
V2 = zeros(60,length(qin)^3);
Re2 = zeros(60,length(qin)^3);
Nu2 = zeros(60,length(qin)^3);
H2 = zeros(60,length(qin)^3);
R2 = zeros(60,length(qin)^3);
% Computation
for i=1:length(Temp)
    for j=1:length(qin)
        for k=1:length(inlet)
            % Inlet Conditions ============================================
            % mass flow rate oil inlet kg/s
            mass_flow(k,j+50*(i-1))=qin(j)/(CL*(Temp(i)-Ta));
            % velocity oil inlet m/s
            Uinf(k,j+50*(i-1))=mass_flow(k,j+50*(i-1))/...
                (rhoL*pi*inlet(k)^2/4);
            % Reynold's number inlet
            Re_inf(k,j+50*(i-1))=rhoL*Uinf(k,j+50*(i-1))*inlet(k)/visco_l;
            % Nusselt number inlet
            if (Re_inf(k,j+50*(i-1))<3000)  % laminar flow
                fr_inf(k,j+50*(i-1)) = 64/Re_inf(k,j+50*(i-1));
                Nu_inf(k,j+50*(i-1))= 4.36;
            else                            % turbulent flow
                % smooth pipe
                fr_inf(k,j+50*(i-1)) = (0.79*log(Re_inf(k,j+50*...
                    (i-1)))-1.64)^-2;
                Nu_inf(k,j+50*(i-1)) = 0.125*fr_inf(k,j+50*(i-1))*...
                    Re_inf(k,j+50*(i-1))*Pr^(1/3);
            end
            % Convective heat transfer coefficient inlet
            H_inf(k,j+50*(i-1)) = Nu_inf(k,j+50*(i-1))*KL/inlet(k);
            % Shell Side  Configuration 1 ================================
            T(1,k+50*((j+50*(i-1))-1)) = Temp(i);
            Q(1,k+50*((j+50*(i-1))-1)) = qin(j);
            A(1,k+50*((j+50*(i-1))-1)) = pi*inlet(k)^2/4;
```

```
            V(1,k+50*((j+50*(i-1))-1)) = Uinf(k,j+50*(i-1));
            Re(1,k+50*((j+50*(i-1))-1)) = Re_inf(k,j+50*(i-1));
            Nu(1,k+50*((j+50*(i-1))-1)) = Nu_inf(k,j+50*(i-1));
            H(1,k+50*((j+50*(i-1))-1)) = H_inf(k,j+50*(i-1));
            R(1,k+50*((j+50*(i-1))-1)) = 1/(A(1,k+50*((j+50*(i-1))-1))...
                *H(1,k+50*((j+50*(i-1))-1)));
            for z=1:59;
                % compute parameters for each section across duct
                % choose section
                section = mod(z,12)+1;
                % number of tubes at section
                if ((section==4)||(section==5)||(section==8)||(section==9))
                    Ntube = 4;
                elseif ((section==6)||(section==7))
                    Ntube = 5;
                else
                    Ntube = 3;
                end
                % Shift index
                l=z+1;
                % choose height
                if ((l>12)&&(l<49))
                    height = baffle_h;
                else
                    height = entry_h;
                end
                % compute geometry of interest
                tube_sa = pi*tube_d*height*Ntube;     % capsule s.area (m2)
                area_cf = ((tube_c)...                % cross flow area (m2)
                    *(Ntube-1)+(2*tube_w))*height;
                area_ff = (tube_p*(Ntube-1)...        % free-flow area
                    +tube_d+2*tube_w)*height;
                area_hx = (0.9*tube_d*height)*Ntube; % heat transfer area
                L_hx = 0.9*tube_d/2;
                Dh = 2*(area_ff)/(height+((Ntube-1)...
                    *tube_p+tube_d+2*tube_w));
                switch section
                    case {1}   % baffle entry
                        % compute flow properties
                        A(l,k+50*((j+50*(i-1))-1)) = baffle_entry;
                        V(l,k+50*((j+50*(i-1))-1)) = mass_flow(k,j+50*(i-
1))/(rhoL*A(l,k+50*((j+50*(i-1))-1)));
                        Re(l,k+50*((j+50*(i-1))-1)) = rhoL*V(l,k+50*((j+50*(i-
1))-1))*baffle_dh/visco_l;
                        if (Re(l,k+50*((j+50*(i-1))-1))<3000)% laminar flow
                            Nu(l,k+50*((j+50*(i-1))-1)) = 3.61;
                        else                                % turbulent flow
                            Nu(l,k+50*((j+50*(i-1))-1)) =
0.023*Re(l,k+50*((j+50*(i-1))-1))^(0.8)*Pr^(0.3);
                        end
                        % compute heat transfer
                        H(l,k+50*((j+50*(i-1))-1)) = Nu(l,k+50*((j+50*(i-1))-
1))*KL/baffle_dh;
                        R(l,k+50*((j+50*(i-1))-1))= 1/(A(l,k+50*((j+50*(i-1))-
1))*H(l,k+50*((j+50*(i-1))-1)));
                    case {2,12} % free flow
                        % compute flow properties
```

```
                        A(l,k+50*((j+50*(i-1))-1)) = area_ff;
                        V(l,k+50*((j+50*(i-1))-1)) = mass_flow(k,j+50*(i-
1))/(rhoL*A(l,k+50*((j+50*(i-1))-1)));
                        Re(l,k+50*((j+50*(i-1))-1)) = rhoL*V(l,k+50*((j+50*(i-
1))-1))*Dh/visco_l;
                        if (Re(l,k+50*((j+50*(i-1))-1))<3000)% laminar flow
                            Nu(l,k+50*((j+50*(i-1))-1)) = 4.12;
                        else                                % turbulent flow
                            Nu(l,k+50*((j+50*(i-1))-1)) =
0.023*Re(l,k+50*((j+50*(i-1))-1))^(0.8)*Pr^(0.3);
                        end
                        % compute heat transfer
                        H(l,k+50*((j+50*(i-1))-1)) = Nu(l,k+50*((j+50*(i-1))-
1))*KL/Dh;
                        R(l,k+50*((j+50*(i-1))-1))= (1/(A(l,k+50*((j+50*(i-
1))-1))*H(l,k+50*((j+50*(i-1))-1))))+R(l-1,k+50*((j+50*(i-1))-1));
                    case {3,11} % cross flow
                        % compute flow properties
                        A(l,k+50*((j+50*(i-1))-1)) = area_cf;
                        V(l,k+50*((j+50*(i-1))-1)) = mass_flow(k,j+50*(i-
1))/(rhoL*A(l,k+50*((j+50*(i-1))-1)));
                        Re(l,k+50*((j+50*(i-1))-1)) = rhoL*V(l,k+50*((j+50*(i-
1))-1))*tube_dh/visco_l;
                        Nu(l,k+50*((j+50*(i-1))-1)) =
0.3+((0.62*Re(l,k+50*((j+50*(i-1))-
1))^(0.5)*Pr^(1/3))/((1+(0.4/Pr)^(2/3))^(1/4)))*((1+(Re(l,k+50*((j+50*(i-1))-
1))/282000)^(5/8))^(4/5));
                        % compute heat transfer
                        H(l,k+50*((j+50*(i-1))-1)) = Nu(l,k+50*((j+50*(i-1))-
1))*KL/tube_dh;
                        R(l,k+50*((j+50*(i-1))-1))=
(1/(tube_sa*H(l,k+50*((j+50*(i-1))-1))))+Ntube*(log(0.8)...
                            /(2*pi*height*Ks))+(L_hx/(KP*area_hx));
                    case {4,10}  % free flow
                        % compute flow properties
                        A(l,k+50*((j+50*(i-1))-1)) = area_ff;
                        V(l,k+50*((j+50*(i-1))-1)) = mass_flow(k,j+50*(i-
1))/(rhoL* A(l,k+50*((j+50*(i-1))-1)));
                        Re(l,k+50*((j+50*(i-1))-1)) = rhoL*V(l,k+50*((j+50*(i-
1))-1))*Dh/visco_l;
                        if (Re(l,k+50*((j+50*(i-1))-1))<3000)% laminar flow
                            Nu(l,k+50*((j+50*(i-1))-1)) = 3.61;
                        else                                % turbulent flow
                            Nu(l,k+50*((j+50*(i-1))-1)) =
0.023*Re(l,k+50*((j+50*(i-1))-1))^(0.8)*Pr^(0.3);
                        end
                        % compute heat transfer
                        H(l,k+50*((j+50*(i-1))-1)) = Nu(l,k+50*((j+50*(i-1))-
1))*KL/Dh;
                        R(l,k+50*((j+50*(i-1))-1))= (1/(A(l,k+50*((j+50*(i-
1))-1))*H(l,k+50*((j+50*(i-1))-1))))+R(l-1,k+50*((j+50*(i-1))-1));
                    case {5,9}  % cross flow
                        % compute flow properties
                        A(l,k+50*((j+50*(i-1))-1)) = area_cf;
                        V(l,k+50*((j+50*(i-1))-1)) = mass_flow(k,j+50*(i-
1))/(rhoL*A(l,k+50*((j+50*(i-1))-1)));
```

```
                        Re(l,k+50*((j+50*(i-1))-1)) = rhoL*V(l,k+50*((j+50*(i-
1))-1))*tube_dh/visco_l;
                        Nu(l,k+50*((j+50*(i-1))-1)) =
0.3+((0.62*Re(l,k+50*((j+50*(i-1))-
1))^(0.5)*Pr^(1/3))/((1+(0.4/Pr)^(2/3))^(1/4)))*((1+(Re(l,k+50*((j+50*(i-1))-
1))/282000)^(5/8))^(4/5));
                        % compute heat transfer
                        H(l,k+50*((j+50*(i-1))-1)) = Nu(l,k+50*((j+50*(i-1))-
1))*KL/tube_dh;
                        R(l,k+50*((j+50*(i-1))-1))=
(1/(tube_sa*H(l,k+50*((j+50*(i-1))-1))))+Ntube*(log(0.8)...
                            /(2*pi*height*Ks))+(L_hx/(KP*area_hx));
                    case {6,8}  % free flow
                        % compute flow properties
                        A(l,k+50*((j+50*(i-1))-1)) = area_ff;
                        V(l,k+50*((j+50*(i-1))-1)) = mass_flow(k,j+50*(i-
1))/(rhoL*A(l,k+50*((j+50*(i-1))-1)));
                        Re(l,k+50*((j+50*(i-1))-1)) = rhoL*V(l,k+50*((j+50*(i-
1))-1))*Dh/visco_l;
                        if (Re(l,k+50*((j+50*(i-1))-1))<3000)% laminar flow
                            Nu(l,k+50*((j+50*(i-1))-1)) = 3.61;
                        else                                   % turbulent flow
                            Nu(l,k+50*((j+50*(i-1))-1)) =
0.023*Re(l,k+50*((j+50*(i-1))-1))^(0.8)*Pr^(0.3);
                        end
                        Nu(l,k+50*((j+50*(i-1))-1)) =
0.023*Re(l,k+50*((j+50*(i-1))-1))^(0.8)*Pr^(0.3);
                        % compute heat transfer
                        H(l,k+50*((j+50*(i-1))-1)) = Nu(l,k+50*((j+50*(i-1))-
1))*KL/Dh;
                        R(l,k+50*((j+50*(i-1))-1))= (1/(A(l,k+50*((j+50*(i-
1))-1))*H(l,k+50*((j+50*(i-1))-1))))+R(l-1,k+50*((j+50*(i-1))-1));
                    case {7}    % cross flow
                        % compute flow properties
                        A(l,k+50*((j+50*(i-1))-1)) = area_cf;
                        V(l,k+50*((j+50*(i-1))-1)) = mass_flow(k,j+50*(i-
1))/(rhoL*A(l,k+50*((j+50*(i-1))-1)));
                        Re(l,k+50*((j+50*(i-1))-1)) = rhoL*V(l,k+50*((j+50*(i-
1))-1))*tube_dh/visco_l;
                        Nu(l,k+50*((j+50*(i-1))-1)) =
0.3+((0.62*Re(l,k+50*((j+50*(i-1))-
1))^(0.5)*Pr^(1/3))/((1+(0.4/Pr)^(2/3))^(1/4)))*((1+(Re(l,k+50*((j+50*(i-1))-
1))/282000)^(5/8))^(4/5));
                        % compute heat transfer
                        H(l,k+50*((j+50*(i-1))-1)) = Nu(l,k+50*((j+50*(i-1))-
1))*KL/tube_dh;
                        R(l,k+50*((j+50*(i-1))-1))=
(1/(tube_sa*H(l,k+50*((j+50*(i-1))-1))))+Ntube*(log(0.8)...
                            /(2*pi*height*Ks))+(L_hx/(KP*area_hx));
                end
                T(l,k+50*((j+50*(i-1))-1)) = T(l-1,k+50*((j+50*(i-1))-1))-
(Q(l-1,k+50*((j+50*(i-1))-1))*R(l,k+50*((j+50*(i-1))-1)));
                delta_t = T(l-1,k+50*((j+50*(i-1))-1))-T(l,k+50*((j+50*(i-1))-
1));
                Q(l,k+50*((j+50*(i-1))-1)) = mass_flow(k,j+50*(i-
1))*CL*T(l,k+50*((j+50*(i-1))-1));
            end
```

```
            % Shell Side Configuration 2 ==================================
            T2(1,k+50*((j+50*(i-1))-1)) = Temp(i);
            Q2(1,k+50*((j+50*(i-1))-1)) = qin(j);
            A2(1,k+50*((j+50*(i-1))-1)) = pi*inlet(k)^2/4;
            V2(1,k+50*((j+50*(i-1))-1)) = Uinf(k,j+50*(i-1));
            Re2(1,k+50*((j+50*(i-1))-1)) = Re_inf(k,j+50*(i-1));
            Nu2(1,k+50*((j+50*(i-1))-1)) = Nu_inf(k,j+50*(i-1));
            H2(1,k+50*((j+50*(i-1))-1)) = H_inf(k,j+50*(i-1));
            R2(1,k+50*((j+50*(i-1))-1)) = 1/(A2(1,k+50*((j+50*(i-1))-
1))*H2(1,k+50*((j+50*(i-1))-1)));
            for z=1:59;
                % compute parameters for each section across duct
                % choose section
                section = mod(z,12)+1;
                % number of tubes at section
                if ((section==7)||(section==5)||(section==4)||(section==6))
                    Ntube = 4;
                elseif ((section==3)||(section==2))
                    Ntube = 5;
                else
                    Ntube = 3;
                end
                % Shift index
                l=z+1;
                % choose height
                if ((l>12)&&(l<49))
                    height = baffle_h;
                else
                    height = entry_h;
                end
                % baffle entry index
                m = mod(l,2);
                % compute geometry of interest
                tube_sa = pi*tube_d*height*Ntube;     % capsule s.area (m2)
                area_cf = ((tube_c)...                % cross flow area (m2)
                    *(Ntube-1)+(2*tube_w))*height;
                area_ff = (tube_p*(Ntube-1)...        % free-flow area
                    +tube_d+2*tube_w)*height;
                area_hx = (0.9*tube_d*height)*Ntube; % heat transfer area
                area_donut = pi*(0.0254*6)^2/4-(4*pi*(tube_d)^2/4);
                area_disc = pi*(shell_id)^2/4-pi*(0.0254*13.5)^2/4;
                L_hx = 0.9*tube_d/2;
                Dh = 2*(area_ff)/(height+((Ntube-1)...
                    *tube_p+tube_d+2*tube_w));
                switch section
                    case {1}   % baffle entry
                        % compute flow properties
                        if (m==0)
                            A2(l,k+50*((j+50*(i-1))-1)) = area_disc;
                            baffle_dh = 4*(area_disc)/(pi*(0.0254*13.5));
                        else
                            A2(l,k+50*((j+50*(i-1))-1)) = area_donut;
                            baffle_dh = tube_dh;
                        end
                        V2(l,k+50*((j+50*(i-1))-1)) = mass_flow(k,j+50*(i-
1))/(rhoL*A2(l,k+50*((j+50*(i-1))-1)));
```

```
                        Re2(l,k+50*((j+50*(i-1))-1)) =
rhoL*V2(l,k+50*((j+50*(i-1))-1))*baffle_dh/visco_l;
                        if (Re2(l,k+50*((j+50*(i-1))-1))<3000)% laminar flow
                            Nu2(l,k+50*((j+50*(i-1))-1)) = 4.36;
                        else                                   % turbulent flow
                            if (m==0)
                                Nu2(l,k+50*((j+50*(i-1))-1)) =
0.228*Re2(l,k+50*((j+50*(i-1))-1))^(0.731)*Pr^(0.3);
                            else
                                Nu2(l,k+50*((j+50*(i-1))-1)) =
0.023*Re2(l,k+50*((j+50*(i-1))-1))^(0.8)*Pr^(0.3);
                            end
                        end
                        % compute heat transfer
                        H2(l,k+50*((j+50*(i-1))-1)) = Nu2(l,k+50*((j+50*(i-
1))-1))*KL/baffle_dh;
                        R2(l,k+50*((j+50*(i-1))-1))= 1/(A2(l,k+50*((j+50*(i-
1))-1))*H2(l,k+50*((j+50*(i-1))-1)));
                    case {11,12} % free flow
                        % compute flow properties
                        A2(l,k+50*((j+50*(i-1))-1)) = area_ff;
                        V2(l,k+50*((j+50*(i-1))-1)) = mass_flow(k,j+50*(i-
1))/(rhoL*A2(l,k+50*((j+50*(i-1))-1)));
                        Re2(l,k+50*((j+50*(i-1))-1)) =
rhoL*V2(l,k+50*((j+50*(i-1))-1))*tube_dh/visco_l;
                        if (Re2(l,k+50*((j+50*(i-1))-1))<3000)% laminar flow
                            Nu2(l,k+50*((j+50*(i-1))-1)) = 4.12;
                        else                                 % turbulent flow
                            Nu2(l,k+50*((j+50*(i-1))-1)) =
0.023*Re2(l,k+50*((j+50*(i-1))-1))^(0.8)*Pr^(0.3);
                        end
                        % compute heat transfer
                        H2(l,k+50*((j+50*(i-1))-1)) = Nu2(l,k+50*((j+50*(i-
1))-1))*KL/tube_dh;
                        R2(l,k+50*((j+50*(i-1))-1))= (1/(A2(l,k+50*((j+50*(i-
1))-1))*H2(l,k+50*((j+50*(i-1))-1))));
                    case {9,10} % cross flow
                        % compute flow properties
                        A2(l,k+50*((j+50*(i-1))-1)) = area_cf;
                        V2(l,k+50*((j+50*(i-1))-1)) = mass_flow(k,j+50*(i-
1))/(rhoL*A2(l,k+50*((j+50*(i-1))-1)));
                        Re2(l,k+50*((j+50*(i-1))-1)) =
rhoL*V2(l,k+50*((j+50*(i-1))-1))*tube_dh/visco_l;
                        Nu2(l,k+50*((j+50*(i-1))-1)) =
0.3+((0.62*Re2(l,k+50*((j+50*(i-1))-
1))^(0.5)*Pr^(1/3))/((1+(0.4/Pr)^(2/3))^(1/4)))*((1+(Re2(l,k+50*((j+50*(i-1))-
1))/282000)^(5/8))^(4/5));
                        % compute heat transfer
                        H2(l,k+50*((j+50*(i-1))-1)) = Nu2(l,k+50*((j+50*(i-
1))-1))*KL/tube_dh;
                        R2(l,k+50*((j+50*(i-1))-1))=
(1/(tube_sa*H2(l,k+50*((j+50*(i-1))-1))))+Ntube*(log(0.8)...
                            /(2*pi*height*Ks))+(L_hx/(KP*area_hx));
                    case {7,8}  % free flow
                        % compute flow properties
                        A2(l,k+50*((j+50*(i-1))-1)) = area_ff;
```

```
                        V2(l,k+50*((j+50*(i-1))-1)) = mass_flow(k,j+50*(i-1))/(rhoL* A2(l,k+50*((j+50*(i-1))-1)));
                        Re2(l,k+50*((j+50*(i-1))-1)) = rhoL*V2(l,k+50*((j+50*(i-1))-1))*tube_dh/visco_l;
                        if (Re2(l,k+50*((j+50*(i-1))-1))<3000) % laminar flow
                            Nu2(l,k+50*((j+50*(i-1))-1)) = 3.61;
                        else                             % turbulent flow
                            Nu2(l,k+50*((j+50*(i-1))-1)) = 0.023*Re2(l,k+50*((j+50*(i-1))-1))^(0.8)*Pr^(0.3);
                        end
                        % compute heat transfer
                        H2(l,k+50*((j+50*(i-1))-1)) = Nu2(l,k+50*((j+50*(i-1))-1))*KL/tube_dh;
                        R2(l,k+50*((j+50*(i-1))-1))= (1/(A2(l,k+50*((j+50*(i-1))-1))*H2(l,k+50*((j+50*(i-1))-1))));
                    case {5,6}  % cross flow
                        % compute flow properties
                        A2(l,k+50*((j+50*(i-1))-1)) = area_cf;
                        V2(l,k+50*((j+50*(i-1))-1)) = mass_flow(k,j+50*(i-1))/(rhoL*A2(l,k+50*((j+50*(i-1))-1)));
                        Re2(l,k+50*((j+50*(i-1))-1)) = rhoL*V2(l,k+50*((j+50*(i-1))-1))*tube_dh/visco_l;
                        Nu2(l,k+50*((j+50*(i-1))-1)) = 0.3+((0.62*Re2(l,k+50*((j+50*(i-1))-1))^(0.5)*Pr^(1/3))/((1+(0.4/Pr)^(2/3))^(1/4)))*((1+(Re2(l,k+50*((j+50*(i-1))-1))/282000)^(5/8))^(4/5));
                        % compute heat transfer
                        H2(l,k+50*((j+50*(i-1))-1)) = Nu2(l,k+50*((j+50*(i-1))-1))*KL/tube_dh;
                        R2(l,k+50*((j+50*(i-1))-1))= (1/(tube_sa*H2(l,k+50*((j+50*(i-1))-1))))+Ntube*(log(0.8)...
                            /(2*pi*height*Ks))+(L_hx/(KP*area_hx));
                    case {3,4}  % free flow
                        % compute flow properties
                        A2(l,k+50*((j+50*(i-1))-1)) = area_ff;
                        V2(l,k+50*((j+50*(i-1))-1)) = mass_flow(k,j+50*(i-1))/(rhoL*A2(l,k+50*((j+50*(i-1))-1)));
                        Re2(l,k+50*((j+50*(i-1))-1)) = rhoL*V2(l,k+50*((j+50*(i-1))-1))*tube_dh/visco_l;
                        if (Re2(l,k+50*((j+50*(i-1))-1))<3000) % laminar flow
                            Nu2(l,k+50*((j+50*(i-1))-1)) = 3.61;
                        else                             % turbulent flow
                            Nu2(l,k+50*((j+50*(i-1))-1)) = 0.023*Re2(l,k+50*((j+50*(i-1))-1))^(0.8)*Pr^(0.3);
                        end
                        % compute heat transfer
                        H2(l,k+50*((j+50*(i-1))-1)) = Nu2(l,k+50*((j+50*(i-1))-1))*KL/tube_dh;
                        R2(l,k+50*((j+50*(i-1))-1))= (1/(A2(l,k+50*((j+50*(i-1))-1))*H2(l,k+50*((j+50*(i-1))-1))));
                    case {2}    % cross flow
                        % compute flow properties
                        A2(l,k+50*((j+50*(i-1))-1)) = tube_ua;
                        V2(l,k+50*((j+50*(i-1))-1)) = mass_flow(k,j+50*(i-1))/(rhoL*A2(l,k+50*((j+50*(i-1))-1)));
                        Re2(l,k+50*((j+50*(i-1))-1)) = rhoL*V2(l,k+50*((j+50*(i-1))-1))*tube_dh/visco_l;
```

```
                        Nu2(l,k+50*((j+50*(i-1))-1)) =
0.3+((0.62*Re2(l,k+50*((j+50*(i-1))-
1))^(0.5)*Pr^(1/3))/((1+(0.4/Pr)^(2/3))^(1/4)))*((1+(Re2(l,k+50*((j+50*(i-1))-
1))/282000)^(5/8))^(4/5));
                        % compute heat transfer
                        H2(l,k+50*((j+50*(i-1))-1)) = Nu2(l,k+50*((j+50*(i-
1))-1))*KL/tube_dh;
                        R2(l,k+50*((j+50*(i-1))-1))=
(1/(tube_sa*H2(l,k+50*((j+50*(i-1))-1))))+Ntube*(log(0.8)...
                            /(2*pi*height*Ks))+(L_hx/(KP*area_hx));
                end
                T2(l,k+50*((j+50*(i-1))-1)) = T2(l-1,k+50*((j+50*(i-1))-1))-
(Q2(l-1,k+50*((j+50*(i-1))-1))*R2(l,k+50*((j+50*(i-1))-1)));
                delta_t = T2(l-1,k+50*((j+50*(i-1))-1))-T2(l,k+50*((j+50*(i-
1))-1));
                Q2(l,k+50*((j+50*(i-1))-1)) = mass_flow(k,j+50*(i-
1))*CL*T2(l,k+50*((j+50*(i-1))-1));
            end
        end
    end
end
% Analysis 1 ==============================================================
% Differential Dimensions
delta_w = shell_id;
delta_l = shell_id;
delta_h = 0.0762;
% In-line configuration
Sn = 1.25*tube_d;
Sp = Sn;
Nn = round(delta_w/Sn);
Np = round(delta_l/Sp);
N = Nn*Np;
% Heat Transfer
C = 0.287;                              % constant in-line configuration
n = 0.620;                              % constant in-line configuration
area_HT = tube_n*pi*tube_d*shell_h;     % heat transfer area (m2)
Umax = max(max(Uinf.*(Sn./(Sn-tube_d))));
H_out = KL/tube_d*C*((Umax*tube_d/visco_l)^n)*Pr^(1/3);
delta_a = delta_w*delta_h;
delta_q = mass_oil*CL*(delta_t);
delta_m = delta_q/latent;
mass_f = mean(mean(Uinf.*rhoL.*delta_a));
Fm = delta_m/mass_pcm;
time_1 = -(mass_oil/mass_f)*log((Tm-Ta)/(Tmax-Ta))*4;
% Analysis 2 ==============================================================
area_cf = ((tube_d^2)*tube_n)/4;
de = 4*(shell_h*shell_id/8.36);
Re3 = (mean(max(mass_flow))*tube_d)/(area_cf*visco_l);
hi = KP/tube_d*(0.023*Re3^0.8*Pr^0.33*visco_l^1.25);
ho = KL/de*0.36*(Re^0.55*Pr^0.33*visco_l^0.14);
%Uo = (1/Ao)/((1/(hi*Ai))+(log(tube_d/tube_d)/(2*KP*tube_l))+(1/(ho*Ao)));
% Analysis 3 ==============================================================
Ua = 1.2;
Ks = 60.5;
Ki = 0.23;
R_total = (1/(2*pi*shell_id*shell_h*H_out))...
    +(log(shell_od/shell_id)/(2*pi*shell_h*Ks))...
```

```
    +(log((shell_od+(0.0254*4))/shell_od)/(2*pi*shell_h*Ki))...
    +(1/(2*pi*(shell_od+(0.0254*4))*shell_h*Ua));
q_loss = (Tmax-Ta)/R_total;
t_loss = E_total/q_loss;
Analysis 4 ===============================================================
Plot Data ================================================================
figure(1)
hold on
for i=1:length(Temp)
    for j=1:length(qin)
        plot(mass_flow(1,j+50*(i-1)),qin(j),'r')
    end
end
title('Input Heat Flux vs. Mass Flow (Duratherm @150-300C)')
xlabel('Mass Flow Rate (kg/s)')
ylabel('Heat Flux (J/s)')
figure(2)
hold on
for i=1:length(Temp)
    for j=1:length(qin)
       for k=1:length(inlet)
          plot(inlet(k),Uinf(k,j+50*(i-1)),'b')
       end
    end
end
title('Inlet Velocity vs. Inlet Diameter (Duratherm @150-300C)')
xlabel('Diameter (m)')
ylabel('Fluid Velocity (m/s)')
figure(3)
hold on
for i=1:length(Temp)
    for j=1:length(qin)
       for k=1:length(inlet)
          plot(mass_flow(1,j+50*(i-1)),Uinf(k,j+50*(i-1)),'g')
       end
    end
end
title('Inlet Velocity vs. Mass Flow (Duratherm @150-300C)')
xlabel('Diameter (m)')
ylabel('Fluid Velocity (m/s)')
```